C.P. No. 983

C.P. No. 983

MINISTRY OF TECHNOLOGY

AERONAUTICAL RESEARCH COUNCIL

CURRENT PAPERS

Low-Speed Wind-Tunnel Tests on a 1/6th Scale Model of an Air-Cushion-Vehicle (Britten-Norman Cushioncraft C.C.2)

by

W. J. G. Trebble, B.Sc.

LONDON: HER MAJESTY'S STATIONERY OFFICE

1968

PRICE 11s 6d NET

U.D.C. No. 533.6.013.67 : 533.682

C.P. No. 983*
December 1966

LOW-SPEED WIND-TUNNEL TESTS ON A 1/6th SCALE MODEL OF AN AIR-CUSHION-VEHICLE (BRITTEN-NORMAN CUSHIONCRAFT C.C.2.)

by

W.J.G. Trebble, B.Sc.

SUMMARY

An investigation has been made into the effects of mainstream speed on the performance and stability of a model of an Air-Cushion-Vehicle. At constant speed of the lifting fan, the lift increases both with reduction in ground clearance and increase in forward speed. The craft has a large drag which is mainly intake momentum drag. Limited speed could be available from tilting the craft bows down, but augmentation from propulsive units would be required for higher speeds.

Large nose-up moments occur at forward speed, reaching a maximum when the mainstream dynamic head is comparable with the cushion pressure. At higher speeds, the front air curtain breaks down with a resultant rearward movement of the centre of cushion lift thus giving some reduction in the nose-up moment. Pitch stiffness is reduced by an increase in either ground clearance or speed and is reduced to zero when the front curtain breaks down; at higher speeds there is some recovery in stability. Attempts to improve pitch control by means of a tailplane or by throttling the front jet proved inadequate.

---

* Replaces R.A.E. Technical Report 66383 - A.R.C. 29280

CONTENTS

3

1 INTRODUCTION

The principle of the Air-Cushion-Vehicle (A.C.V.) has now been well established and many types have been built both in this country and abroad. So far they have only been operated over a speed range where the mainstream dynamic head is much less than the cushion pressure. Future developments will obviously include increases in forward speed and it was felt that the balance of pressures at high speed might lead to a collapse of the front air-curtain hence causing severe stability problems. A programme of low-speed wind-tunnel research was therefore called for to investigate A.C.V. behaviour at high speed.

The possibility of testing a full-scale craft above a ground-board in the 24 ft wind-tunnel was considered and rejected. This would have avoided the problems of reproducing, on model scale, the full scale fan characteristics and the internal duct losses but it would have meant that a craft would have been unavailable for flight testing for a long period and any detailed modifications suggested as the work proceeded would not have been easy.

Furthermore, there are great uncertainties in the mainstream speed when ground effect tests are made on relatively large models in open-jet tunnels. It was therefore decided to build a scale model of the Britten-Norman C.C.2 for testing in a closed tunnel at the R.A.E. Separate models for investigating the effects of intake and exit flows independently had their attractions as the complicated fan aerodynamics could then be removed but, in view of the urgent need for results on a complete model to supplement full-scale research, a 1/6th scale fan-powered model was constructed.

One great disadvantage in testing complete models at low Reynolds number is that the internal flow may not be truly representative of that in the full-scale A.C.V. For this reason it would be imprudent to assume that the results can necessarily be scaled up in detail though the general trends should apply.

2 MODEL DETAILS

A 1/6th scale model of the Britten-Norman C.C.2 (Figs.1-4) was manufactured from wood structural members covered with an outer skin of dural sheeting. The model construction was similar to that used by the firm for their own dynamic model but the extra weight and rigidity required for wind-tunnel balance measurements was provided by a solid wooden cabin containing the heavy variable-frequency three-phase electric motor used to drive the lifting fans while heavier gauge metal sheeting was used throughout. Thus the basic model weight was increased from 20 to 80 lb.

A pair of Heba 100 type fans (Fig.4(a)), were fitted in the model. Originally the fan design incorporated rather sharp intake lips (Fig.4(b)), but alternative lips were also provided to give lip radii of 5% and 10% of the inlet throat diameter. The fans exhausted through a plenum chamber to a peripheral blowing slot which was inclined inwards at 30° to the horizontal. Additional longitudinal blowing slots (Fig.3), were fitted on the full-scale craft to provide pitch and roll stability. These could be represented on the model, if required, and guide vanes were avialable to give a vertical jet or ±30° deflection fore and aft. On the full-scale vehicle, the fans rotate in opposite directions but, for simplicity of construction, the model fans both rotated in the same direction, clockwise when viewed from above. This may have caused some difference in the velocity distribution around the circumference of the blowing slot.

Behind and outboard of the rear intake, a pair of fixed fins could be mounted on the craft and a rudder capable of deflections up to 30° was cut in each fin (Fig.3). Furthermore, a tailplane could be mounted in a high position between the two fins (Fig.2). Provision was also made for the installation of a pair of propulsion motors ahead of the cabin with each motor driving a two-bladed propeller (Fig.1 and 2).

3 TEST DETAILS

The tests were made in the No.1, $11\frac{1}{2} \times 8\frac{1}{2}$ ft low-speed wind-tunnel at R.A.E. Farnborough during 1963 and 1964. The model was suspended in an upright position from the overhead 6-component balance, using a conventional V-wire rig on which the wire lengths could be adjusted so that different hover heights could be represented. The 'ground' consisted of a 2 in thick elliptic-nosed wooden board spanning the tunnel. It split the tunnel cross-sectional area approximately in the ratio 2 : 1 and extended 2 ft ahead of and 4 ft behind the model extremities. The wind-speed at the model position had been determined, before the model was installed, from measurements made with a suitably located pitot-static tube for a series of values of the pressure differential between the usual two reference stations in the tunnel circuit. Experience has shown that a model of normal size has little or no effect on the total mass flow rate through the tunnel, so that a corrected value of wind-speed at the model could be obtained by measuring the changes of the mean velocity in the air passage below the ground board. No constraint corrections have been applied except for this velocity re-distribution.

Measurements were made at four hover heights of the lift, drag and pitching moment of the unyawed model, both with and without stability jets, at mainstream speeds up to 75 ft/sec over an incidence range that was limited solely by the bow or stern touching the ground. Usually the chosen fan speed was that required for dynamic similarity (1288 rpm) though some tests were also made over a range from 1030 to 1800 rpm. The fan speed was measured by counting pulses on a tacho-generator in the motor and could be controlled quite easily to within ±0.1% of the desired value. At a hover height representative of 14 in full scale (h/t = 3.57), the directional and lateral stability were investigated for a range of values of the ratio of mainstream dynamics head to cushion pressure. Tests were also made with a pair of propulsive motors installed and their performance was examined for a range of propeller blade settings.

Lift and moment contributions from the air cushion were obtained from eleven static pressure orifices fitted along the centreline of the under-surface of the model and a further ten orifices distributed over the port half of that surface. Mass flow rate through the model and the exit momentum were estimated crudely from measurements of the total and static pressures at seven peripheral stations in the port half of the nozzle (Fig.6); two pitot tubes were fitted at each station whilst the static pressure was obtained at orifices in the inner and outer walls of the slot. Similarly the flow through the stability jets was obtained from single pitot and static tubes at seven stations along the length of the port jet.

4 RESULTS

In order to facilitate more general use of the information obtained from these tests, the results are mainly quoted in a non-dimensional form in which the forces and moments have been made non-dimensional by dividing by the lift (L) and also for the pitching moments by the craft length (c); lift itself has been non-dimensionalised by dividing by the hover lift (L_o) at zero incidence for the appropriate hover height. In addition a velocity parameter $\left(\sqrt{\frac{q_o}{P_{c_o}}}\right)$ has been formulated where q_o is the mainstream dynamic head and P_{c_o} is the mean value of cushion pressure at hover. The yawing moments, sideforces and rolling moments have all been non-dimensionalised in the standard aerodynamic way.

It should be remembered that these tests were made at very low Reynolds number (about 1/15th of full scale) and thus it is unlikely that the internal

flow regime was truly representative of that apertaining to the full-scale craft, particularly as regions of separated flow were observed. Consequently it must not be assumed that the results necessarily apply quantitatively to the full-scale craft though general trends would be expected to be similar.

4.1 Aerodynamics of the basic shape

The aerodynamics of the basic craft with intake-lips removed and intakes and exits sealed are given in Fig.5(a)-(i). The forces and moments are here given in the usual aerodynamic coefficient form with the measured values divided by the mainstream dynamic head (q_o) and plan area (S) and also, for the moments, by the overall length of the model (c) or width (b) as appropriate. As expected, the lift slope increased as the model was brought nearer to the ground but there was negligible lift at zero incidence ($C_L \approx 0.02$). Integration of the pressure measurements on the under surface of the craft at zero incidence gave the negative values of lift coefficient indicated in the table below; the difference between these values and the balance measurements gave lift external to the cushion area which varied between C_L-values of 0.15 and 0.20 over the tested height range.

h/t	C_L Overall	C_L Cushion area	C_L External to cushion
1.95	+0.02	-0.18	+0.20
3.57	+0.02	-0.16	+0.18
4.95	+0.02	-0.15	+0.17
7.92	+0.01	-0.14	+0.15

From the pitching moment curves (Fig.5(b)), it could be deduced that the aerodynamic centre was at about one sixth of the overall length at zero incidence but moved back towards the mid-point as the incidence was increased. The profile drag ($C_{D_o} \approx 0.05$) was virtually independent of ground clearance (Fig.5(c)) though there was the usual reduction in induced drag as the ground was approached.

Without fins the model was directionally unstable though the chosen fin design gave stability at sideslip angles up to 17^o (Fig.5(g)).

4.2 Calibration of mass flow rate in model with optimised intake lips

An exploration of the peripheral jet with pitot- and static-pressure tubes in the plane of the nozzle exit indicated that, even in the hover, there were

variations in the jet velocity (V_J) and total head around the periphery (Fig.6). Increases in the mainstream speed reduced the mass flow rate through the front sections of the nozzle but this loss was more than compensated for by increased flow through the remainder of the nozzle; similar variations were also observed in the stability jets. Thus overall some benefit appeared to be derived from the mainstream ram pressure but flow separations from the front portions of the intake lips (Section 4.4) precluded any further gains once the mainstream speed had become comparable with the intake velocity.

4.3 Static hover

The effect of hover height on the static lift is illustrated in Fig.7 where the results have been converted to lb and ft full scale. Opening the stability jets led to some loss in lift at moderate hover heights as this imposed some decrease in the flow-rate through the peripheral jet but close to the ground the stability jets had little effect as the large back pressure of the cushion then reduced the flow-rate through them to a negligible amount. The majority of the lift could be attributed to the cushion pressure (P_c) acting on the area (A_c) within the peripheral jet (Section 4.7) though, of course, there was some contribution from the jet momentum flux (m_j). Typically, at an h/t- value of 3.57, $\frac{L}{P_c A_c} = 1.16$ and 1.10 with stability jets closed and open respectively. Throughout the investigated height range, good agreement was achieved with the Stanton-Jones exponential theory[1] for the cushion pressure produced by a simple peripheral jet of total head H_J (Fig.8):-

$$\frac{P_c}{H_J} = 1 - e^{-2x} \text{ where } x = t/h\ (1 + \cos\theta) \ .$$

Some reduction in lift was observed if the craft was tilted from zero incidence.

In general, the pitching moments become increasingly nose-drum as the incidence was increased (Figs.12(c), 13(c), 14(c)) thus demonstrating inherent stability though the static margin was reduced as the hover height increased. The few measurements made with the stability jets closed indicated that they had negligible effect on the pitch stability.

4.4 Intake modification

The original air intake (Fig.4(b)) had been designed to give maximum efficiency in hover. Unfortunately this resulted in an installation with relatively sharp intake lips whose performance in a cross-flow was rather suspect. A tuft

survey was therefore made and this revealed significant flow separations in the intakes even at quite low mainstream speeds. Consequently further intakes were built with the more generous lip radii of 5.4% and 10.8% of the inlet throat diameter (Fig.4(b)). These gave appreciable lift gains in the presence of mainstream flow (Fig.9(a)) although they had no measurable effect at hover. Further benefits were achieved by fairing the cabin lines into the rear intake and extending the front centre part of the forward intake to the bows of the craft as detailed in Figs.3 and 4(b).

By increasing the intake efficiency, these improvements gave a greater intake mass flow-rate and hence an increase in momentum drag but, as the associated lift gains were proportionately greater, there was a slight reduction in the drag/lift ratio (Fig.9(b)). Only small changes in the moment characteristics were induced by these modifications (Fig.9(c)).

The effects of forward speed and incidence (Sections 4.2, 4.5, 4.6, 4.7) were investigated in detail with this optimised intake design installed but the remainder of the tests were made early in the programme when the sharp lipped intakes were fitted and lack of time prevented repeat testing after the manufacture of the improved intakes.

4.5 Effect of mainstream speed at zero incidence

The combined effects of mainstream speed and hover height at zero incidence are illustrated in Figs.10 and 11 with and without the stability jets represented. No simple relationship could be established for the variation of the lift-values with height and speed but this was hardly surprising in view of the effects of the various parameters on the several contributions to lift (see Appendix). Although integration of the cushion pressure distribution (Section 4.7) indicated some slight reduction in the cushion lift as the mainstream speed was initially increased from rest, the aerodynamic characteristics external to the cushion were sufficient to produce continuously increasing overall lift throughout the tested speed range.

The drag was also made up of several components each of which was influenced by various parameters and thus again complex changes were observed as the height and speed were altered. At low mainstream speed the drag/lift ratio (Figs.10(b) and 11(b)) increased virtually linearly with the speed parameter $\sqrt{\frac{q_o}{P_{c_o}}}$ and nearly all the drag could be attributed to the loss in horizontal momentum at the intake. The reduction in the rate of growth of the drag/lift

ratio at high speeds was mainly due to the rapid rise in aerodynamic lift mentioned above though there was also some reduction in the growth rate of the intake momentum drag once the mainstream speed became comparable with the intake velocity as flow separations from the intake lips then reduced the fan efficiency and mass flow rate (Section 4.2). A very significant result was the substantial drag rise as the ground clearance was increased thus indicating that operation of ACVs at excessive height would incur penalties in propulsive power as well as in lifting power.

The lift and drag changes were accompanied by a forward movement of the effective centre of pressure as the mainstream speed was raised from zero (Figs.10(c) and 11(c)) until a critical speed was attained after which there was a fairly sudden rearward movement of the centre of pressure back towards the centre of area. This critical condition occured when the mainstream dynamics pressure was comparable with the cushion pressure as under this condition the front air curtain broke down with a consequential rearward movement of the centre of cushion lift (Section 4.7). Unsuccessful attempts were made to delay this flow breakdown by fitting a spoiler immediately behind the front jet aligned firstly tangential to the jet and later perpendicular to it.

Large nose-up moments must be expected from a design incorporating upper surface intakes as their associated momentum drag must effectively act high up on the craft. From simple sink flow considerations, Whitley and Bissell[2] predicted that the momentum drag should act half a diameter above the intake lips, a suggestion used in estimating the momentum drag contributions on Fig.10(c) but this could not account for even half of the indicated moment. Other experimental work at the R.A.E. on lifting-fan models[3] has also indicated that momentum drag effectively acts far higher than suggested by simple sink theories and consequently the intake flow phenomenon needs further consideration.

4.6 Effect of incidence

At low mainstream speeds, the overall lift was reduced by angular deflections of the model in either the positive or negative sense (Figs.12(a), 13(a), 14(a), and 15(a)). However, at speeds where the mainstream dynamic head had become comparable with cushion pressure, the influence of external aerodynamics gave some lift increase at positive attitude and appreciable gains were available at higher speeds.

Throughout the investigated range of hover height the craft was statically stable $\left(\left(\frac{dC_m}{d\alpha}\right) \text{ negative}\right)$ at low mainstream speeds (Figs.12(c), 13(c), 14(c)) but

the pitch stiffness was reduced by increases in either hover height or mainstream speed (Fig.16) leading to almost neutral stability in the vicinity of the critical speed ($q_o \approx P_{c_o}$). Fortunately, further increase in speed led to some recovery in stability. Thus, extra pitch controls (Section 4.10) would be required for safe acceleration through the critical speed range.

Forward propulsion would be available from negative tilt (Figs.12(b), 13(b), 14(b), 15(b)) but the resulting speed would be limited by the angle at which the bows touched the ground. Higher speeds would require separate propulsive system (Section 4.8). At high speed the optimum performance would no longer be achieved at negative incidence as the powerful effect of the positive slope of the lift/incidence curve on the drag/lift ratio would imply a large positive inclination for the most economic operation.

4.7 Pressure distribution under the model

The static pressure distribution on the lower surface of the model was investigated over ranges of hover height, mainstream speed and incidence; values along the centreline being illustrated in Figs.17 and 18 for the model with stability jet nozzles closed and open respectively. Increase of hover height gave the anticipated reduction in cushion pressure and, as already mentioned (Section 4.3), integration of the pressure measurements gave good agreement with the Stanton-Jones exponential theory[1] (Fig.8). However, with stability jets open, the $\frac{P_c}{H_J}$ - values were somewhat greater than predicted by the theory though, of course, the absolute values of cushion pressure were reduced by opening the stability jets (compare Figs.17(a) and 18(a)).

Increase of mainstream speed from zero initially caused some reduction in cushion pressure towards the rear of the cushion (Fig.17(a)) but when the mainstream dynamic head exceeded cushion pressure the resulting breakdown of the front curtain led to a rapid reduction in pressure in the front part of the cushion which was accompanied by a pressure rise in the rear part of the cushion. Integration of the overall pressure distribution implied that there was an initial slight loss in cushion lift associated with a forward movement of the centre of pressure but above the critical speed the breakdown of the front curtain led to a substantial rearward movement of the centre of cushion lift.

Angular deflections of the hovering model led to some pressure increase under the downward going part of the craft but there was an even greater pressure

loss under the upward moving part of the craft so that there was an overall lift loss (Figs.18(a), (c) and (d)). Increase in mainstream speed at positive incidence resulted in an initial reduction in the cushion pressure but, at higher speeds, there was an increase in pressure originating at the front of the cushion though rapidly extending rearwards as the speed was further increased (Fig.18(c)). At negative incidence, the mainstream interference effects produced pressure losses at both the front and back of the cushion (Fig.18(d)) and thus, although there was a lift loss, the centre of pressure movement was less rapid than on the undeflected model.

4.8 Directional and lateral stability

Yawing moments, sideforces and rolling moments have been plotted against sideslip angle in Fig.19 for a cruising speed just below the critical speed. The negative values of yawing moment at zero sideslip angle arose from the precessional moment produced on the model by the rotation of both fans in the same direction; full-scale they rotate in opposite directions so this effect would not be expected. With fins installed, the model was directionally stable over the range $\pm 12^{\circ}$ of sideslip though it was completely unstable in the absence of fins. As might be expected from their high position, the fins increased the negative value of ℓ_v as well as doubling the value of Y_v.

The effect of variation of mainstream speed was only investigated on the model without fins (Fig.20). Although the results show linearity at $\sqrt{\frac{q_o}{P_{c_o}}}$ - values below unity, some non-linearity was present at higher speeds. Reductions in the values of $-\frac{dC_Y}{d\beta}$ and $-\frac{dC_\ell}{d\beta}$ with increase in speed were consistent with the effects of the intake momentum drag component acting in the sideforce direction:-

$$\Delta C_Y \text{ (intake)} \propto \frac{V_i}{V_o} \sin \beta \quad .$$

4.9 Propulsion motors

In general, the model propellers were driven at 6860 rpm which was the dynamic scale speed for the proposed full-scale installation though a few check tests were also made at 80% of this speed. Blade pitch could be manually adjusted and a range of blade tip angle (ϕ_{tip}) between 7.5° and 16.75° was

tested so that the effect of blade coarseness could be investigated through the speed range. The resulting thrust coefficient $\left(K_T = \frac{\text{thrust per propeller}}{\rho\, n^2\, d^4}\right)$ has been plotted against the advance factor $\left(J = \frac{V_o}{nd}\right)$ in Fig.21(a) where the implied full-scale values of thrust and mainstream speed are also indicated. Measurements were also made on a Weston analyser of the input power to the electric motors; the measured values (which make no allowance for motor efficiency) were non-dimensionalised with respect to the power consumption with the blade tip set at 11.5° at zero mainstream speed (Fig.21(b)).

In the hover, there was little change in thrust with blade setting, suggesting that the blades stalled at a ϕ_{tip} value of 9°. At fine pitch settings the thrust decayed rapidly as the mainstream speed was increased but this decay could be delayed by coarsening the blade angle though more power would then be required from the motors. Operation of the rear lifting fan gave large reductions in the apparent thrust at low mainstream speed (approximately 25% loss at hover) as some of the slipstream was drawn into the rear intake.

At zero incidence the propellers gave some benefit to the lifting system (Fig.22) presumably through the slipstream augmenting the inlet total pressure but at negative incidence this was counterbalanced by the downward component of thrust. In consequence of their high position on the craft, the propeller thrust produced a useful nose-down moment increment and analysis of the results at zero incidence (Fig.23) showed that the simple relationship:-

$$\Delta M \text{ (propellers)} = 0.85\ \Delta D \text{ (propellers) lb ft}$$

applied throughout the incidence range. This showed excellent agreement with the fact that the propeller axes were 0.85 ft above the moment centre.

The lateral and directional stability of the craft with propellers and fins fitted was only investigated at one speed $\left(\sqrt{\frac{q_o}{P_{c_o}}} = 0.87\right)$ and the results show that the directional stability was now limited to ±5° of sideslip angle (Fig.24). Consequently larger fins would be required to give the same handling characteristics as those experienced on the basic craft. An engine failure was simulated by rotating the starboard propeller whilst holding the port propeller stationary.

Originally, directional control on the C.C.2 had been obtained by deflection of vanes in the peripheral jet but this was insufficient at the higher

speeds available with propulsive units installed. Extra control was therefore provided by cutting rudders in the fins (Fig.2). Curves of yawing moment, sideforce and rolling moment have been plotted against sideslip angle for a range of rudder angle in Fig.25. At low sideslip angles the directional stability was unaffected by sideslip angle but fin stall gave an antisymmetric set of yawing moment curves at higher sideslip angles.

4.10 Tailplane

As previously mentioned (Section 4.5), the nose-up moment increased rapidly as the mainstream speed was increased and some form of trim control was thus desirable. One possible solution was to carry a tailplane between the fins though this would need to be mounted high up to allow for the operation or rudders.

Measurements were made of the lift, drag and pitching moment of one such installation (Fig.2) with the tailplane at various settings between 0 and 25° and, in order to obtain the tailplane contributions, measurements were also made with the tailplane removed. The tailplane contribution to pitching moment has been plotted against tailplane angle (Fig.26) for a range of mainstream speed. From these curves, the mean downwash angle at the tailplane was determined as that tailplane setting required to give zero contribution to pitching moment; values so deduced have been plotted against mainstream speed in Fig.27. As expected from consideration of the effects of the flow into the rear intake, the downwash angle decreased rapidly at first with increase in mainstream speed but only at a very slow rate once the mainstream speed exceeded about a half the intake velocity. Operation of the propulsion motors caused some increase in the mean downwash angle at low mainstream speed but had negligible effect at $\sqrt{\frac{q_o}{P_{c_o}}}$ values above 1.

Overall pitching moments are plotted against speed parameter in Fig.28 with the tailplane set to give maximum nose-down moment contribution on the model both with and without the external propulsion units; curves are also shown for the model without a tailplane. At $\sqrt{\frac{q_o}{P_{c_o}}}$ - values above 0.7 insufficient thrust was being produced to balance the drag (Section 4.9) so an attempt was made to assess true performance by estimating the moment contribution produced by the additional propeller thrust required to give zero net drag; in Section 4.9 it was demonstrated that propeller thrust acted along the propeller axes. The estimated overall moment on the model with drag trimmed in this manner is given in Fig.29 where it can be seen that the tailplane would be inadequate below the critical speed. Some improvements may be possible by fitting the tailplane on low booms behind the craft so that the favourable lift arm could be increased whilst eliminating the adverse drag arm.

4.11 *Effect of sealing front peripheral jet*

An alternative method considered for trim control was the variation of flow through the front part of the peripheral nozzle. A simple test was made at an h/t-value of 1.73 with the extreme condition represented by complete closure of the front nozzle between the stability jets; i.e. just over a tenth of the air curtain was removed. The results have been compared in Fig.30 with those for a fully open nozzle.

In the hover, a lift centre movement of 1.1% of the craft length was obtained at zero incidence though tilting the craft reduced the available trim control which also deteriorated with increase in mainstream speed. Naturally some benefit would be available from a more forward position of the centre of gravity. As was only to be expected, at the higher speeds complete closure of the front nozzle had negligible effect as even with the front nozzle open the air-curtain was blown back and adhered to the under-surface if the mainstream dynamic head exceeded the cushion pressure.

Throughout the speed range, closing the front nozzle had little effect on lift and drag.

5 CONCLUDING REMARKS

These tests have shown that serious trim and stability problems require solution before air-cushion-vehicles can operate at relatively high speeds. The nose-up moment contribution associated with the intake momentum drag predominates over trim considerations at low mainstream speed, but when the mainstream dynamic pressure become comparable with the cushion pressure the front air curtain breaks down leading to a rearward movement of the centre of lift whilst simultaneously the pitch stiffness is reduced to zero. There is some recovery at higher speeds.

Forward propulsion can conveniently be obtained by the installation of propellers mounted above the craft; their thrust moment then tends to counteract the intake momentum drag moment. However, care should be taken in positioning propellers so that their high energy slipstream is not swallowed by the intakes as such an eventually would lead to increased intake momentum drag.

Operation of craft at excessive ground clearance would not only incur a high lift power penalty but greater propulsive power would also be required.

Analysis of the results on this composite model has proved difficult because the effects of varying mainstream speed on the aerodynamics of the upper and lower surfaces are interconnected; i.e. intake efficiency changes with speed and this leads to changes in internal mass flow rate and cushion pressure. Consequently a full understanding of the problems would require three models:-

(a) an intake model for the upper surface aerodynamics;

(b) an efflux model to study the air cushion; and,

(c) a composite model to check the interference effects.

Appendix

ANALYSIS OF LIFT AND DRAG FORCES

The lack of uniformity of flow through the nozzles precluded any rigorous analysis of the results but an attempt has been made to give a crude estimate of the various components of lift and drag.

In order to investigate the importance of the lift external to the air-curtain, the integrated cushion lift ($P_c S_c$) and vertical components of jet moments ($m_j \sin \theta$) were subtracted from the overall balance measurements. Curves of these deduced values plotted against mainstream dynamics head (Fig.31) were parallel indicating that at all speeds and heights there was a constant C_L-value of 0.28 (based on overall plan area) attributable to the external aerodynamics. The slight stagger of the curves may have been produced by the entrainment of air into the standing vortice external to the curtain. Thus the major components of lift could be expressed in the form:-

$$\text{LIFT} = P_c S_c + 0.28 q_o S + \Sigma m_j \sin \theta$$

Simple consideration of the drag results showed that after removal of the intake momentum drag, derived from measured mass flow rate (Section 4.2), the remaining drag varied directly with both hover height and mainstream dynamic head. Thus drag could be expressed:-

$$\text{DRAG} = \{A + B\,(h/t)\} q_o + \rho V_o V_1 A_1 \quad .$$

The first two terms represented the profile drag external to the air-curtain and a term which, being dependent on the cross-sectional area of the passage under the craft, could be regarded as 'curtain drag'. Transposition of these terms into more appropriate forms gave:-

Profile drag	$= 0.03 q_o S$
'Air-curtain' drag	$= 0.667 q_c h b_c$
Intake momentum drag	$= \rho V_o V_i A_i$

The implied profile drag component was only just over half the value established for the basic craft without fans (Section 4.1). Such an improvement could be attributed to the elimination of skin friction on the lower surface of the craft and also to B.L.C. effects on the stern of the craft induced by the air curtain.

A comparison of measured drag with empirical values derived from this analysis is given in Fig.32 where the importance of the intake momentum drag component is clearly demonstrated.

Table 1

Model details

Plan area	S	13.05 sq ft
Cushion area (area within peripheral jet)	S_c	8.95 sq ft
Intake area (at throat)	A_i	0.94 sq ft
Peripheral jet exit area	A_j	0.70 sq ft
Stability jet exit area	A_s	0.51 sq ft
Overall length of craft	ℓ	5.00 ft
Overall width of craft	b	3.00 ft
Length of cushion	c	4.17 ft
Width of cushion	b_c	2.33 ft
Thickness of peripheral nozzle	t	0.667 in
Inclination of peripheral jet to horizontal	θ°	30° inwards
Propeller diameter	D_p	0.995 ft
Tailplane area	S_T	0.923 sq ft
Tailplane chord	c_T	0.500 ft
Tailplane arm ($\frac{1}{4}$ chord point to C.G.)	ℓ_T	2.04 ft

SYMBOLS

Geometric

S	plan area
S_c	cushion area
A_i	intake throat area
A_j	exit area of peripheral nozzle
A_s	exit area of a stability jet
ℓ	length of craft
c	length of cushion (between fore and aft nozzles)
b	width of craft
h	height of peripheral nozzle exit above ground
t	nozzle thickness
θ	inclination of peripheral jet to horizontal
n	fan speed rpm

Pressures and velocities

P_o	cushion pressure
H_j	total head at exit of peripheral nozzle
H_s	total head at exit of stability jet nozzles
q_o	mainstream dynamic head
V_o	mainstream speed
V_i	intake velocity
V_j	exit velocity from peripheral nozzle
V_s	exit velocity from nozzles of stability jets
m_j	exit momentum flux
q_j	peripheral jet dynamic head
q_s	stability jet dynamic head

Forces and moments

L	lift
D	drag
Y	sideforce
m	pitching moment
n	yawing moment
ℓ	rolling moment

SYMBOLS (Contd)

$C_L = \frac{L}{q_o s}$

$C_D = \frac{D}{q_o s}$

$C_Y = \frac{Y}{q_o s}$

$C_m = \frac{m}{q_o s \ell}$

$C_n = \frac{n}{q_o s b}$

$C_\ell = \frac{\ell}{q_o s b}$

Propeller characteristics

D_P propeller diameter

N propeller speed (revs per second)

J advance factor $\frac{V_o}{ND_p}$

ϕ_{tip} blade angle (tip section)

K_T thrust coefficient $= \frac{\text{thrust}}{\rho N^2 D_p^4}$

P power input

P_o power input at $V_o = 0$ with $\phi_{tip} = 11.5^\circ$

REFERENCES

No.	Author	Title, etc
1	Stanton-Jones	Some design problems of Hovercraft. I.A.S. Report No.61-45, A.R.C. 23752 1961
2	Whitley-Bissel	On the nature of aerofoil characteristics with a sink located in the upper surface including comparison of theory with some fan-in-wing experiments. 8th Anglo-American Aeronautical Conference, September 1961
3	W.J.G. Trebble	Wind tunnel experiments on a lifting-jet in a bluff body with and without wings. A.R.C. C.P. 859 July 1964

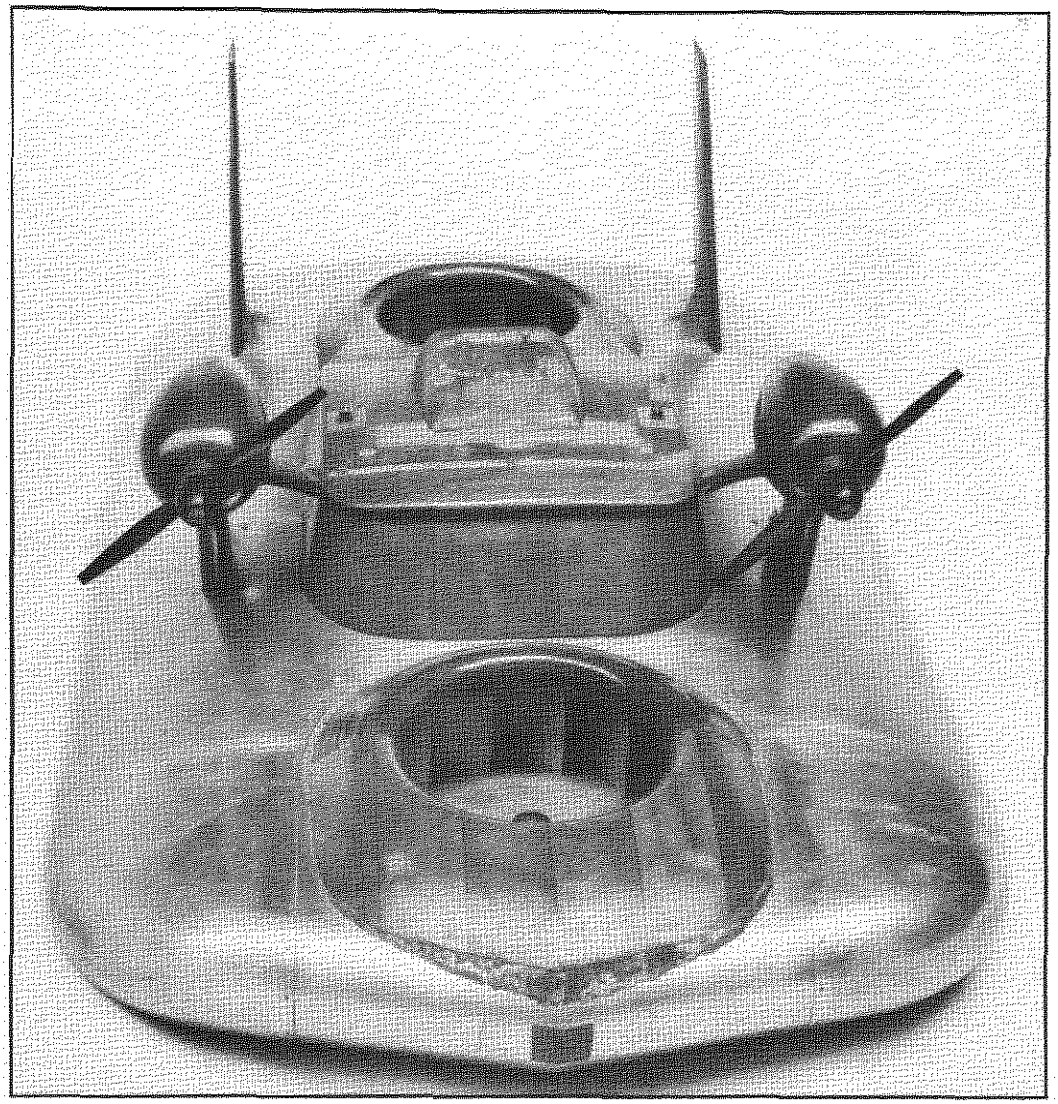

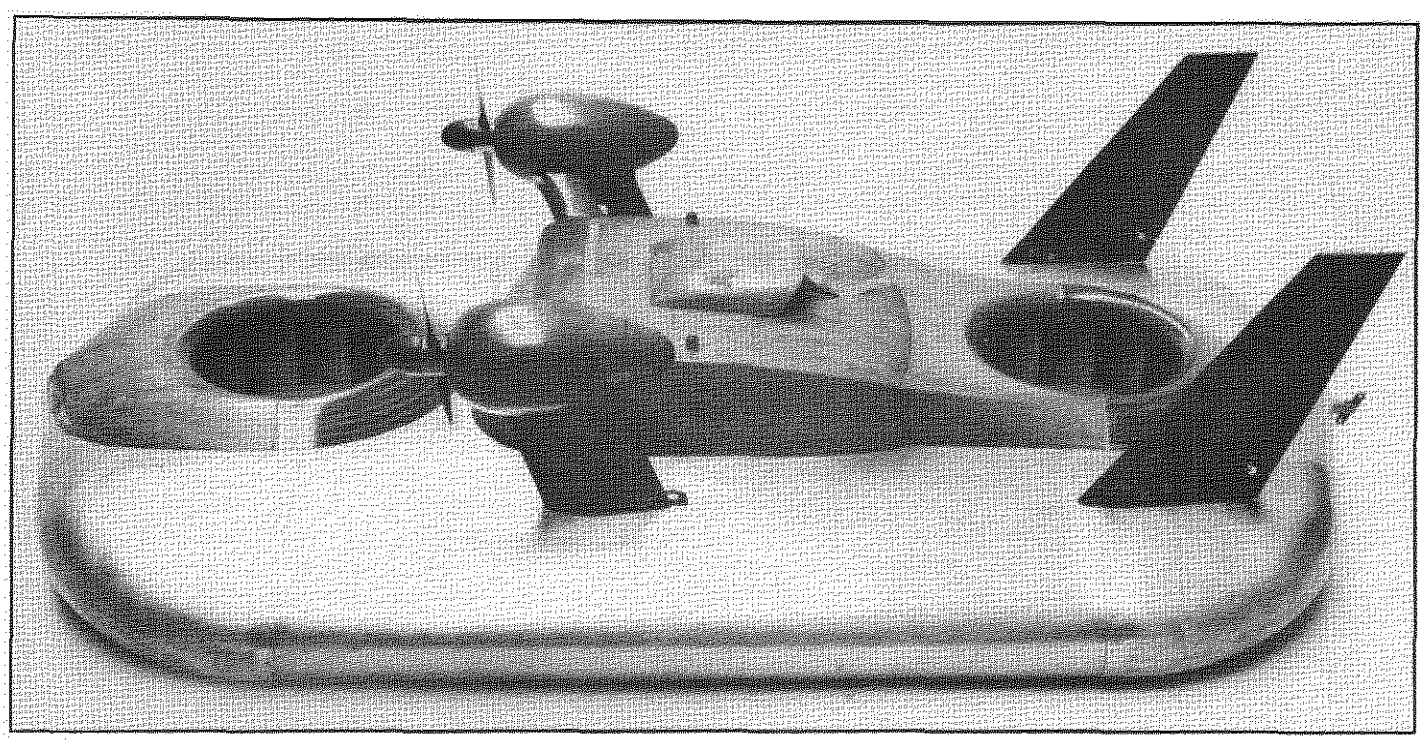

Fig.1 Model with final modification to intake lips

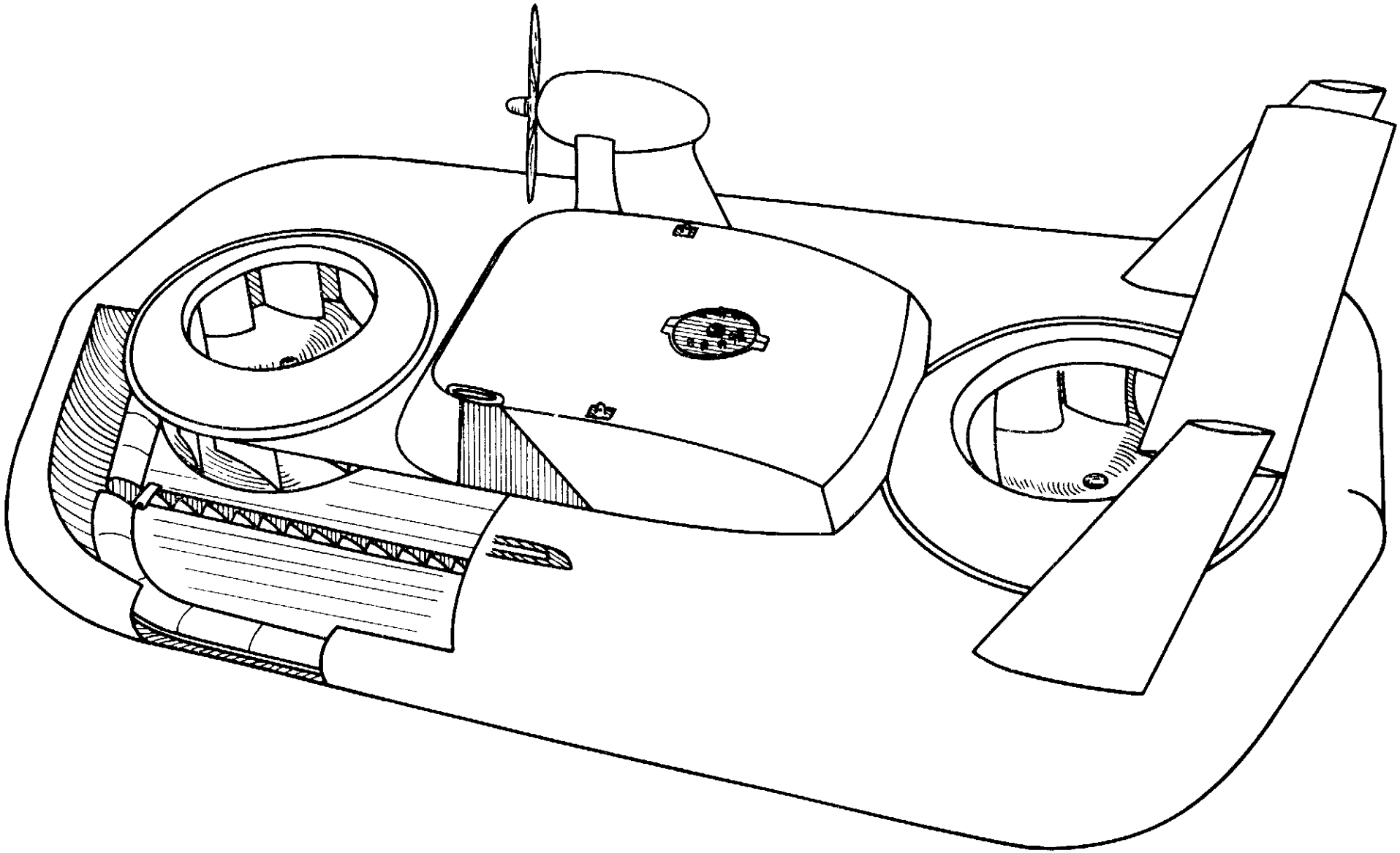

FIG. 2 SCHEMATIC VIEW OF MODEL

NOTE:- PORT NACELLE AND PROPELLER NOT SHOWN

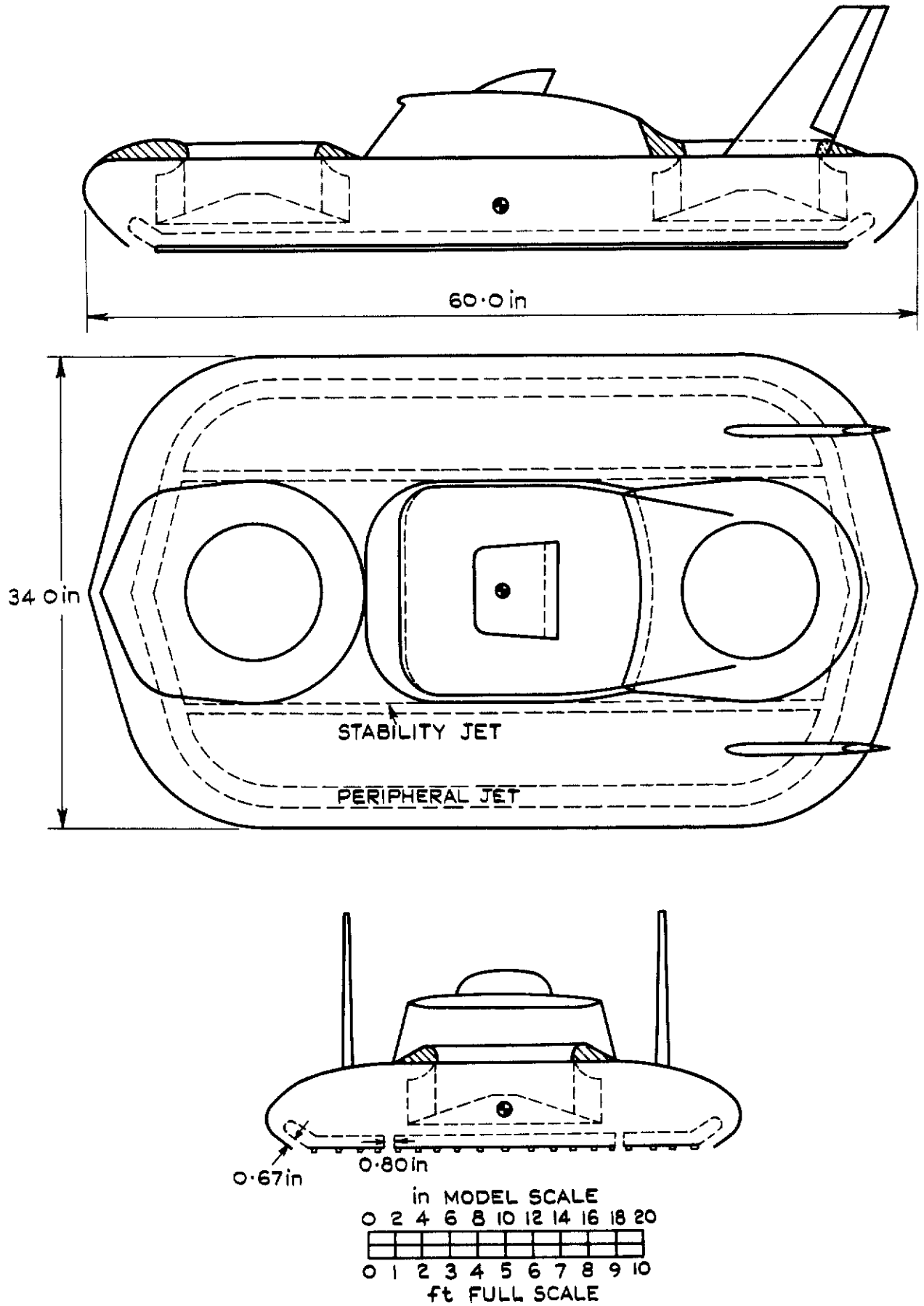

FIG. 3 G A OF MODEL WITH HEBA FANS AND MODIFIED INTAKES

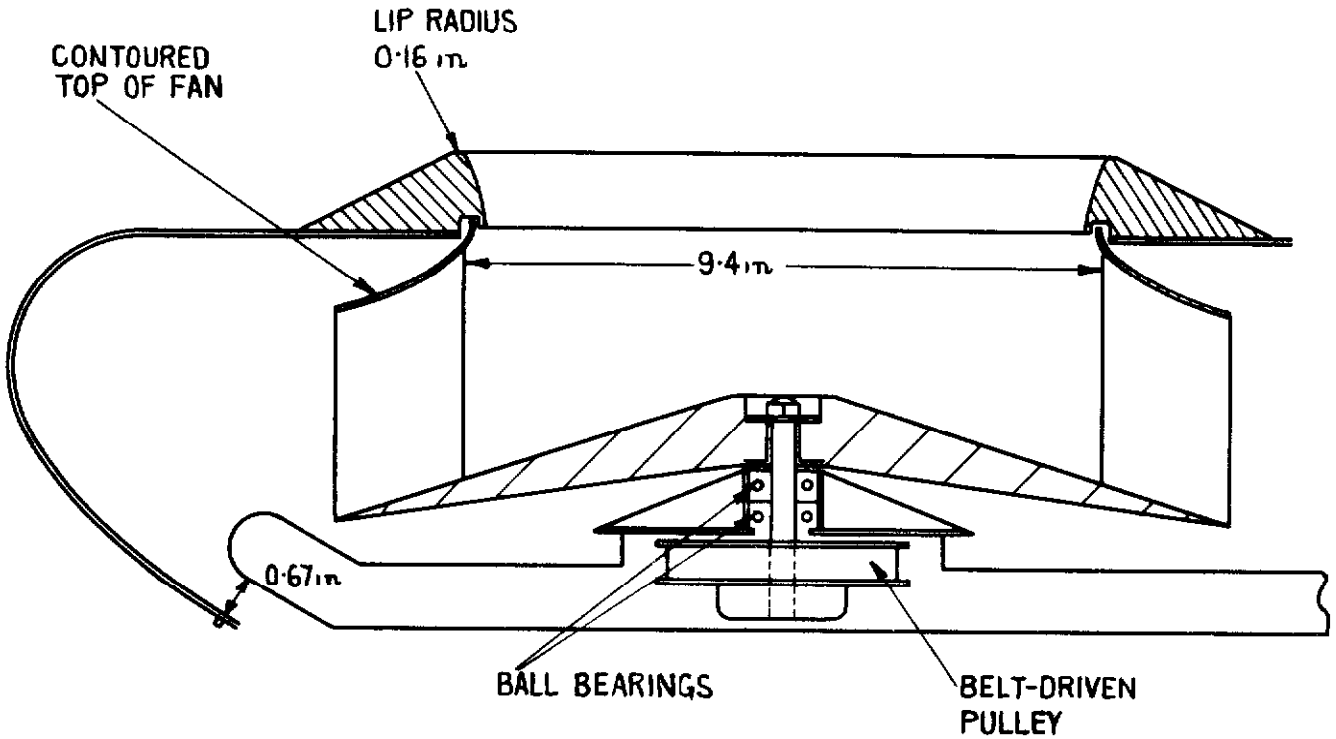

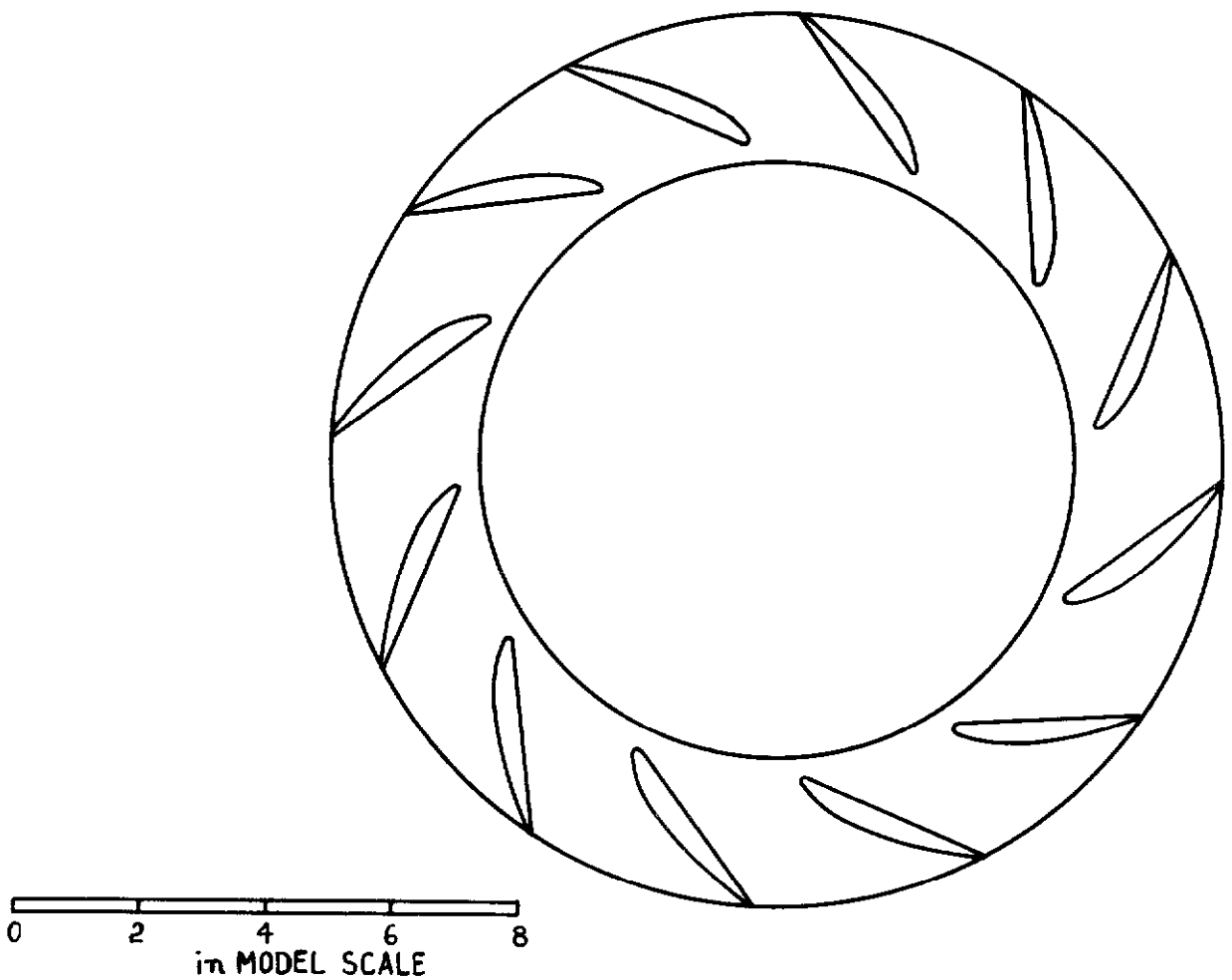

FIG.4 a DETAILS OF HEBA FANS AND INTAKES

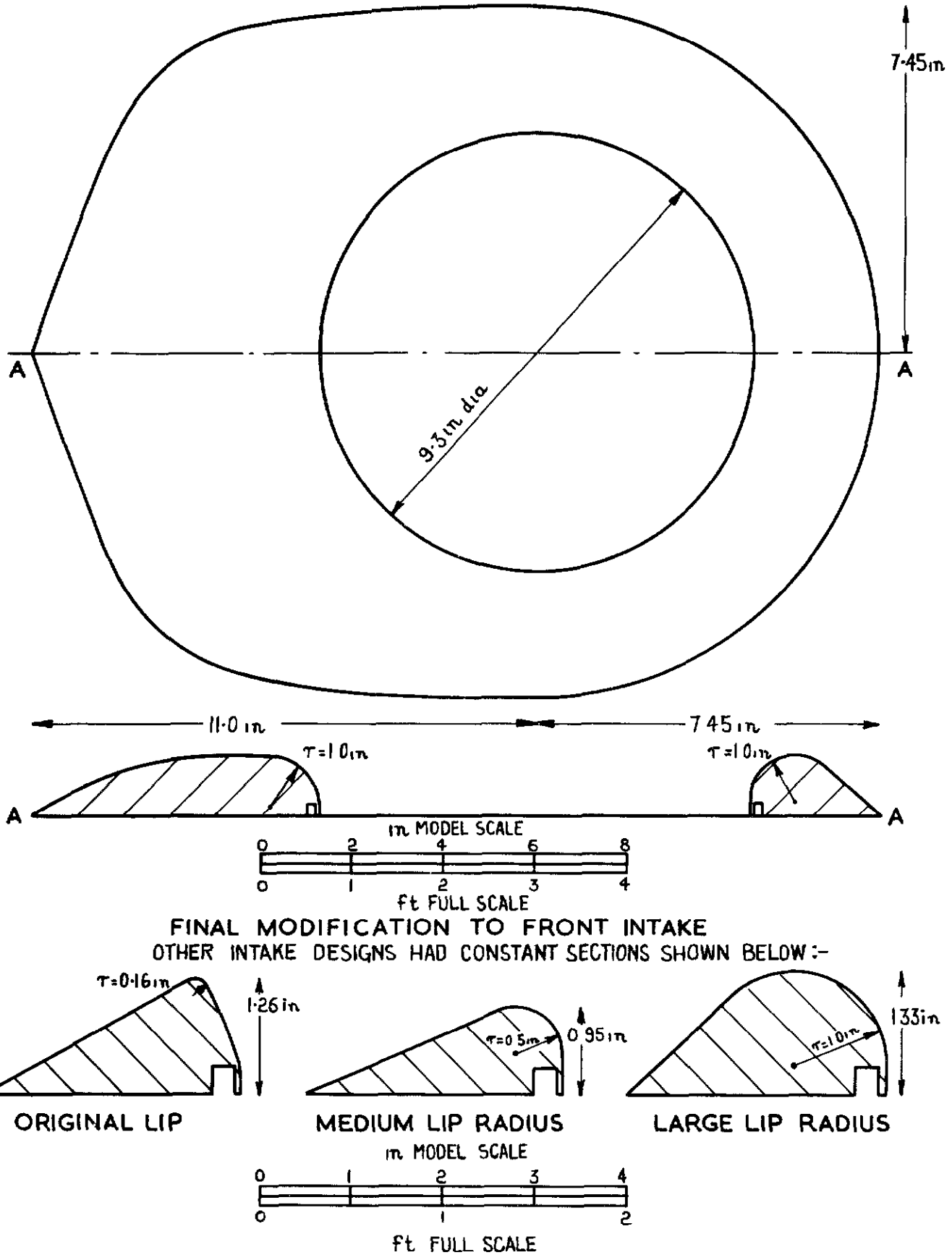

FIG 4 b DETAILS OF INTAKE LIP SHAPES FOR HEBA CONFIGURATION

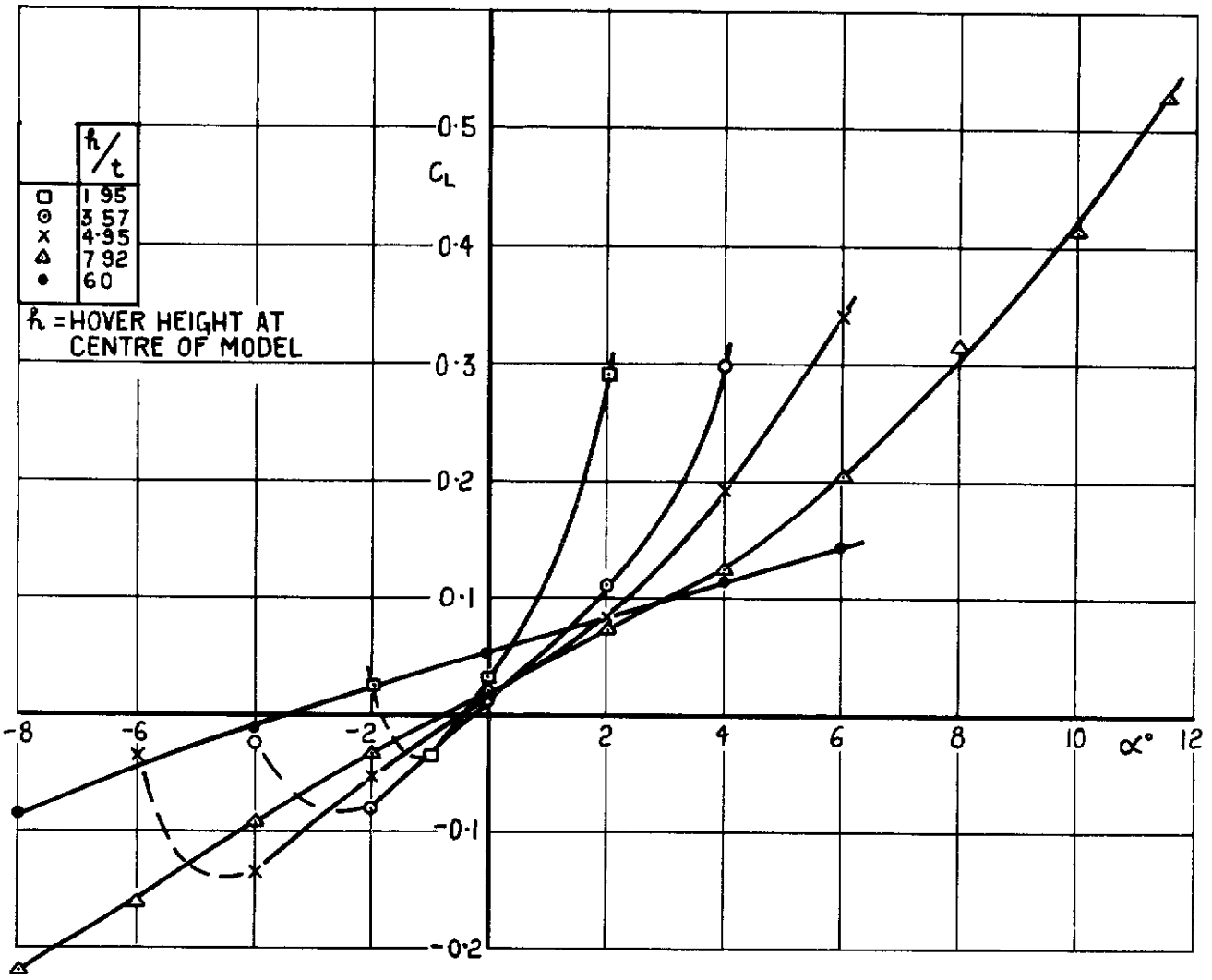

a LIFT AT ZERO SIDESLIP

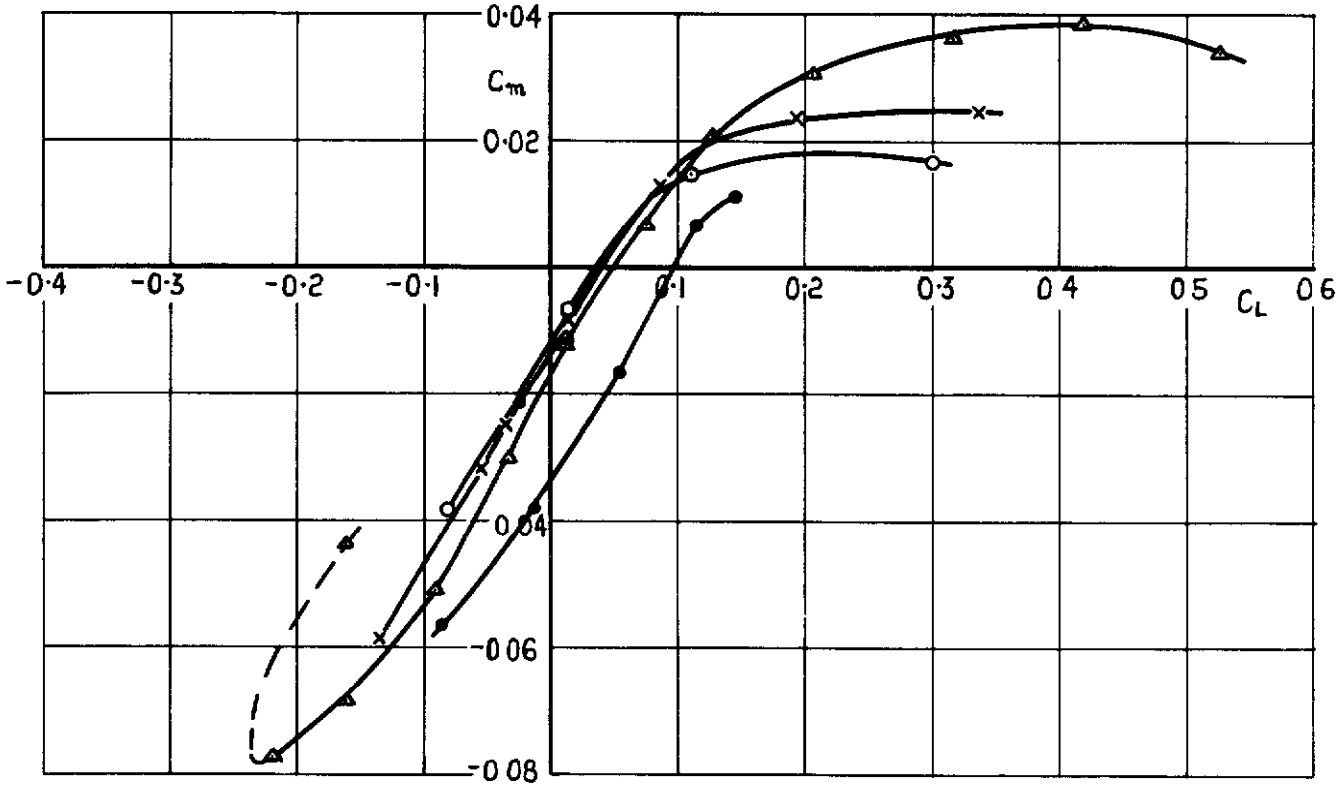

b PITCHING MOMENT AT ZERO SIDESLIP

FIG. 5 a & b AERODYNAMIC CHARACTERISTICS OF BASIC MODEL INTAKES AND EXITS SEALED; NO FINS

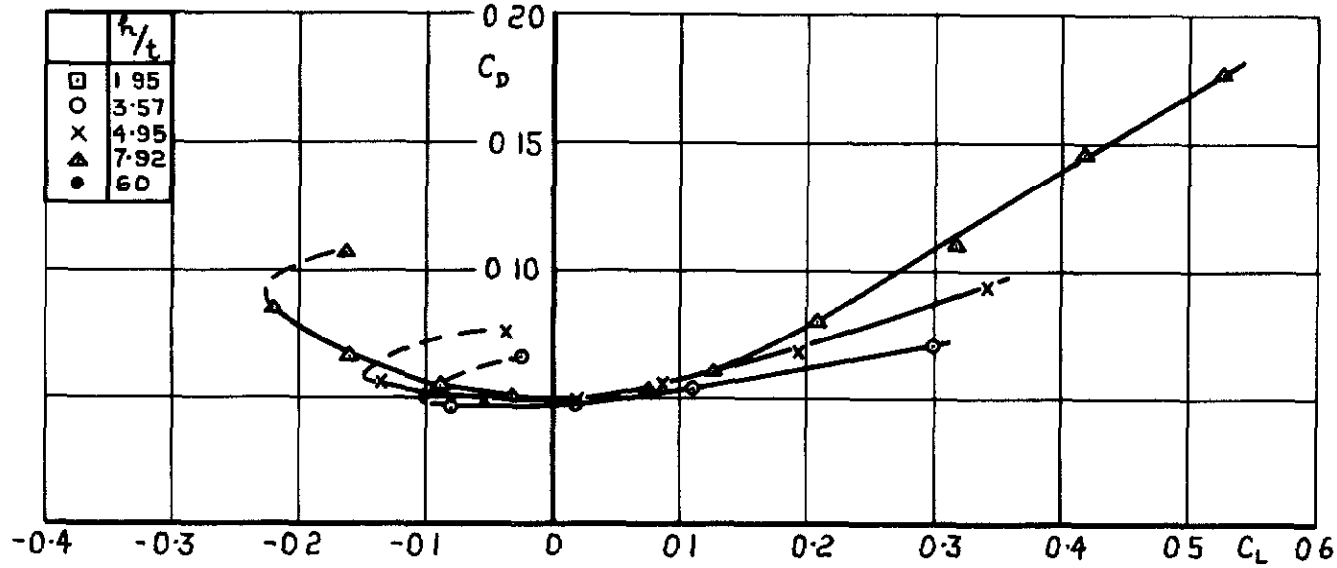

c DRAG AT ZERO SIDESLIP

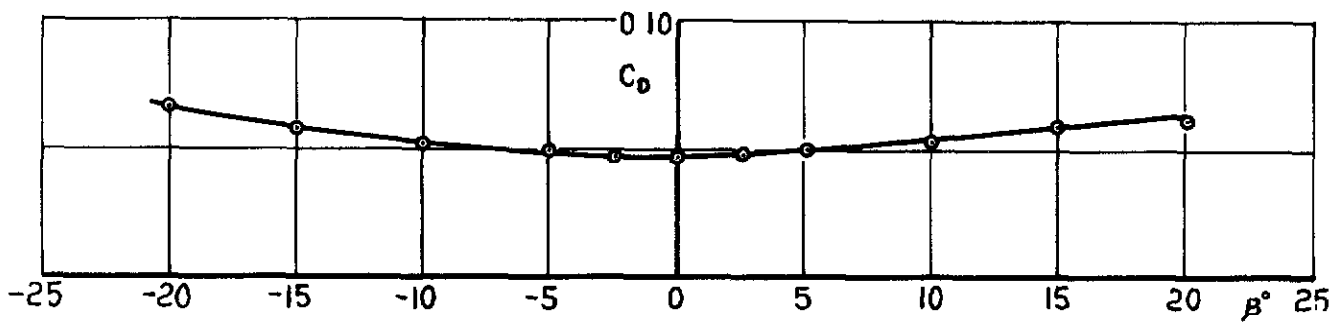

d DRAG AT ZERO INCIDENCE

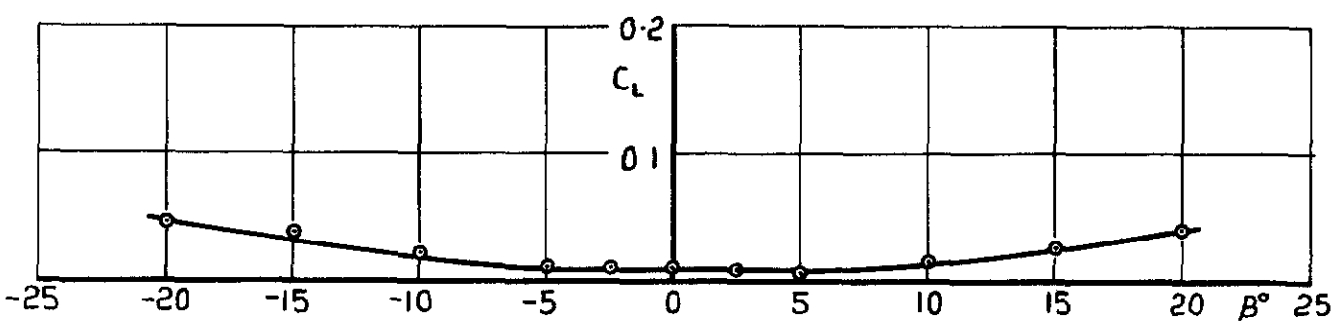

e LIFT AT ZERO INCIDENCE

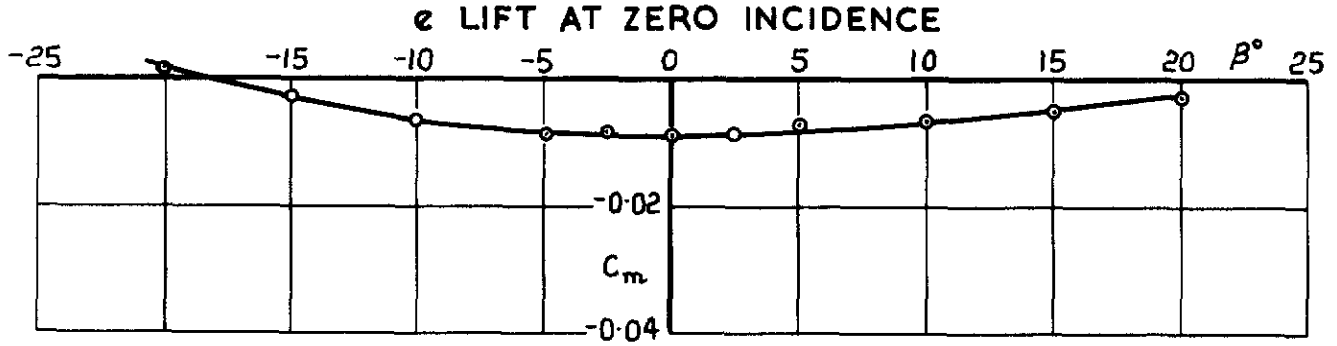

f PITCHING MOMENT AT ZERO INCIDENCE

FIG. 5 c - f AERODYNAMIC CHARACTERISTICS OF BASIC MODEL INTAKES AND EXITS SEALED; NO FINS

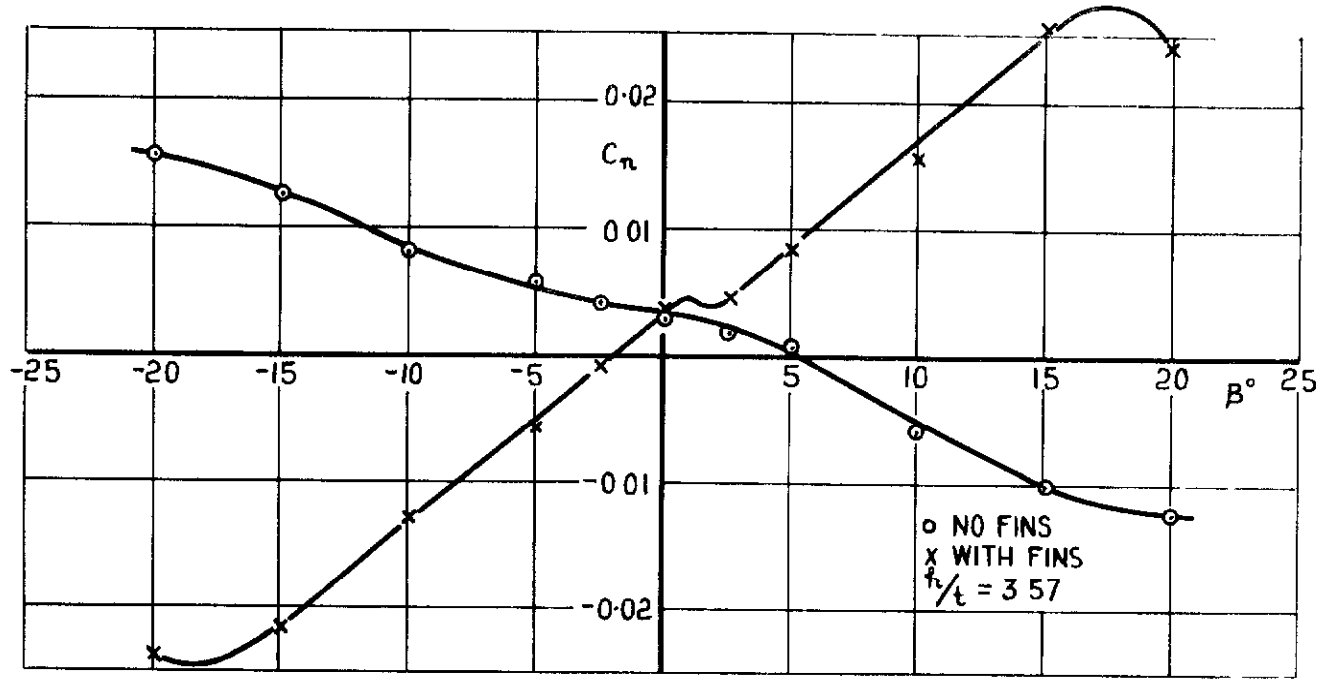

g YAWING MOMENT AT ZERO INCIDENCE

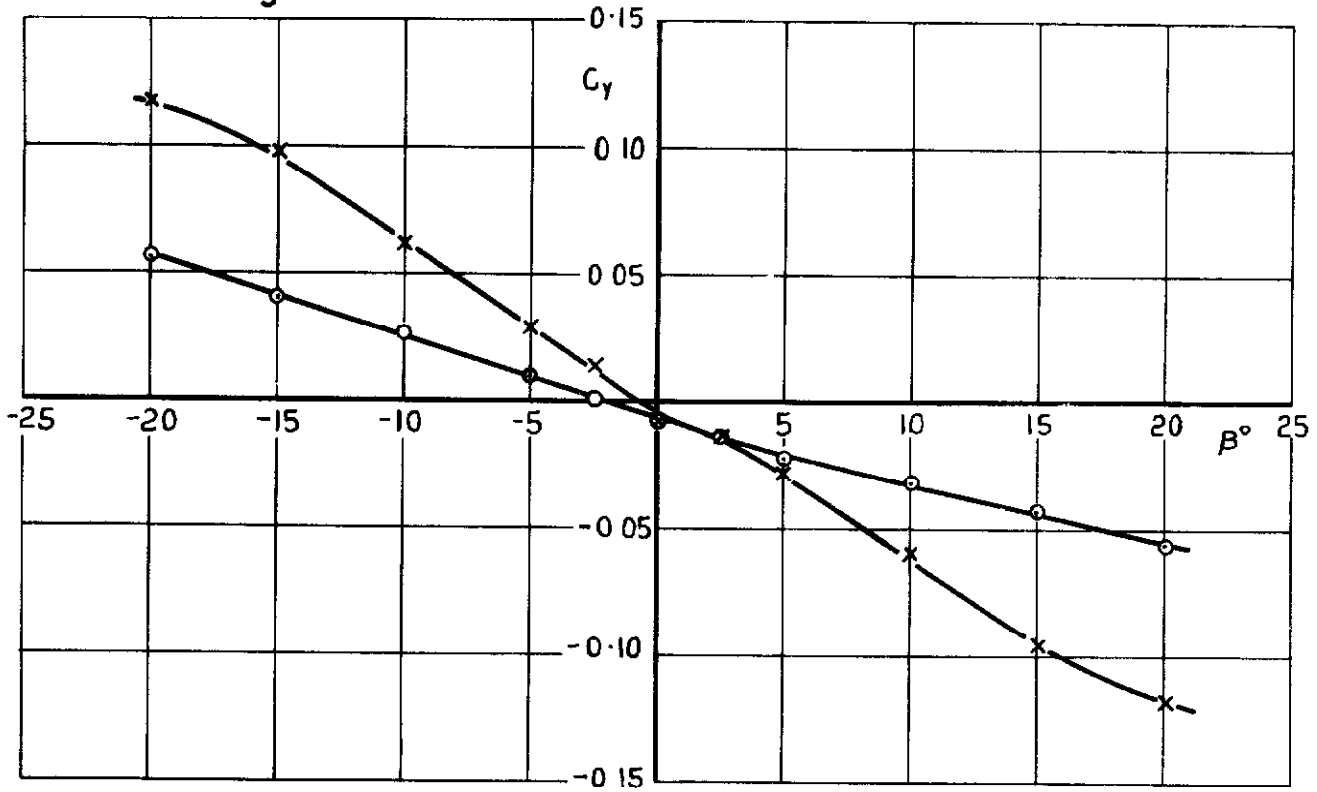

h SIDEFORCE AT ZERO INCIDENCE

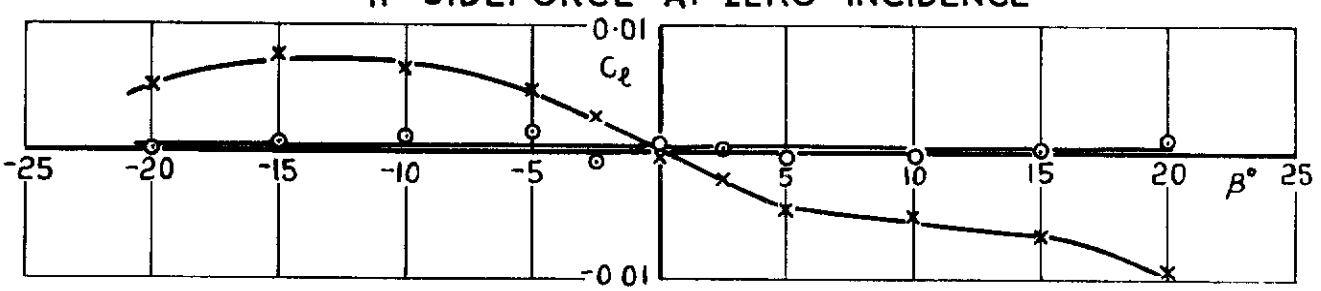

i ROLLING MOMENT AT ZERO INCIDENCE

FIG.5 g–i AERODYNAMIC CHARACTERISTICS OF BASIC MODEL INTAKES AND EXITS SEALED

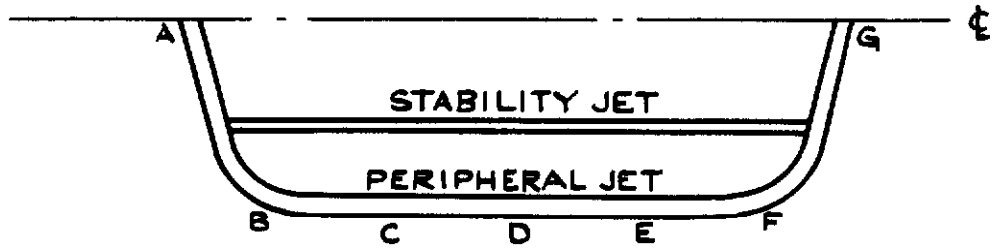

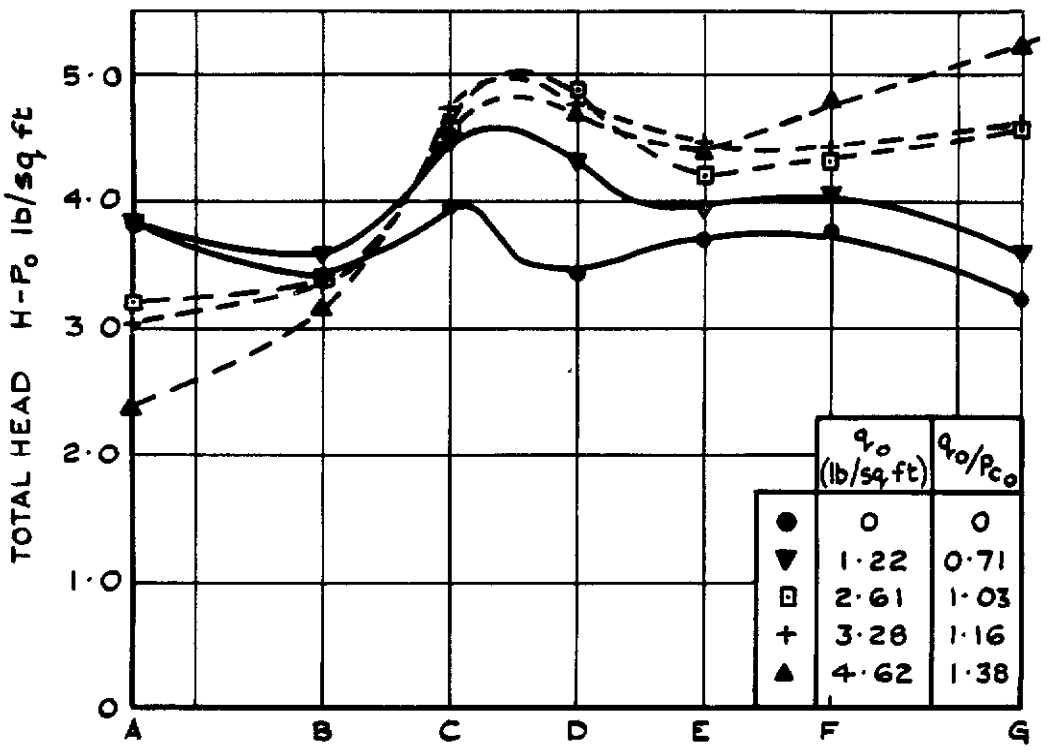

a TOTAL HEAD

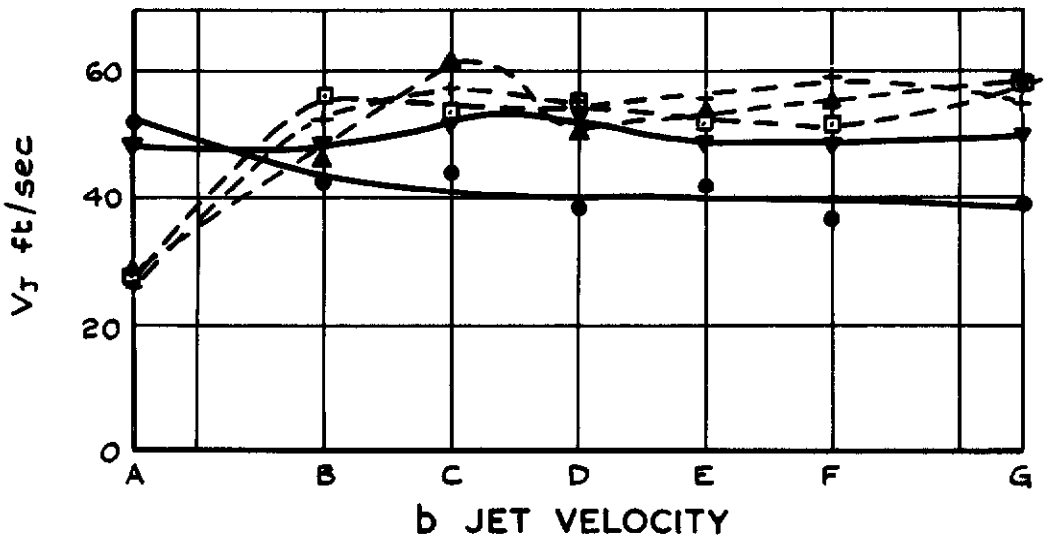

b JET VELOCITY

FIG. 6 a & b TOTAL HEAD AND VELOCITY OF PERIPHERAL JET AT NOZZLE
$^{h}/_{t} = 3{\cdot}57$; $\alpha = 0$; $P_{c_o} = 2{\cdot}45$ lb/sq ft

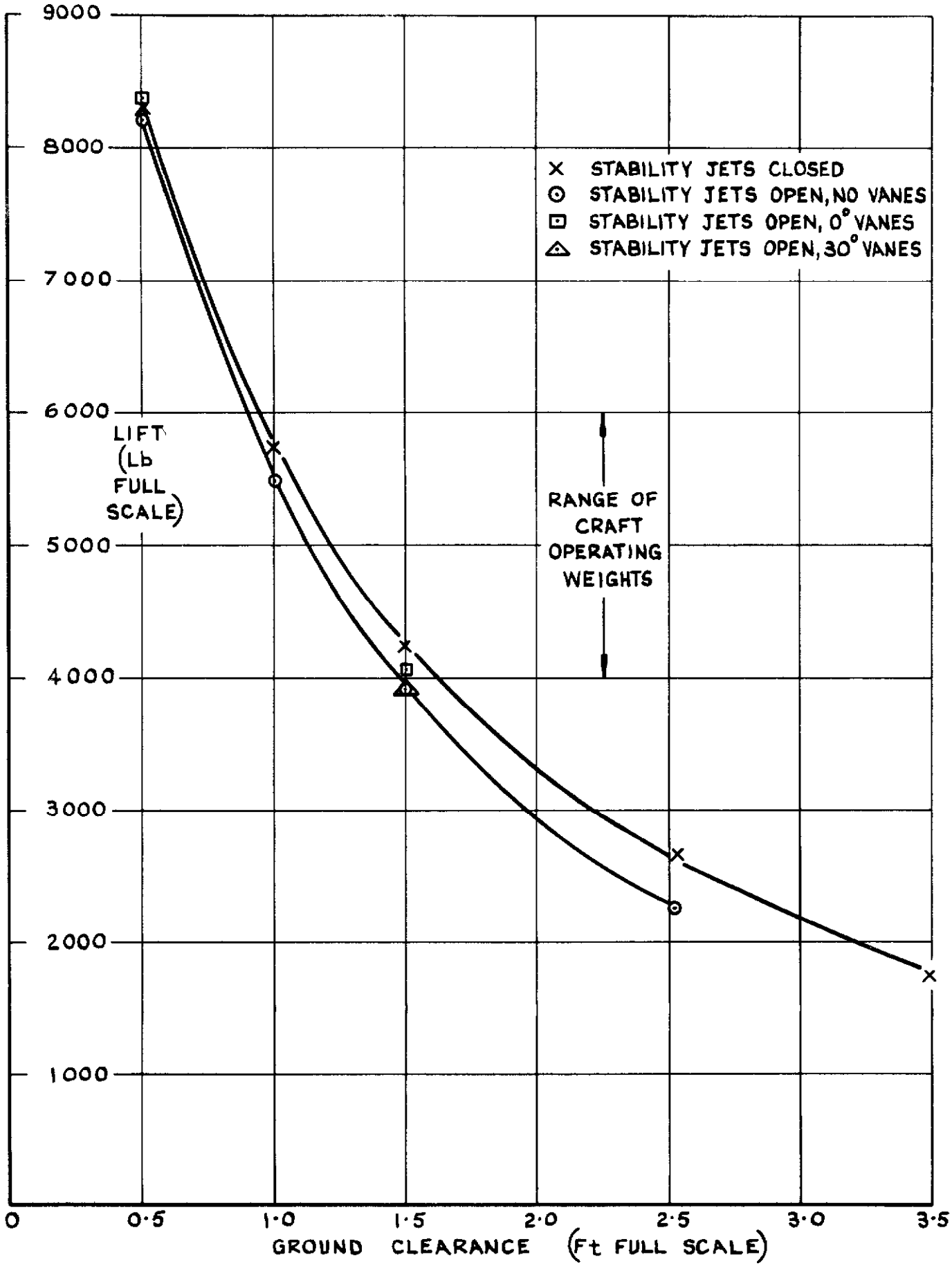

FIG. 7 EFFECT OF HOVER HEIGHT

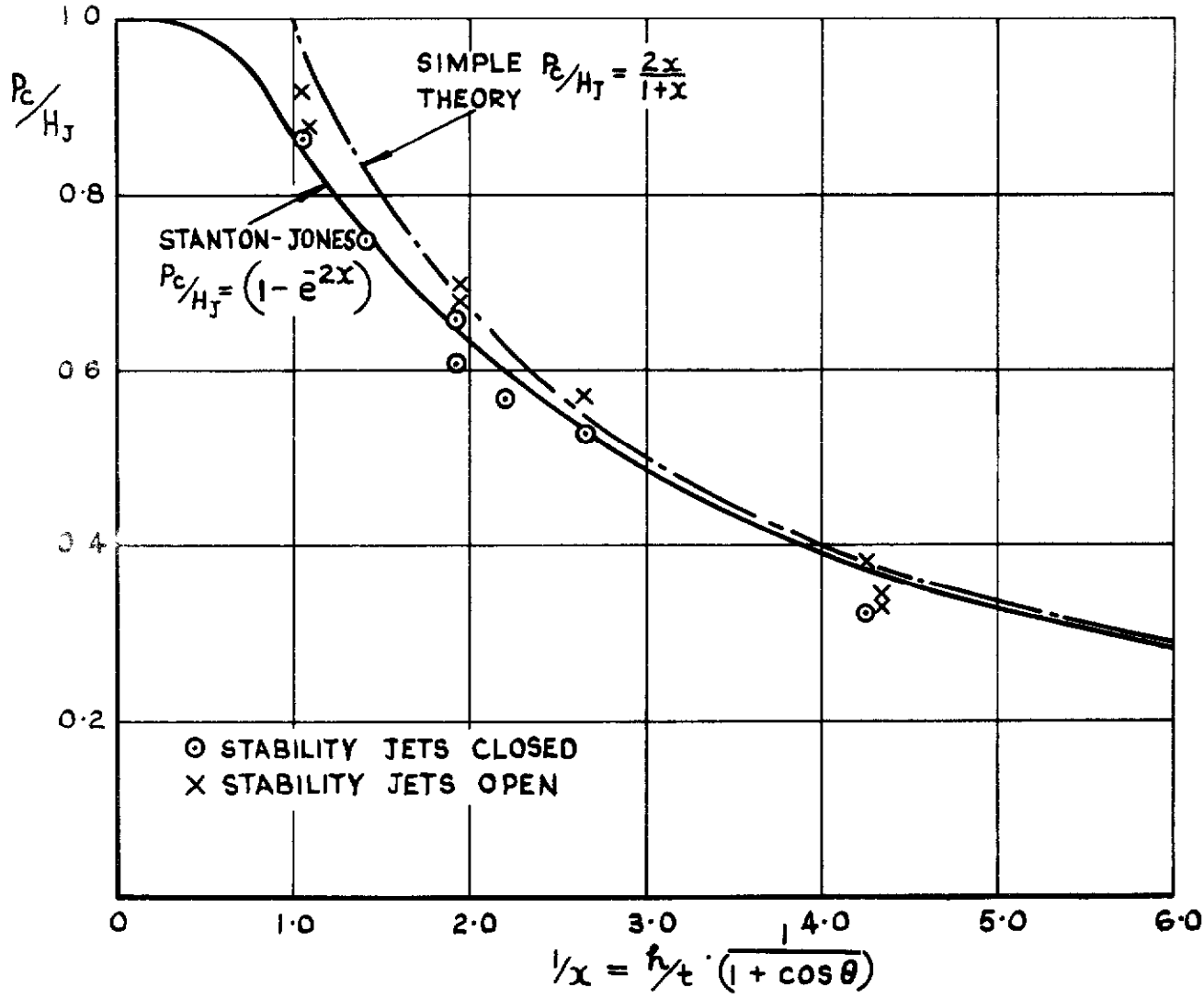

FIG. 8 EFFECT OF HOVER HEIGHT ON CUSHION PRESSURE

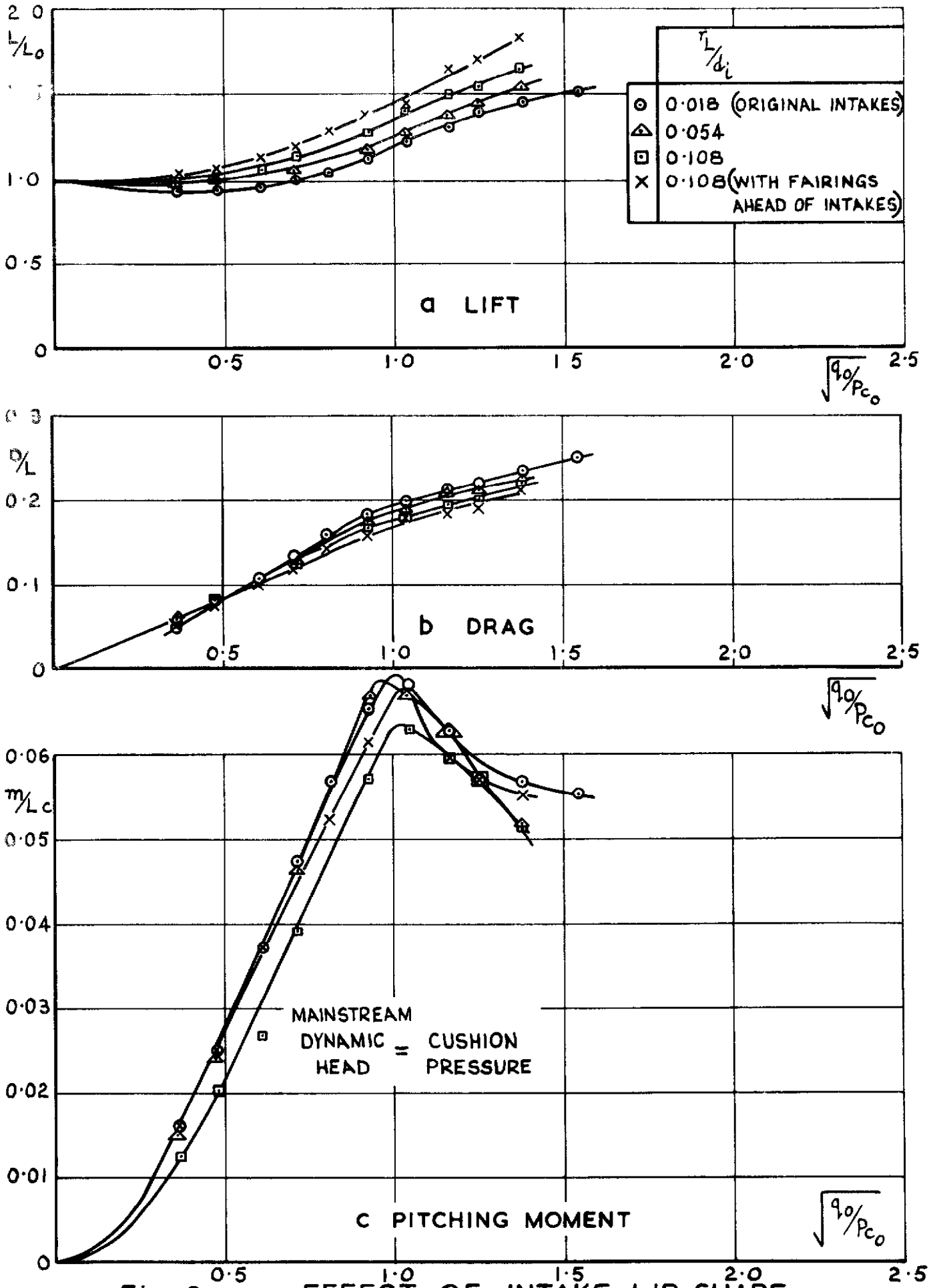

Fig. 9 a – c EFFECT OF INTAKE LIP SHAPE
h/t = 3·57; n = 1288 rpm
STABILITY JETS OPEN

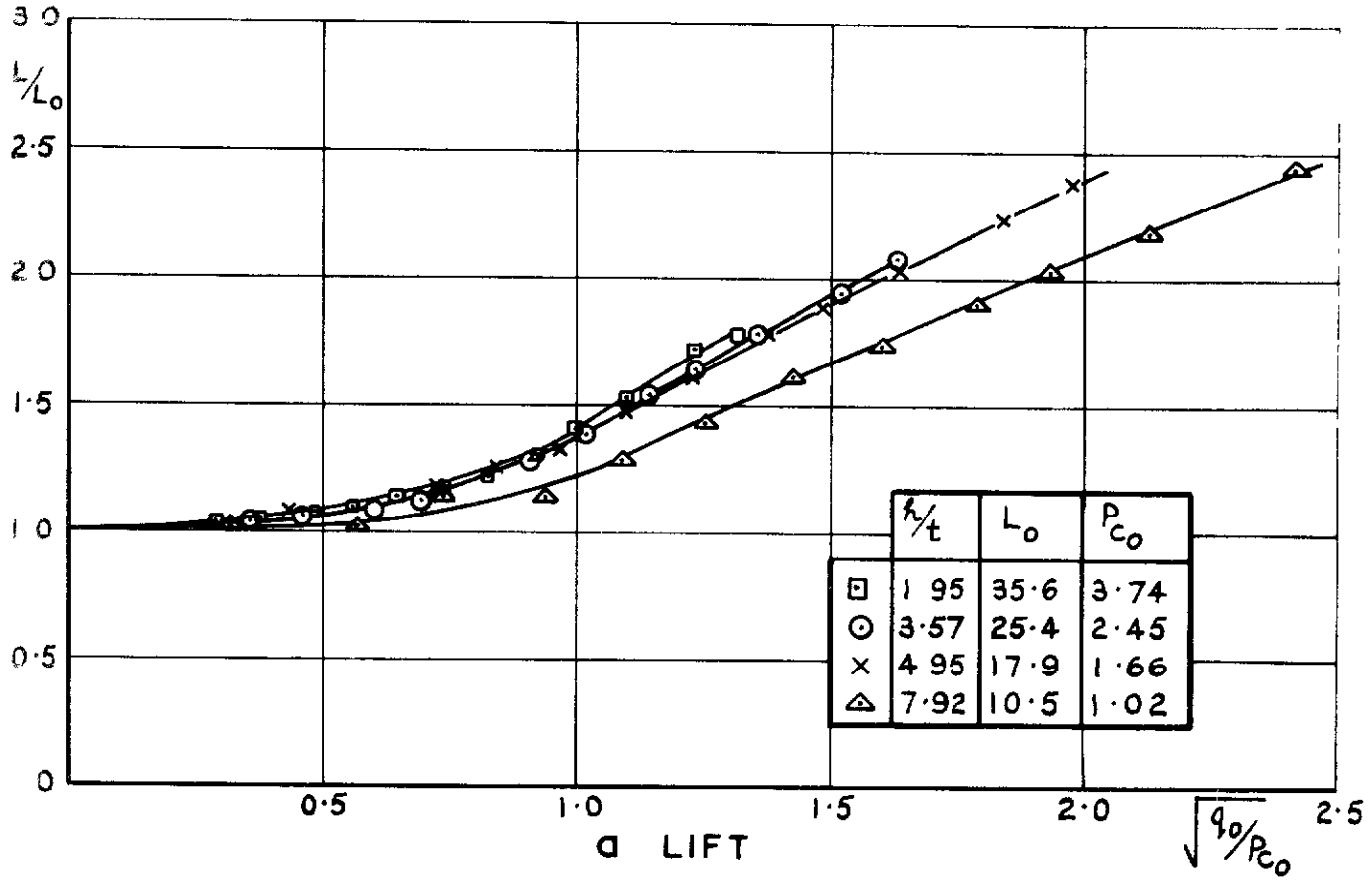

a LIFT

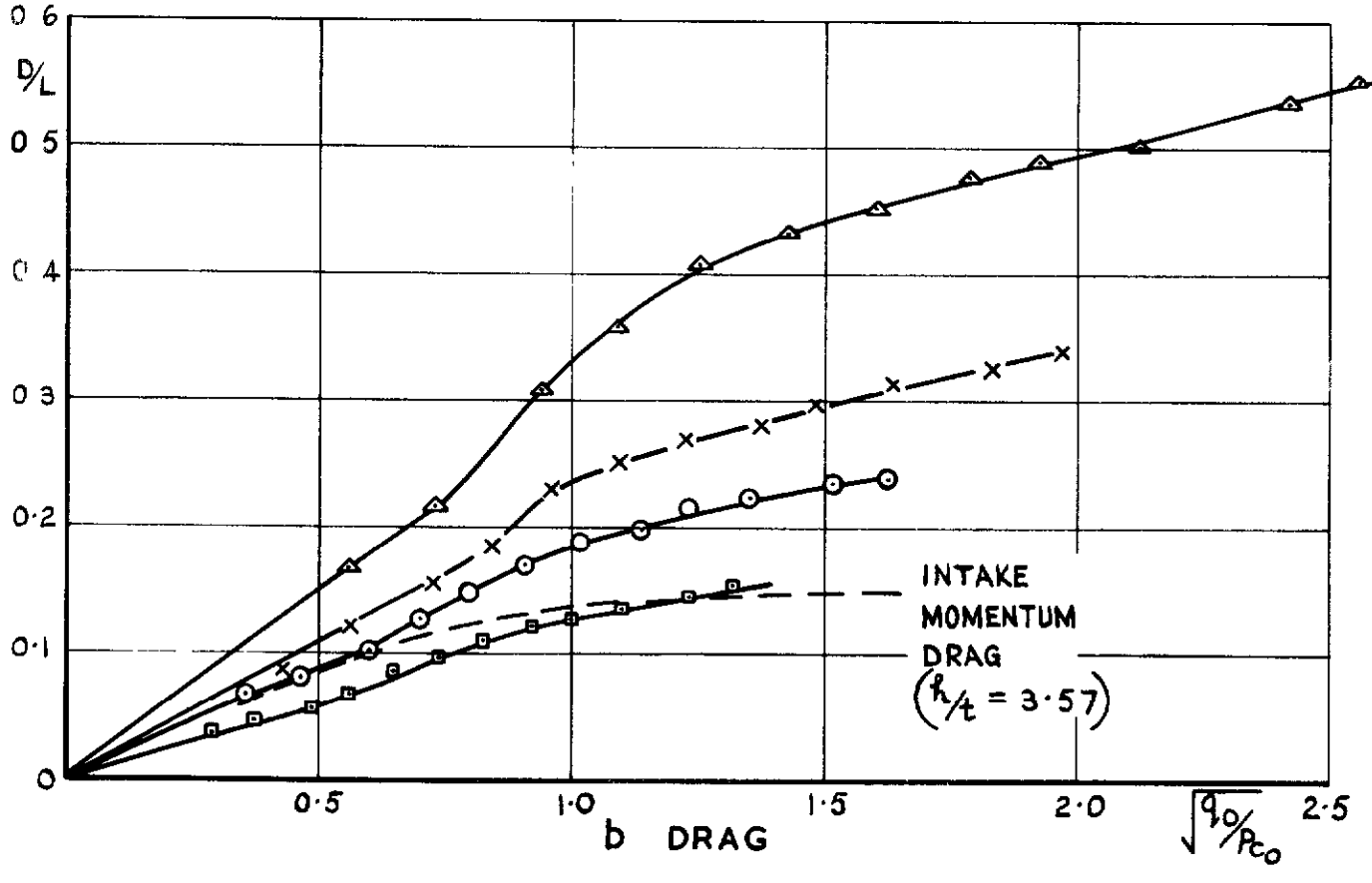

b DRAG

FIG. 10a & b EFFECT OF HEIGHT AND MAINSTREAM SPEED AT ZERO INCIDENCE

STABILITY JETS OPEN

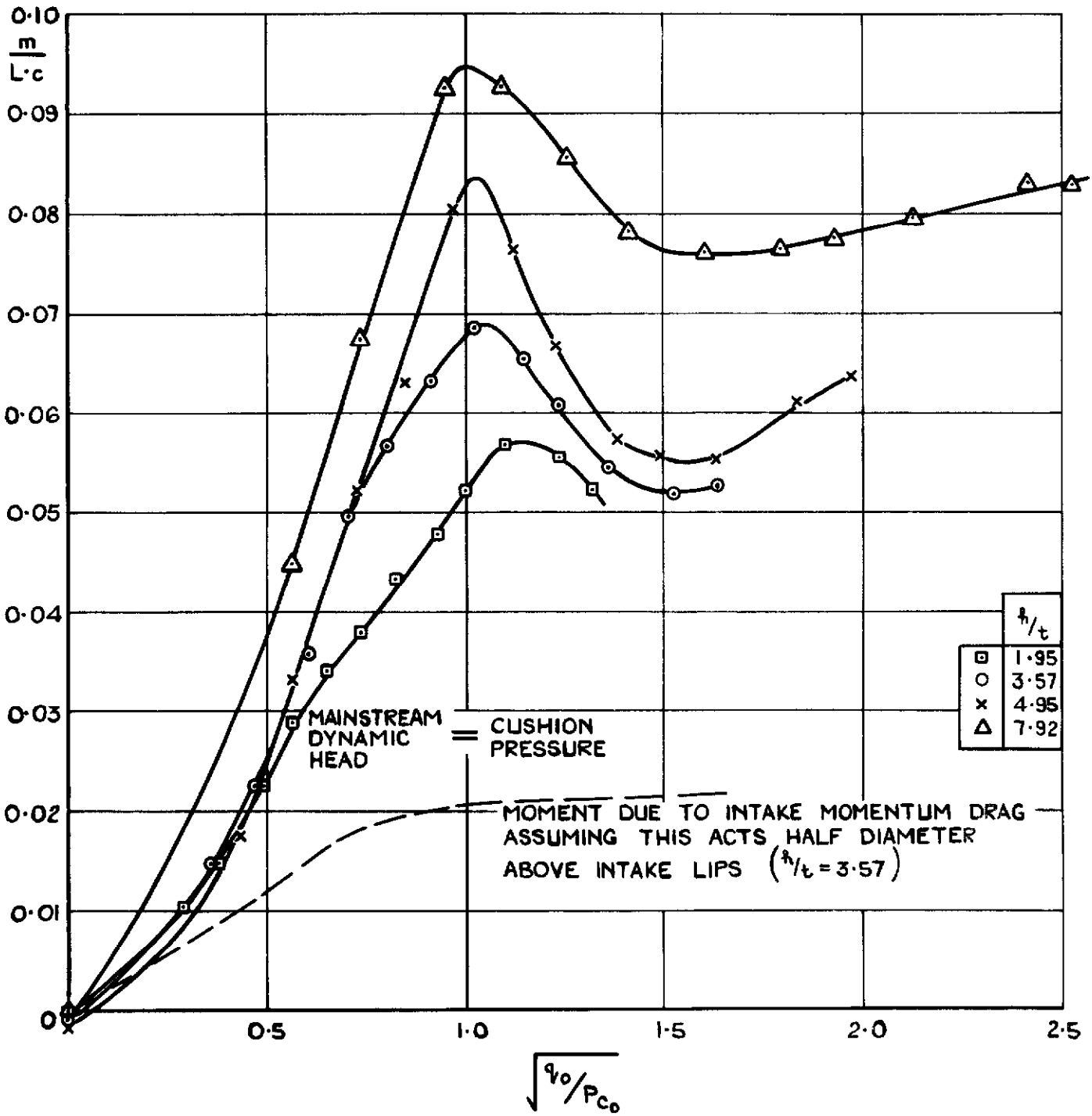

C PITCHING MOMENT

FIG. 10c EFFECT OF HEIGHT AND MAINSTREAM SPEED AT ZERO INCIDENCE
STABILITY JETS OPEN

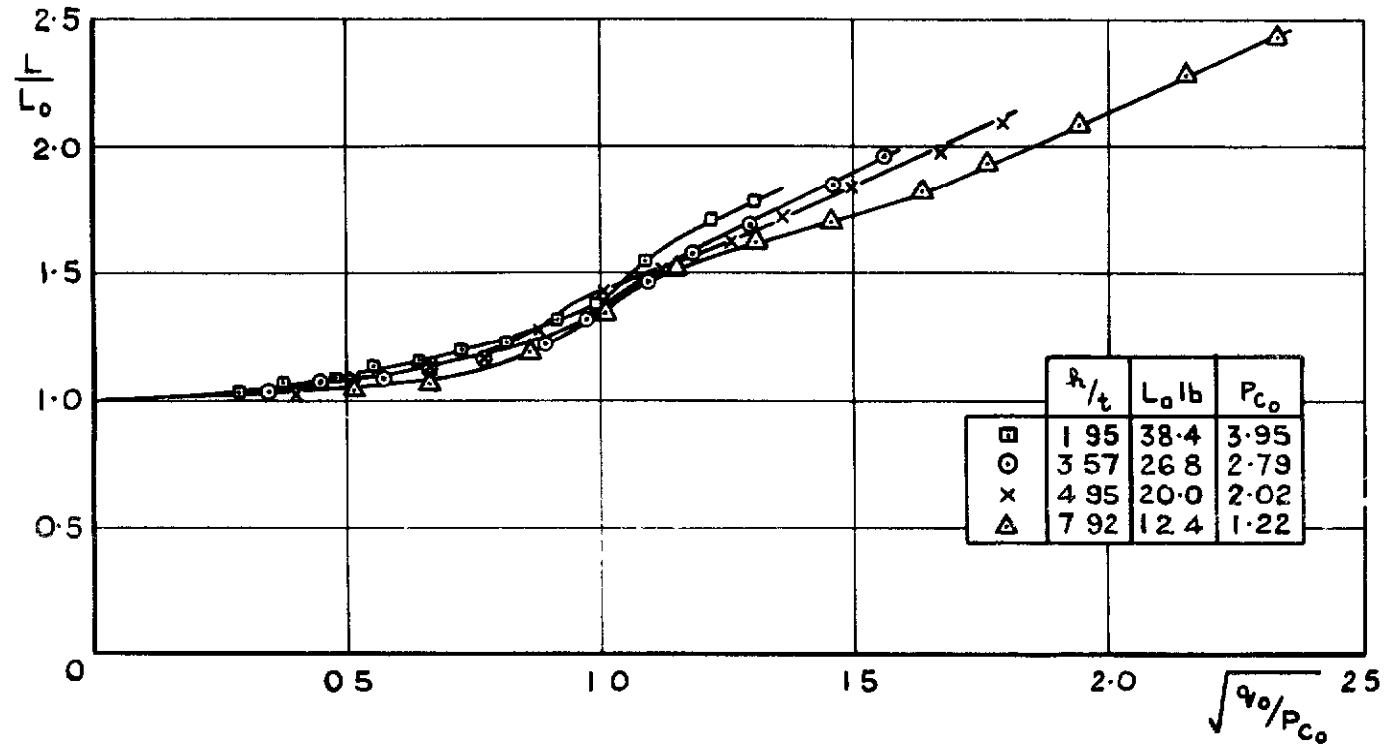

a LIFT

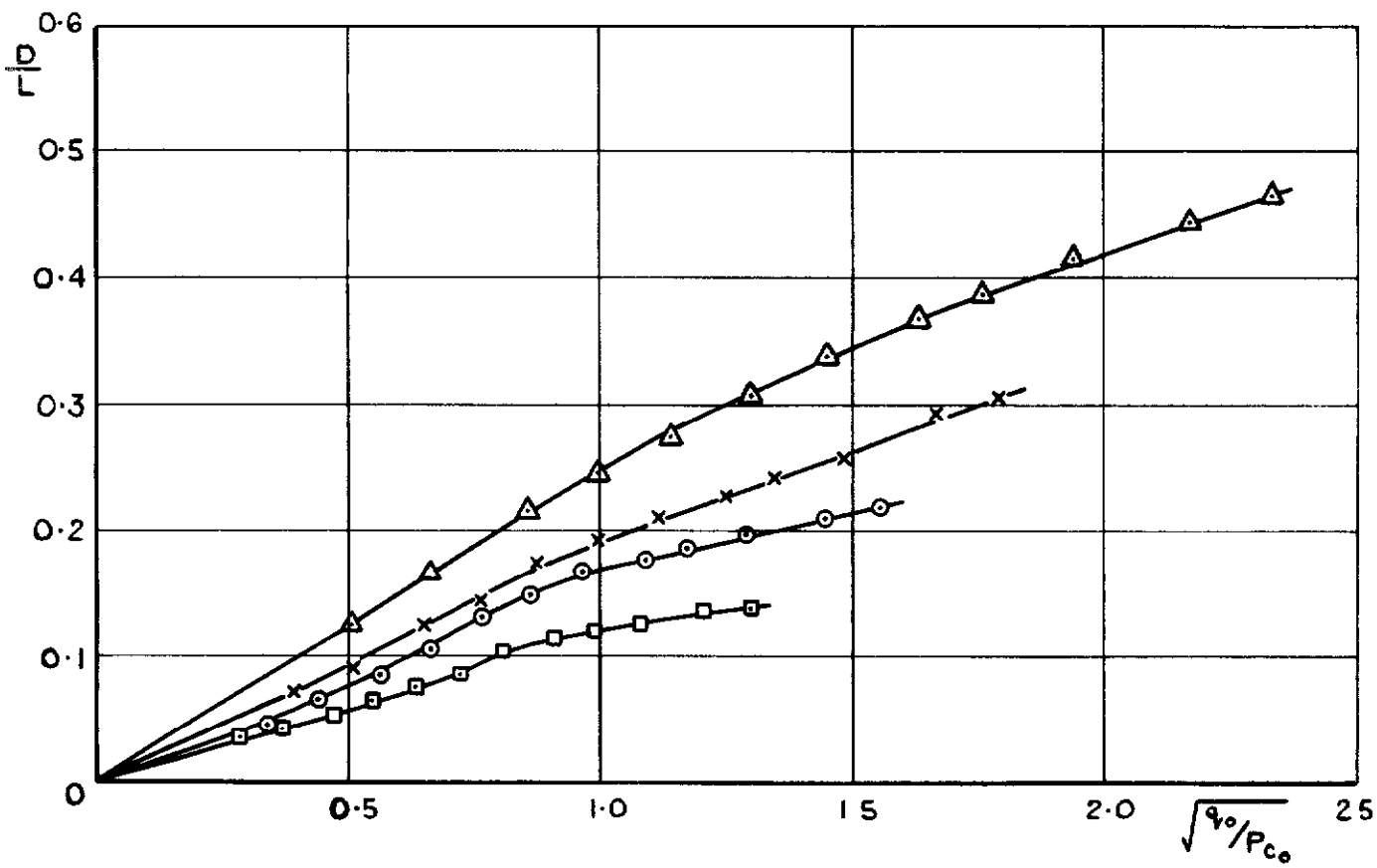

b DRAG

FIG. 11a&b EFFECT OF HEIGHT AND MAINSTREAM SPEED AT ZERO INCIDENCE
NO STABILITY JETS

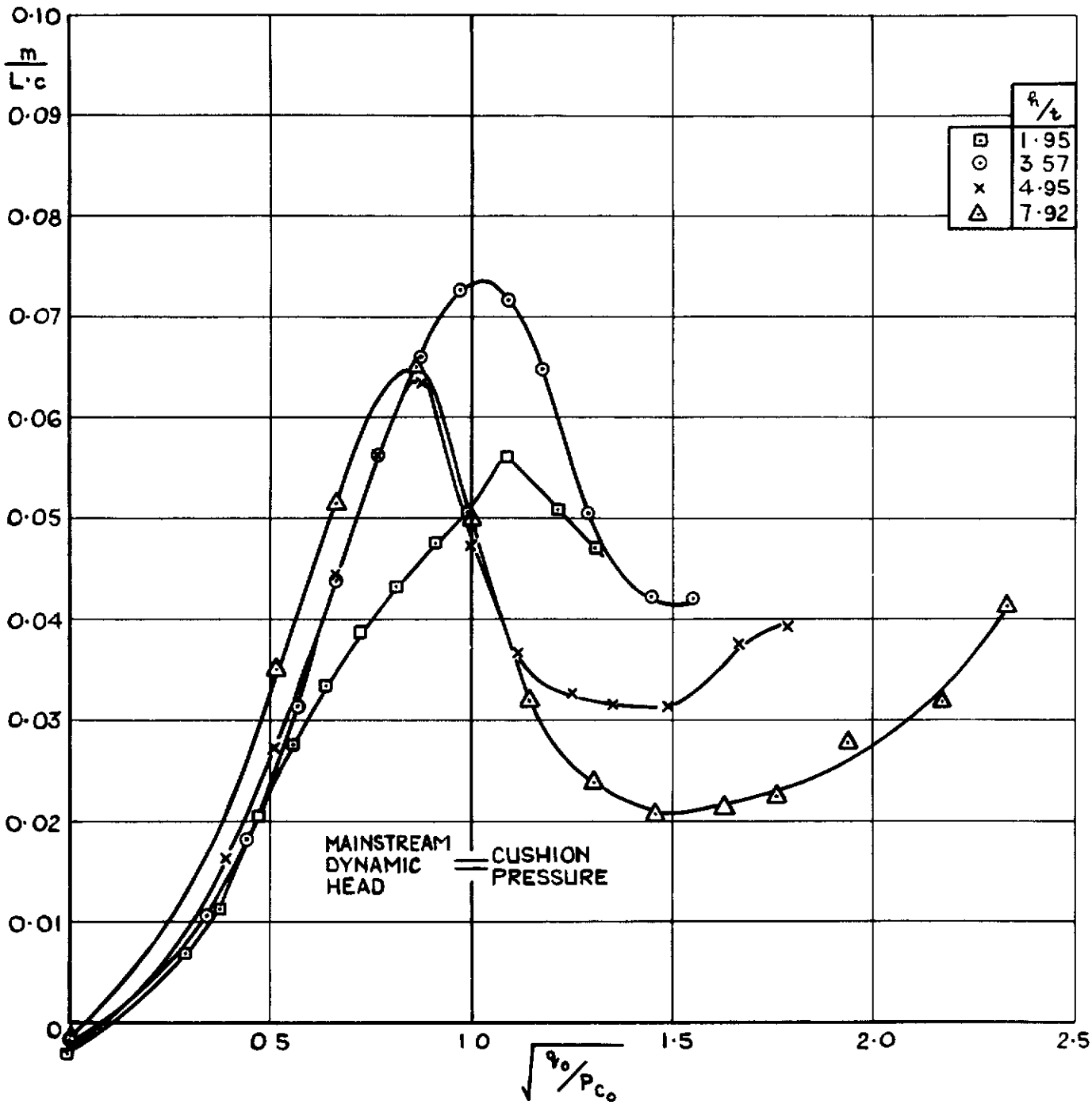

c PITCHING MOMENT

FIG. 11c EFFECT OF HEIGHT AND MAINSTREAM SPEED AT ZERO INCIDENCE
NO STABILITY JETS

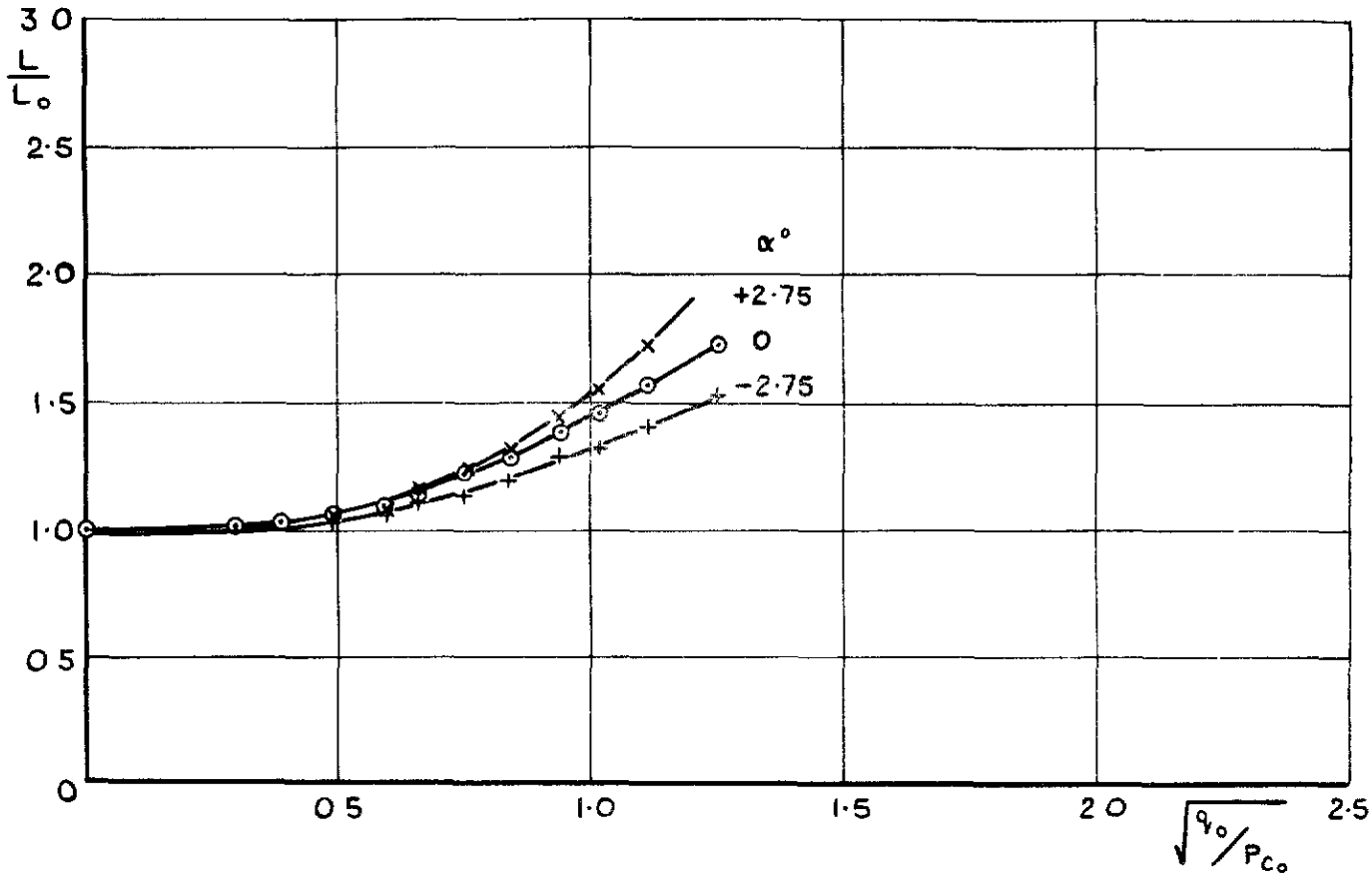

a LIFT ($L_o = 35{\cdot}6$ lb, $P_{C_o} = 3{\cdot}74$ lb/sq ft)

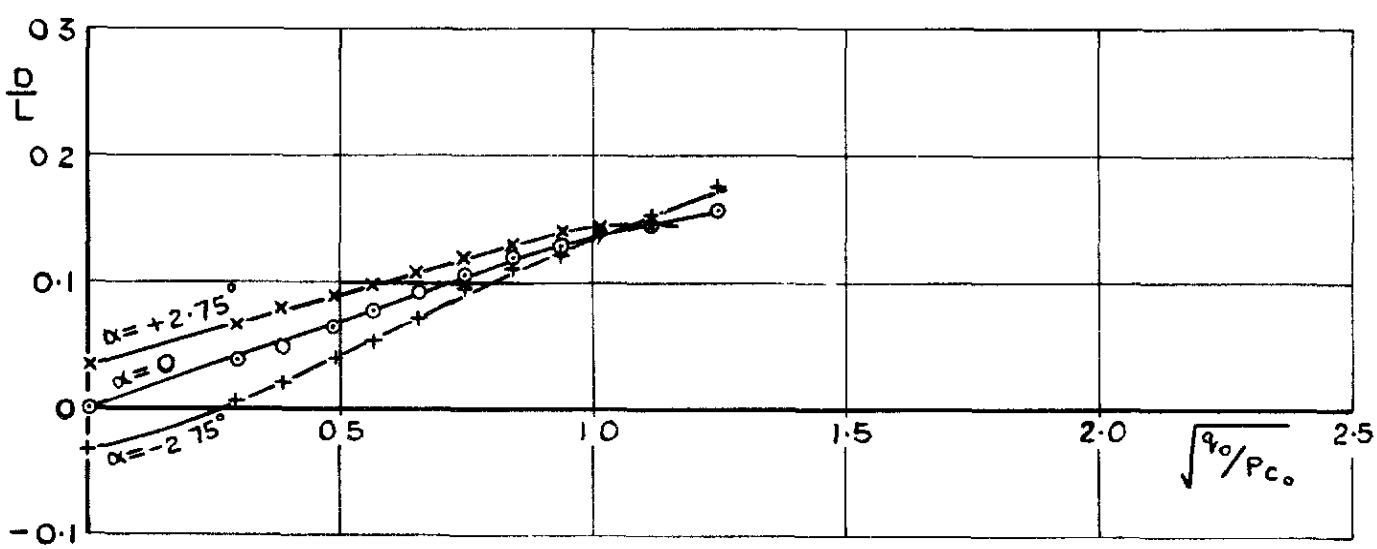

b DRAG

FIG. 12 a & b EFFECT OF INCIDENCE AT $h/t = 2{\cdot}25$
STABILITY JETS OPEN

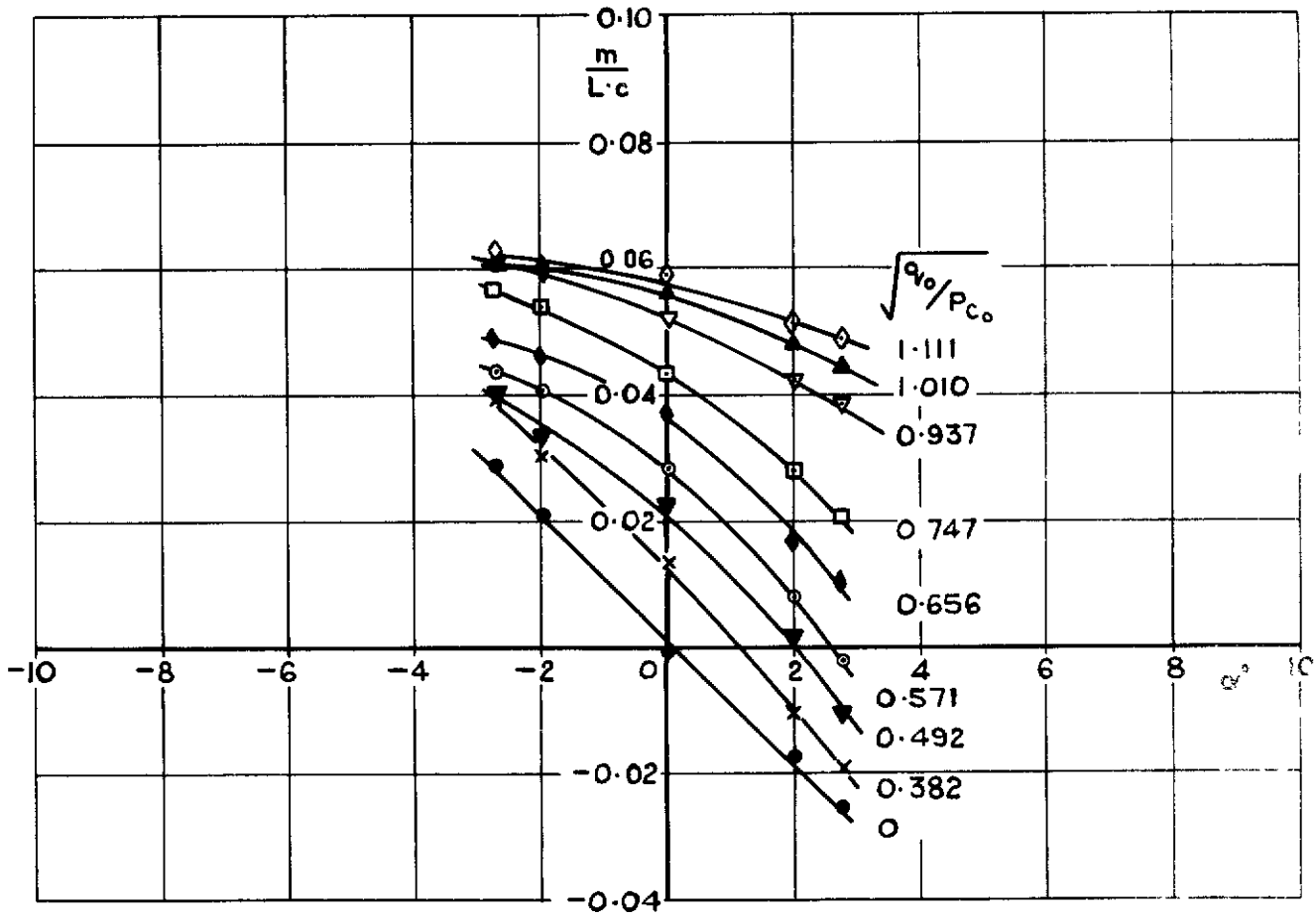

c PITCHING MOMENT

FIG. 12c EFFECT OF INCIDENCE AT $h/t = 2{\cdot}25$
STABILITY JETS OPEN

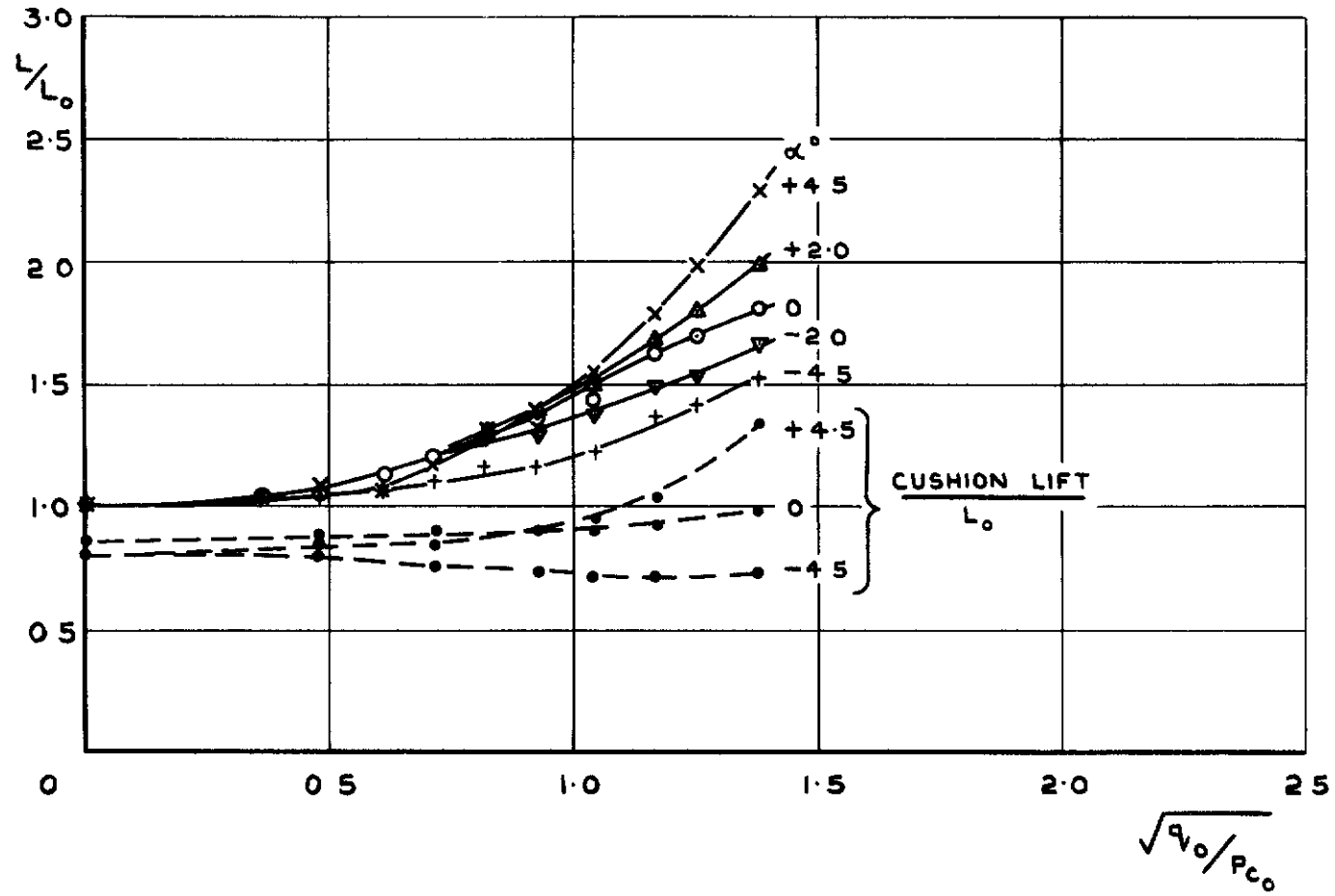

a LIFT ($L_0 = 25{\cdot}4$ lb, $P_{c_0} = 2{\cdot}45$ lb / sq ft)

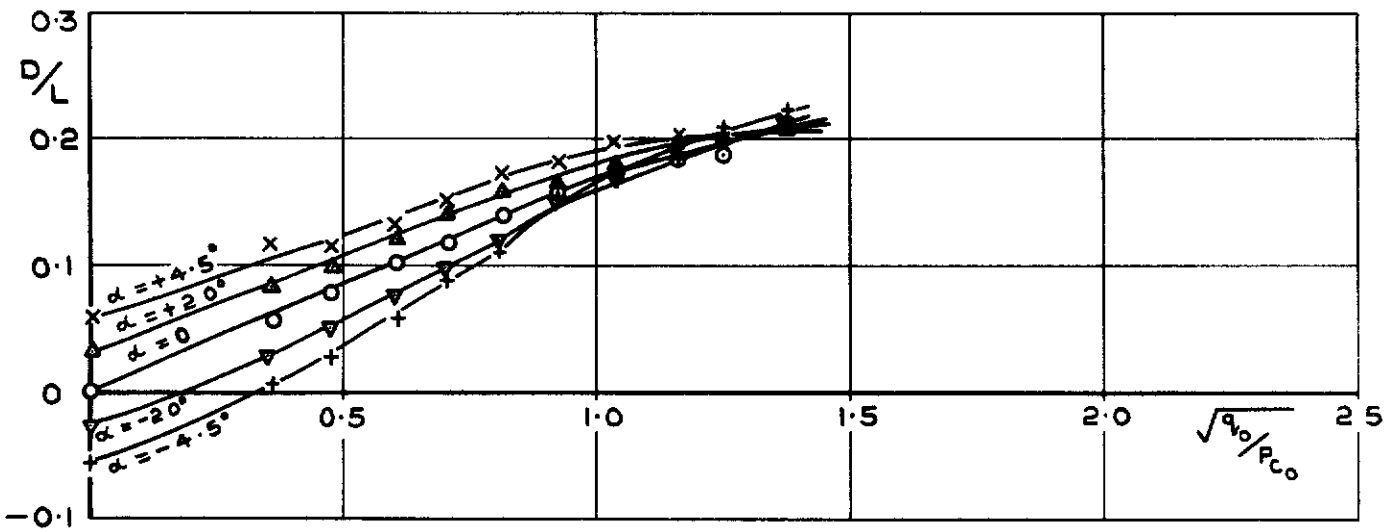

b DRAG

FIG.13 a & b EFFECT OF INCIDENCE AT $h/t = 3{\cdot}57$

STABILITY JETS OPEN

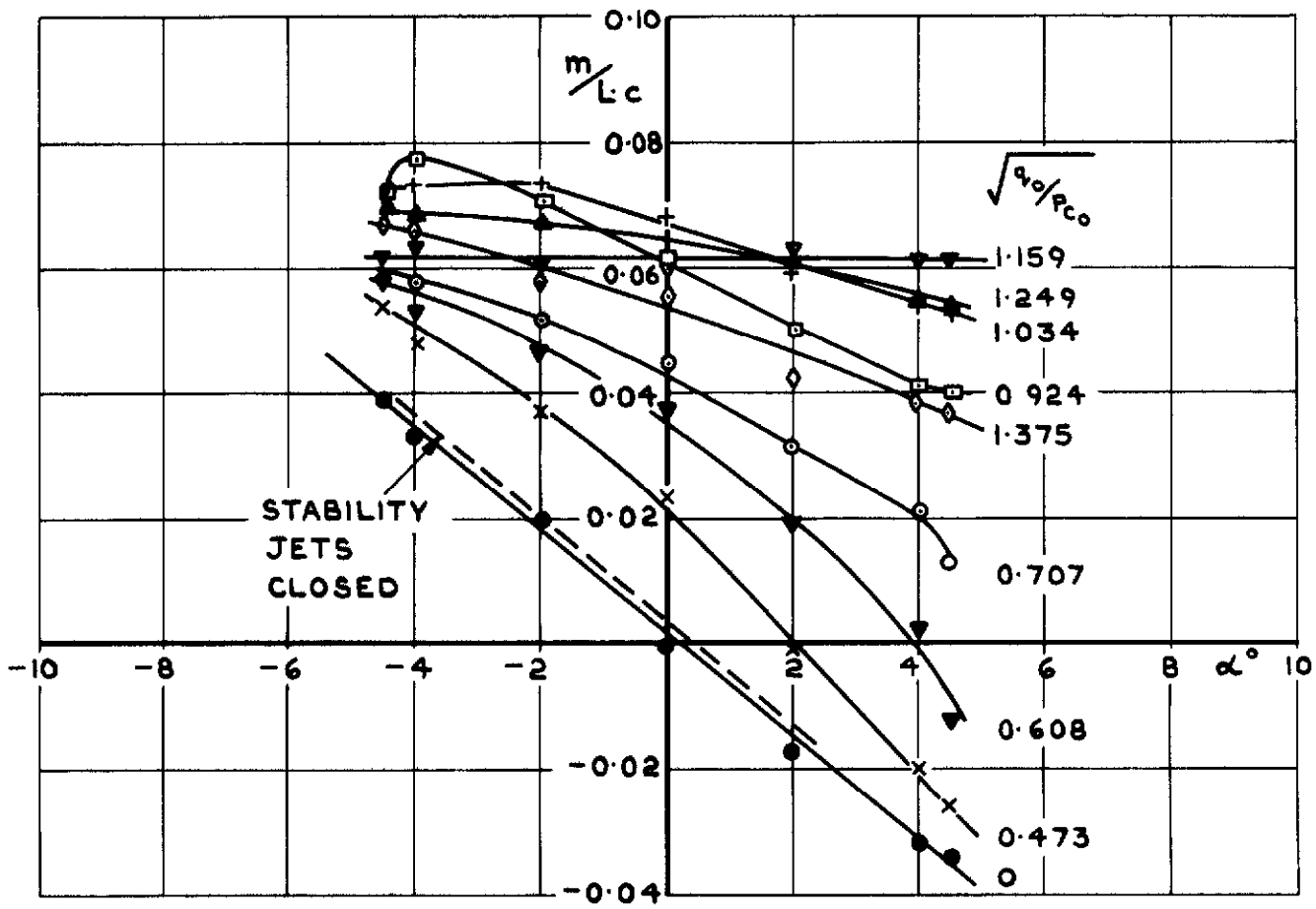

c PITCHING MOMENT

FIG.13c EFFECT OF INCIDENCE AT $h/t = 3{\cdot}57$

STABILITY JETS OPEN

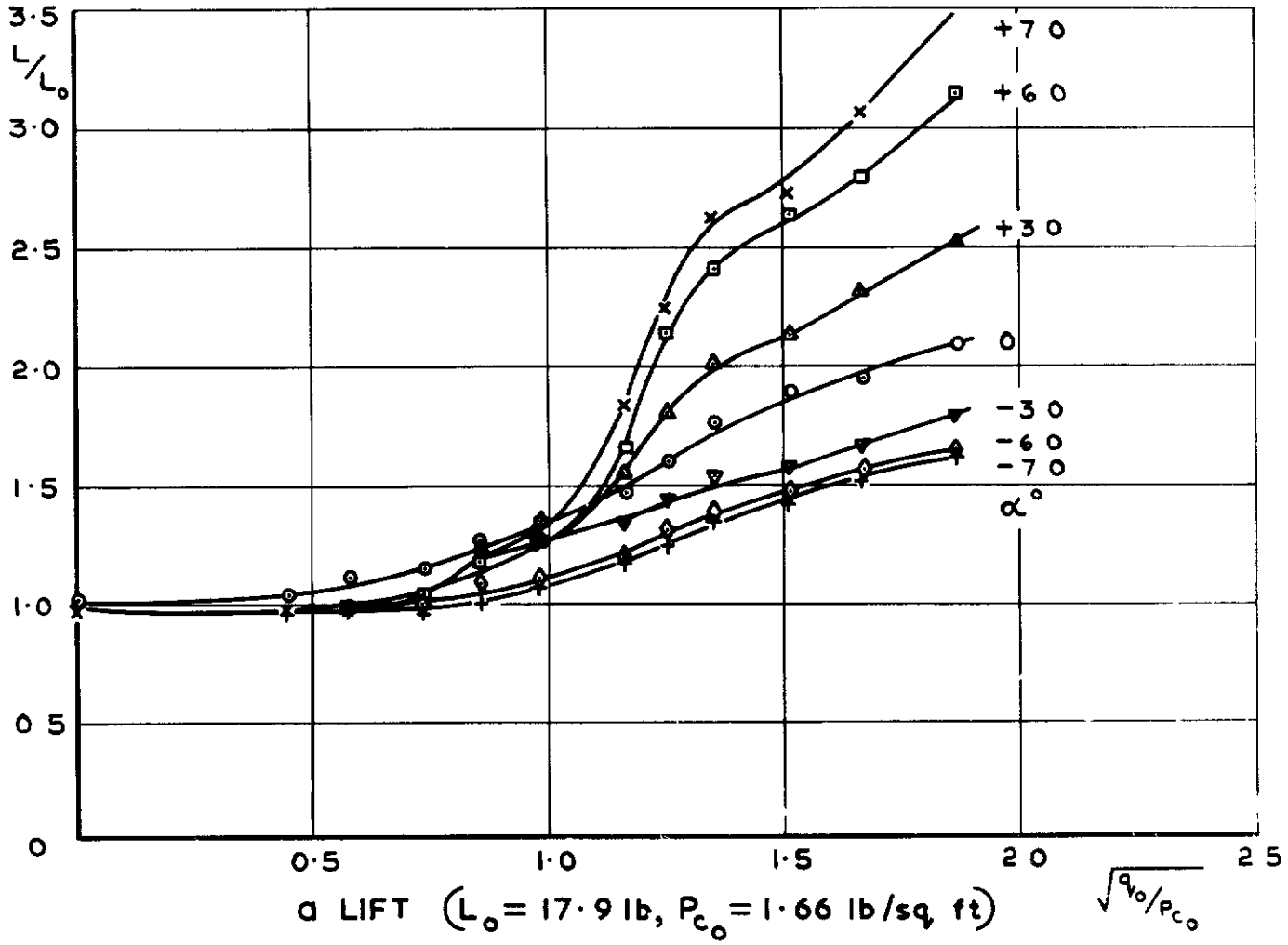

a LIFT (L_o = 17·9 lb, P_{c_o} = 1·66 lb/sq ft)

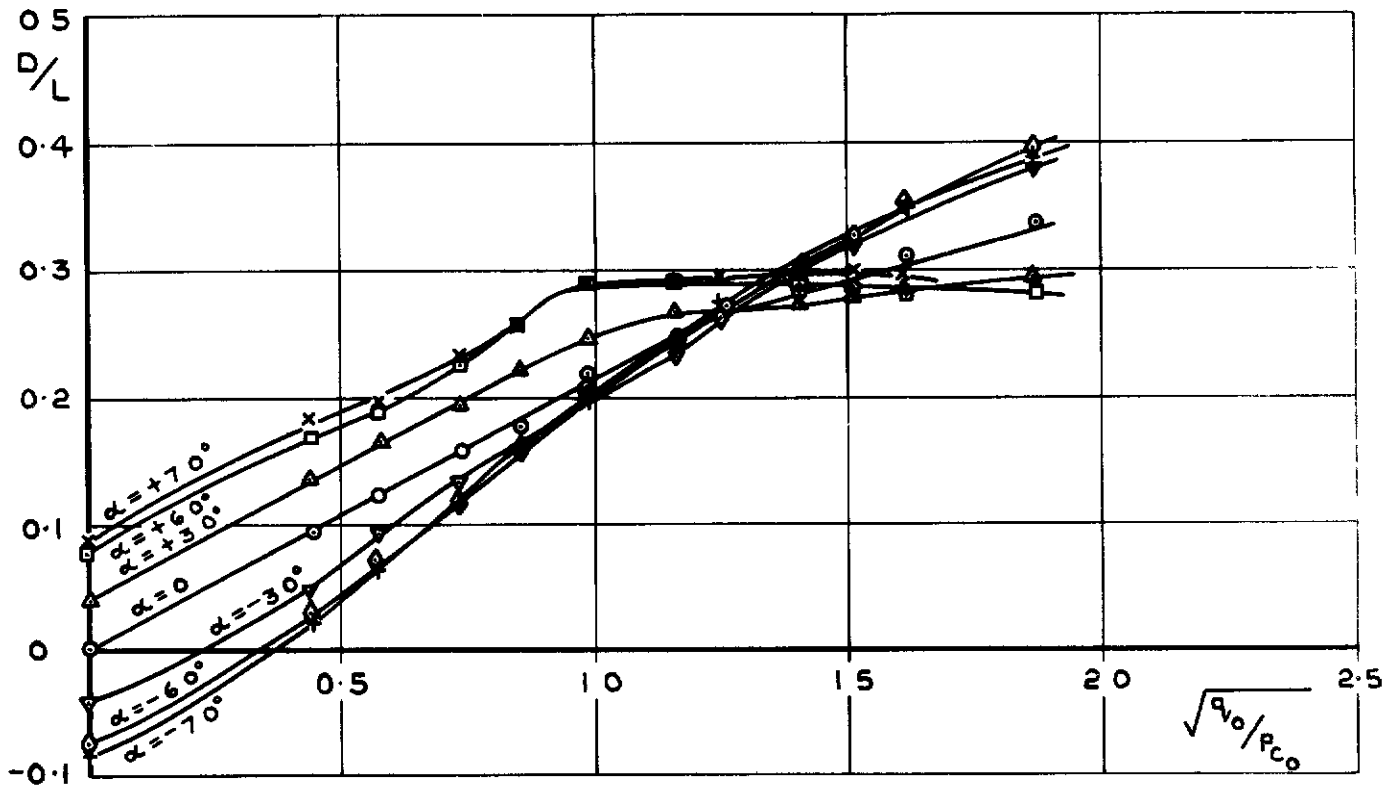

b DRAG

FIG. 14 a & b EFFECT OF INCIDENCE AT $h/t = 4·95$

STABILITY JETS OPEN

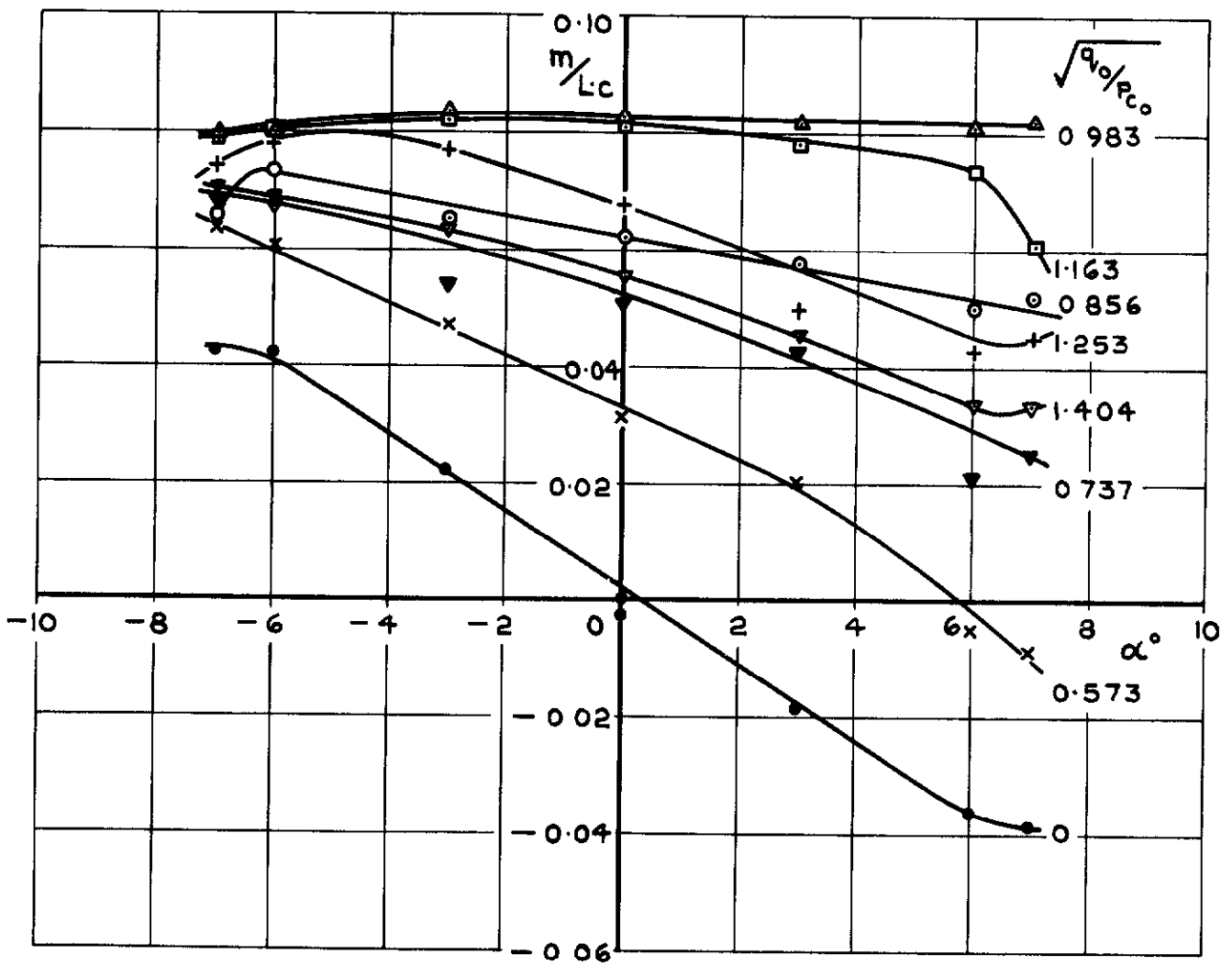

c PITCHING MOMENT

FIG.14 c EFFECT OF INCIDENCE AT $^{h}/_{t} = 4{\cdot}95$
STABILITY JETS OPEN

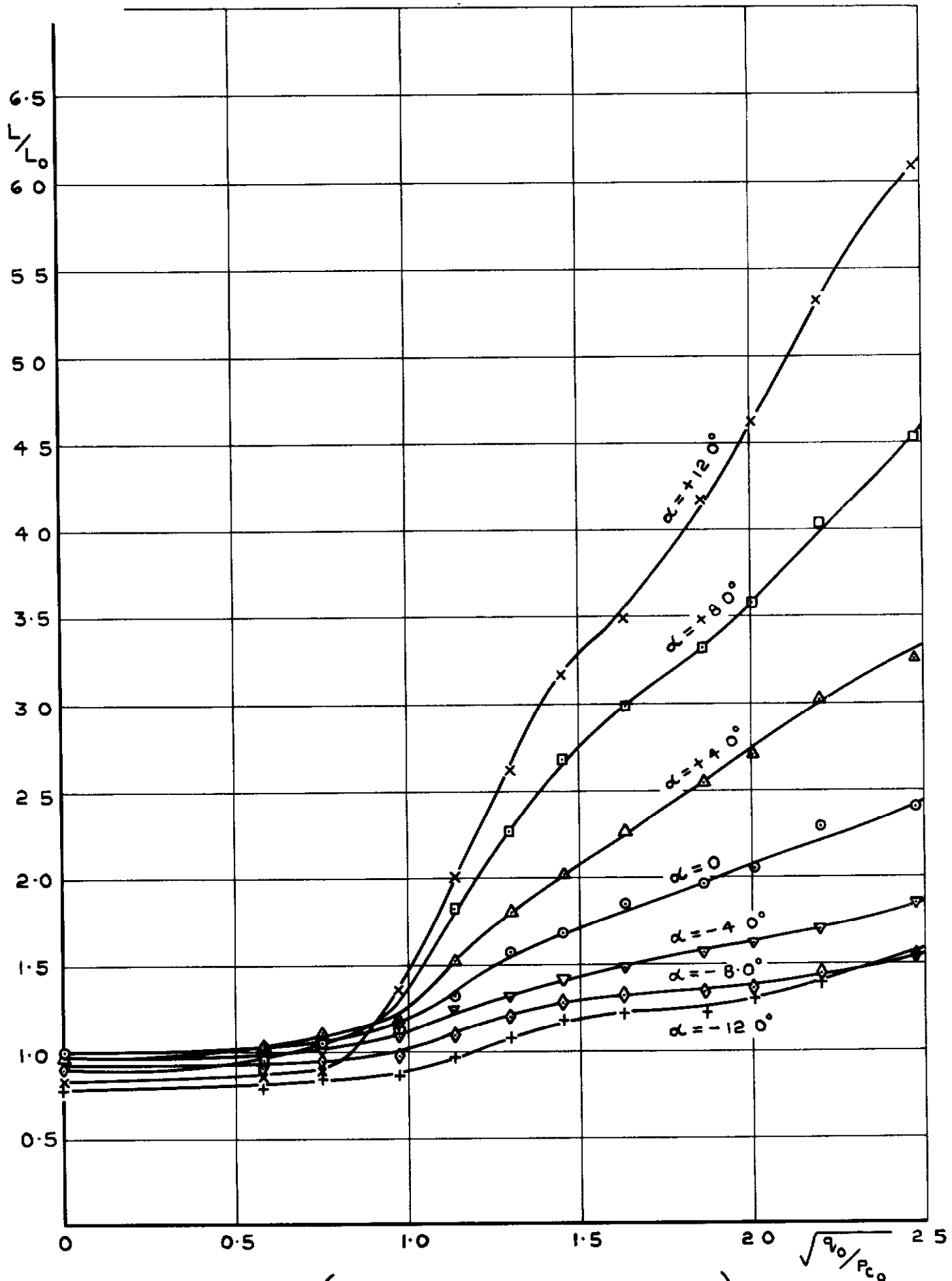

a LIFT $\left(L_o = 10{\cdot}5\ \text{lb},\ P_{c_o} = 1{\cdot}02\ \text{lb/sq ft}\right)$

FIG 15a EFFECT OF INCIDENCE AT $h/t = 8{\cdot}10$
STABILITY JETS OPEN

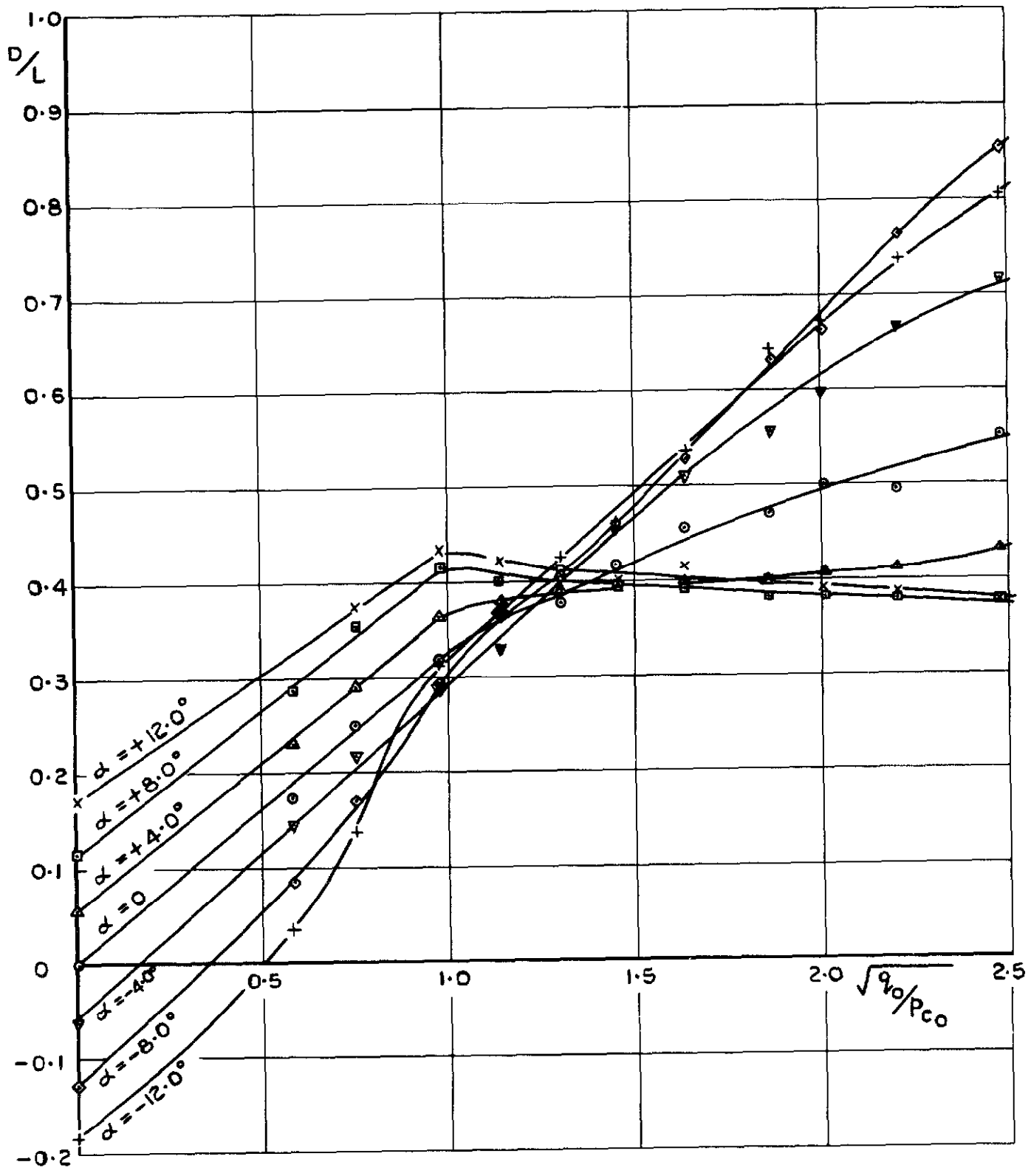

b DRAG

FIG.15b EFFECT OF INCIDENCE AT $^{h}/_{t} = 8{\cdot}10$
STABILITY JETS OPEN

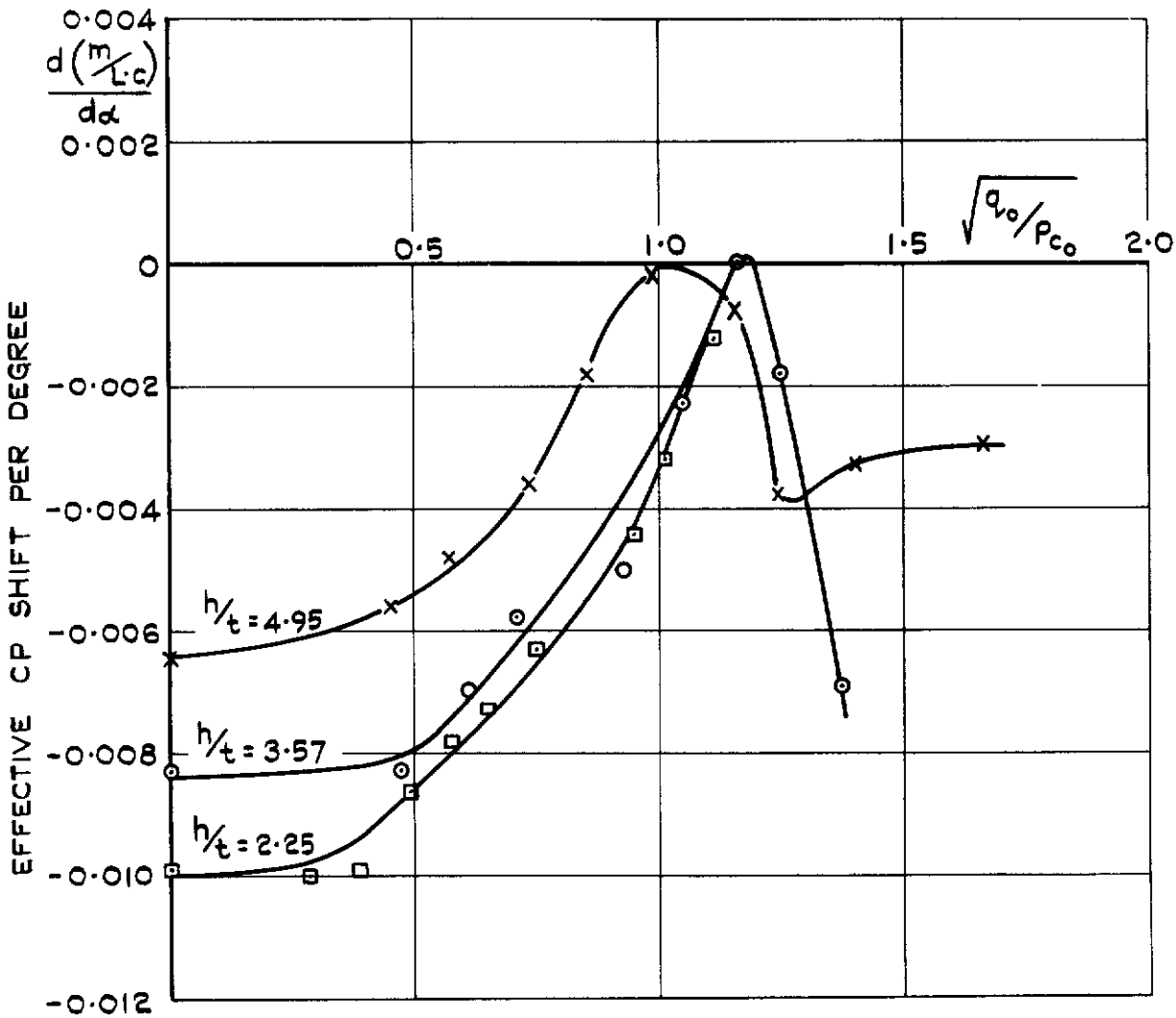

FIG. 16 EFFECT OF MAINSTREAM SPEED ON PITCH STABILITY

STABILITY JETS OPEN

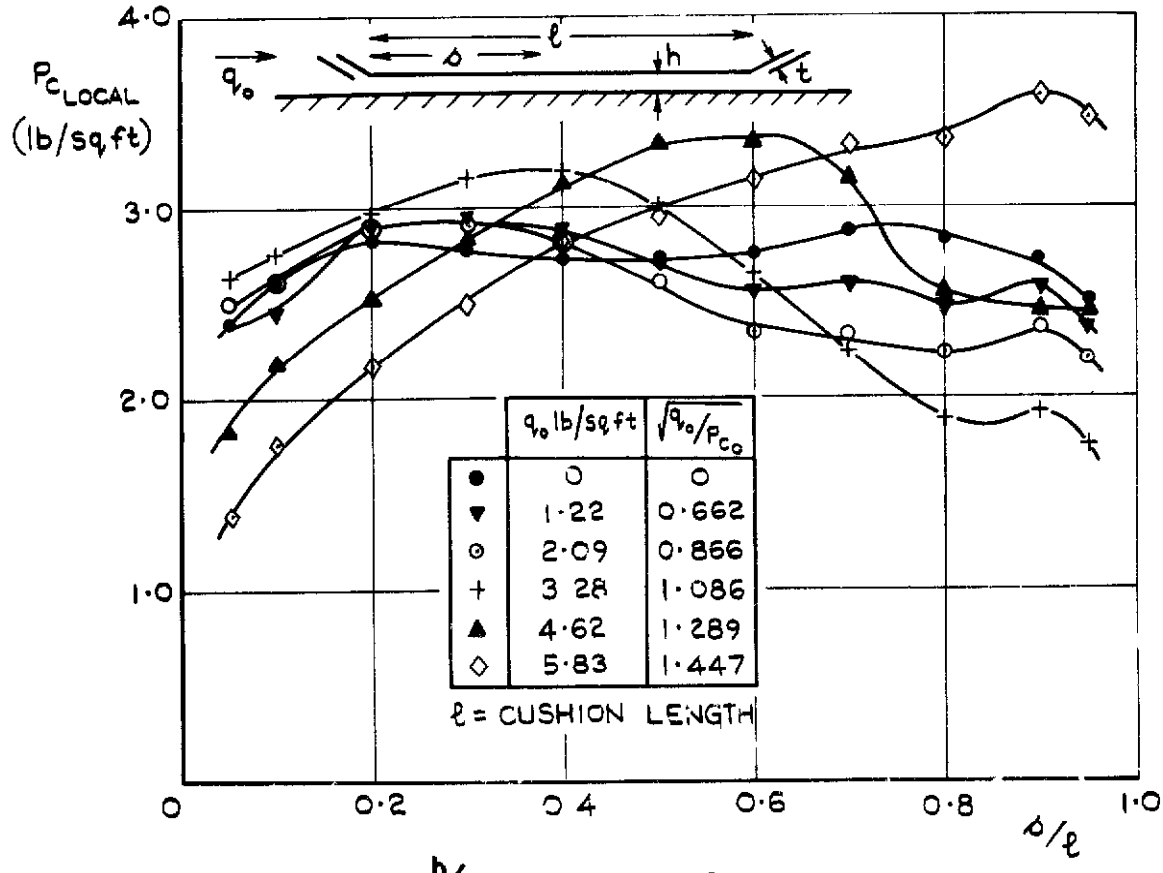

a $h/t = 3 \cdot 57$; $\alpha = 0$

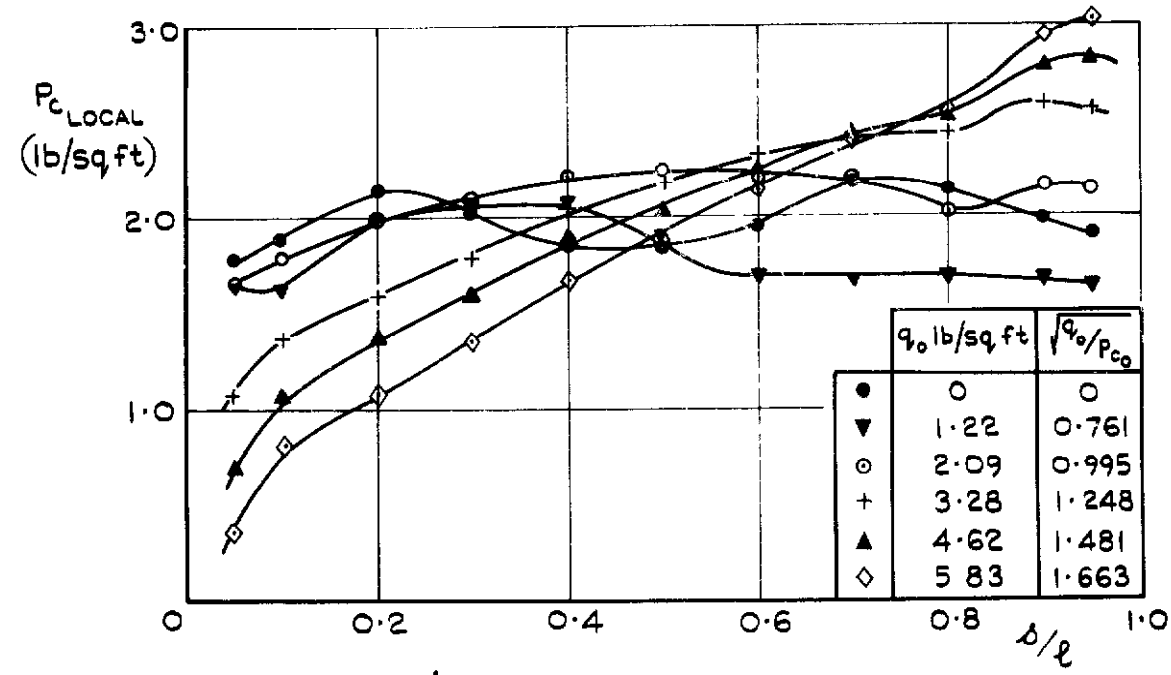

b $h/t = 4 \cdot 95$; $\alpha = 0$

FIG. 17 a & b PRESSURE DISTRIBUTION ALONG CENTRE - LINE OF UNDER - SURFACE OF CRAFT WITHOUT STABILITY JETS

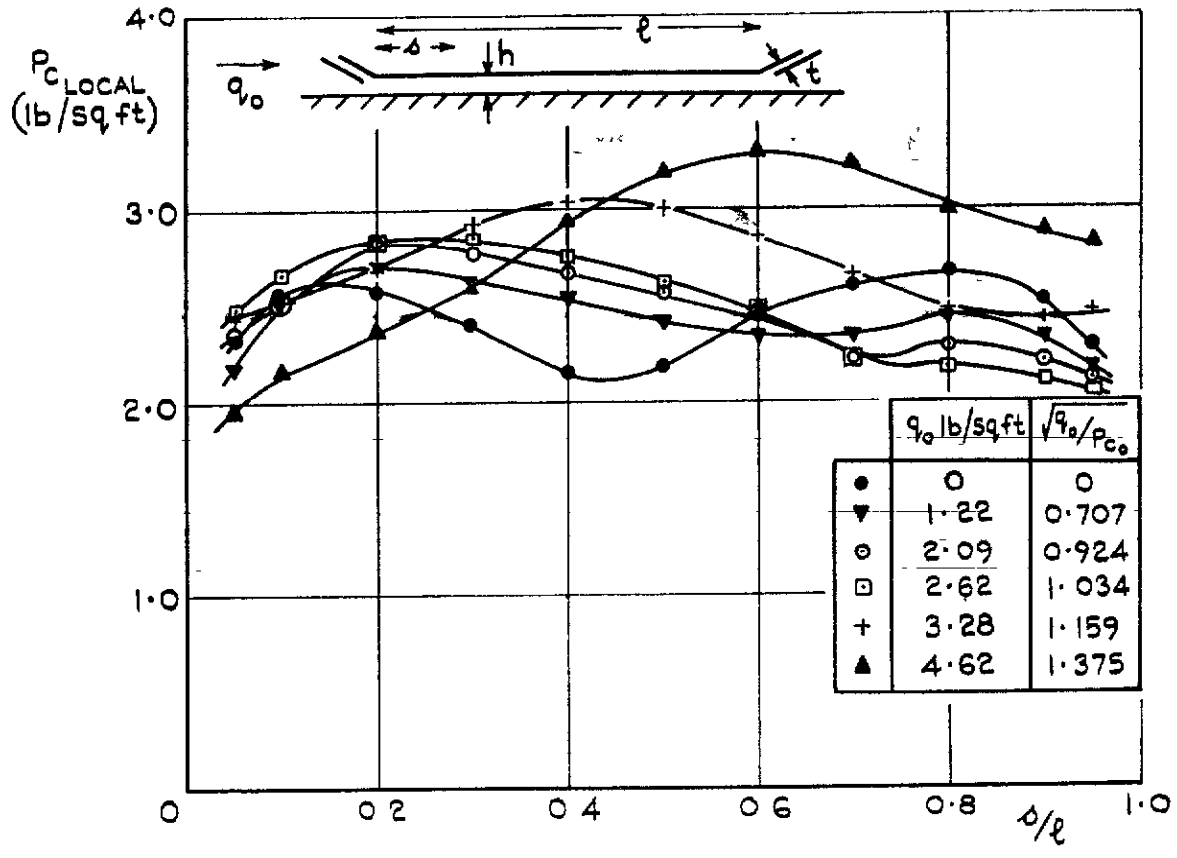

a $h/t = 3 \cdot 57$; $\alpha = 0$

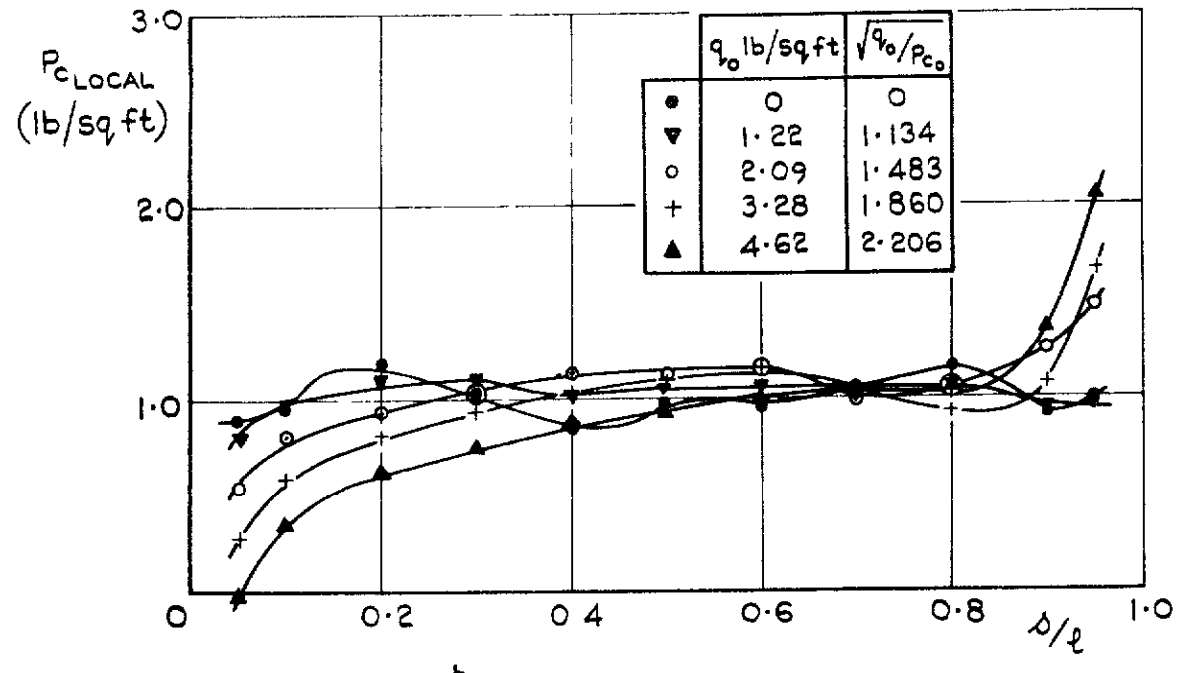

b $h/t = 8 \cdot 10$; $\alpha = 0$

FIG. 18 a & b PRESSURE DISTRIBUTION ALONG CENTRE - LINE OF UNDER - SURFACE OF CRAFT WITH STABILITY JETS

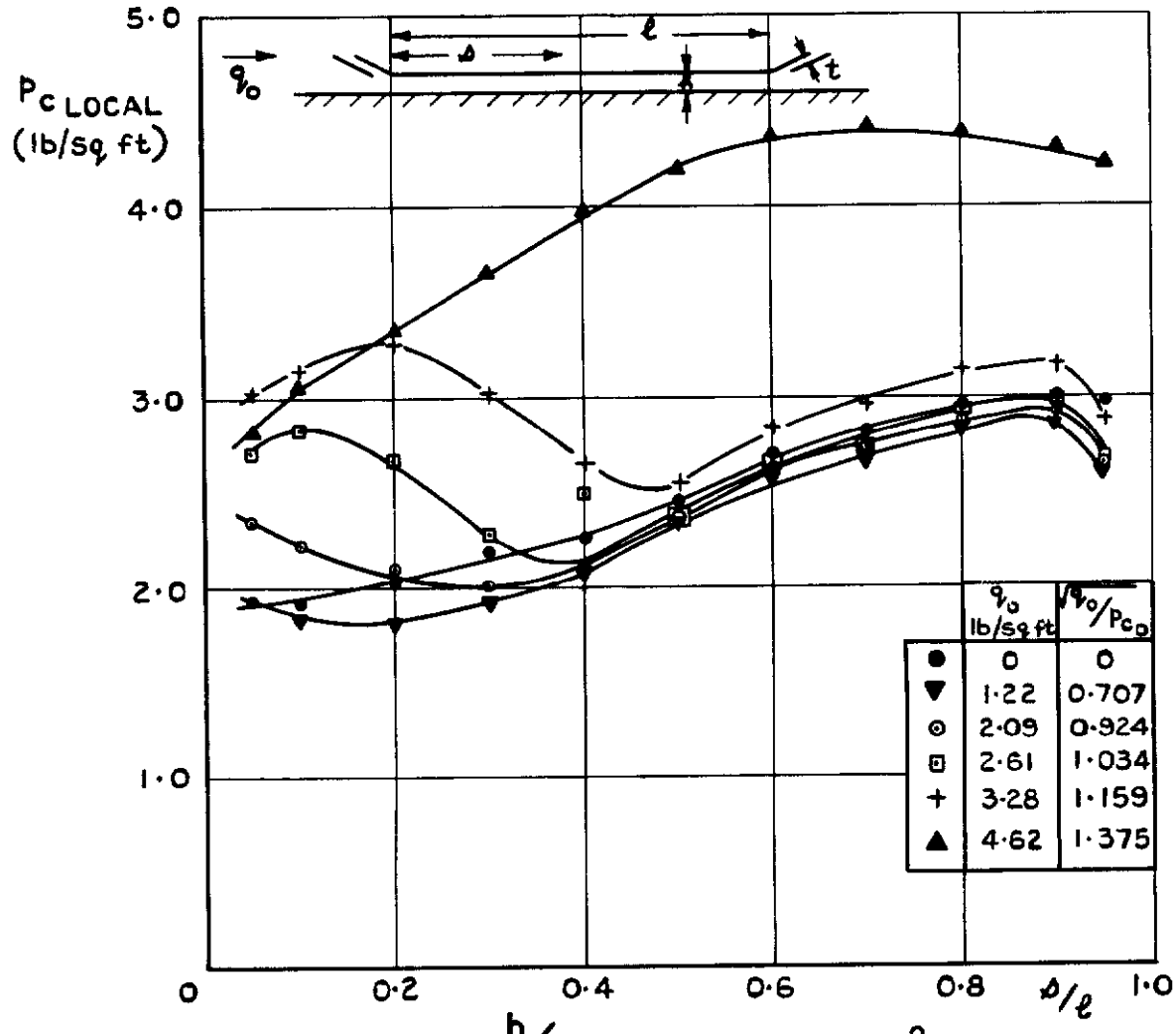

c $h/t = 3.57$; $\alpha = +4.5°$

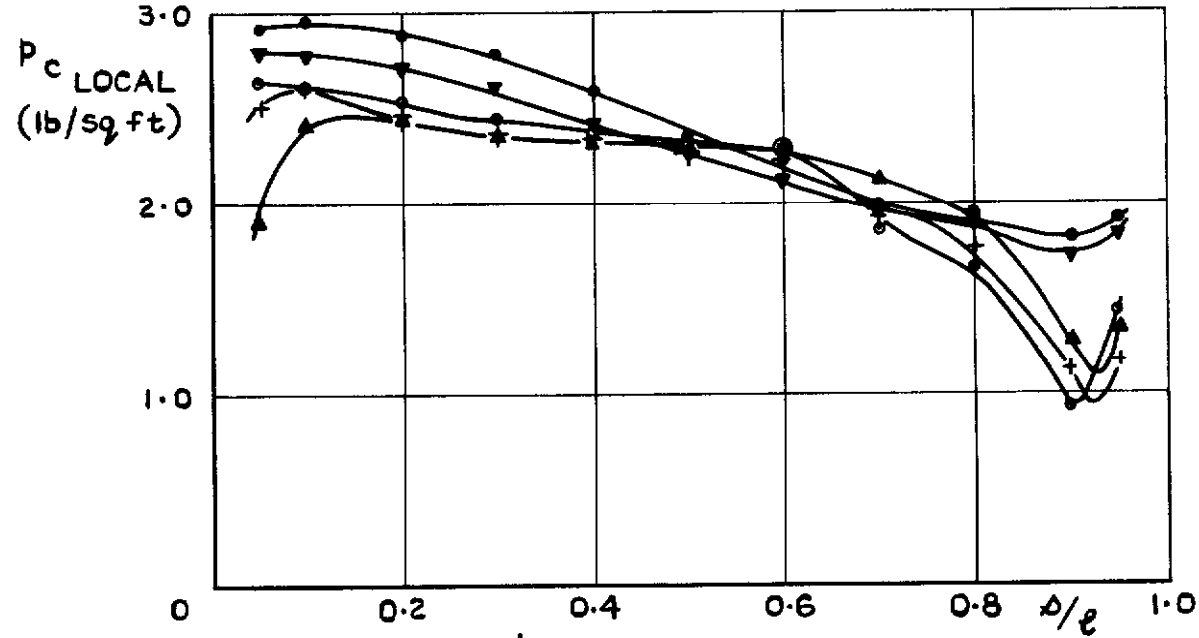

d $h/t = 3.57$; $\alpha = -4.5°$

FIG. 18 c & d PRESSURE DISTRIBUTION ALONG CENTRE-LINE OF UNDER-SURFACE OF CRAFT WITH STABILITY JETS

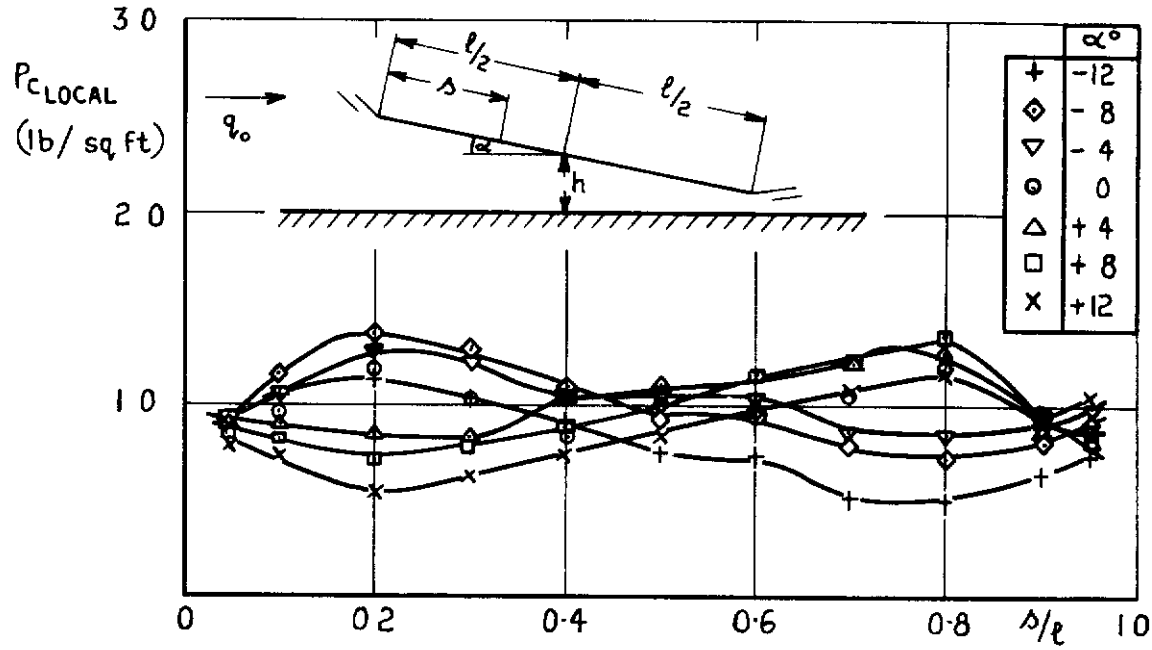

e $h/t = 8 \cdot 10$; $q_o = 0$

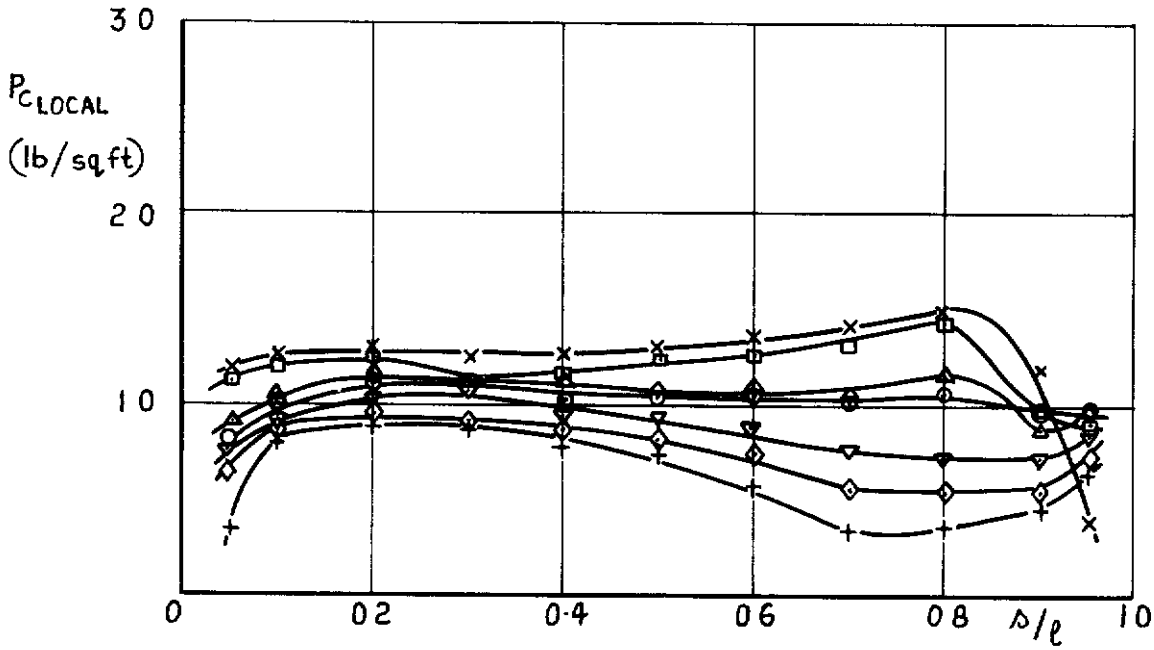

f $h/t = 8 \cdot 10$; $q_o = 1 \cdot 22$ lb/sq ft ; $\sqrt{q_o/p_{c_o}} = 1 \cdot 13$

FIG. 18 e & f PRESSURE DISTRIBUTION ALONG CENTRE-LINE OF UNDER-SURFACE OF CRAFT WITH STABILITY JETS

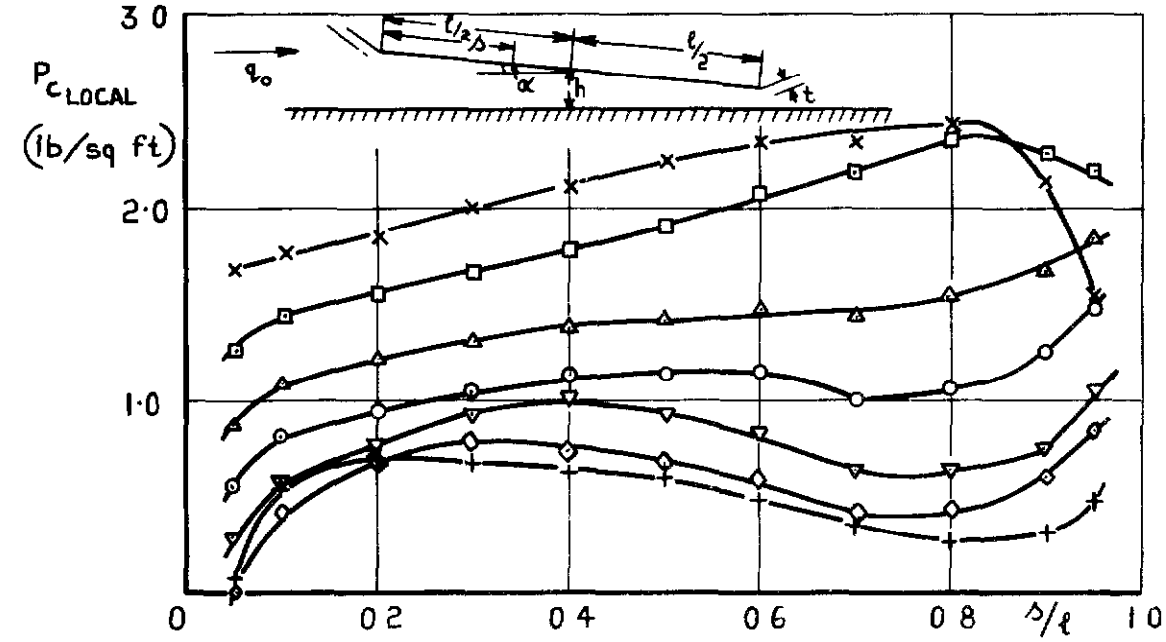

g $h/t = 8{\cdot}10$, $q_o = 2{\cdot}09$ lb/sq ft ; $\sqrt{q_o/p_{C_o}} = 1{\cdot}48$

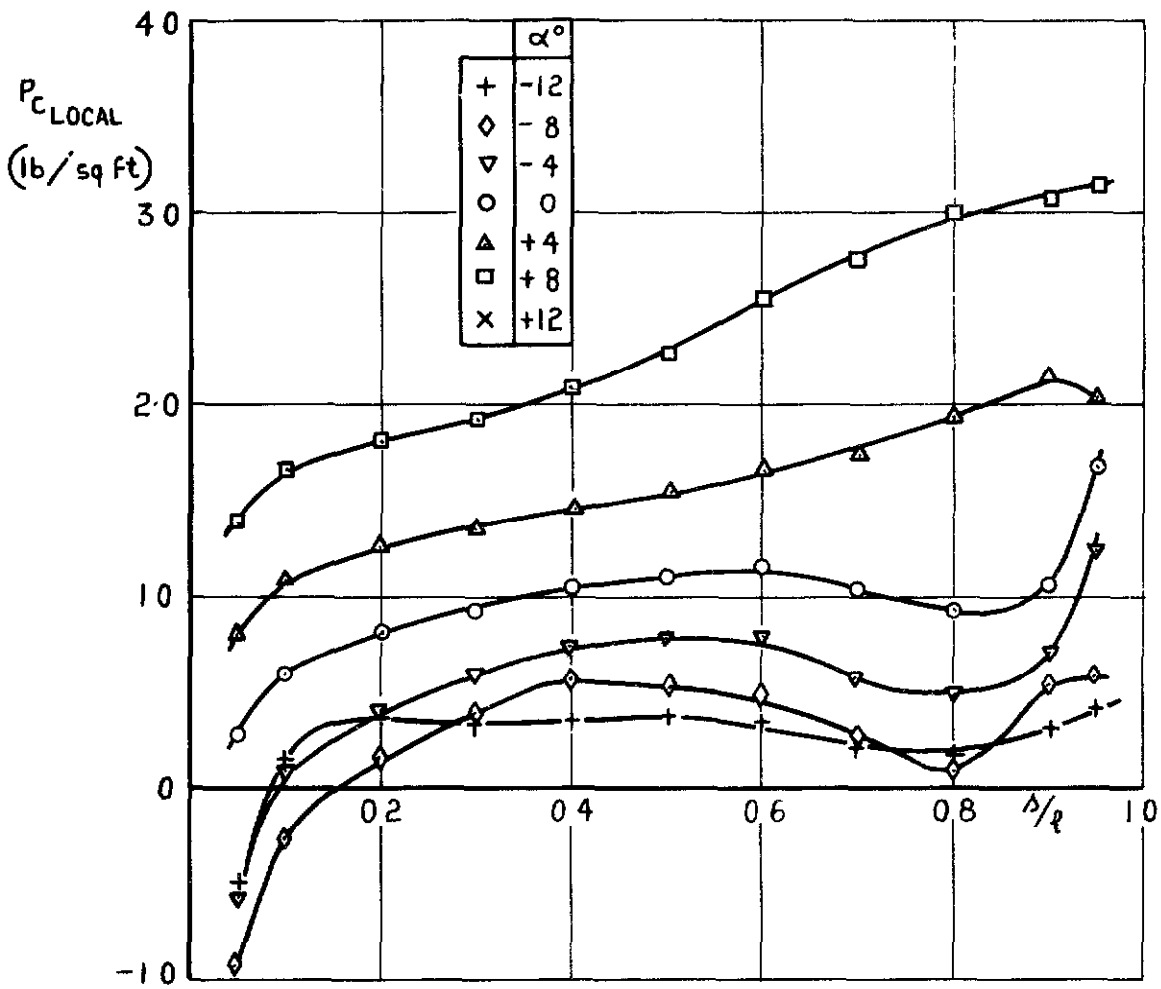

h $h/t = 8{\cdot}10$; $q_o = 3{\cdot}28$ lb / sq ft ; $\sqrt{q_o/p_{C_o}} = 1{\cdot}86$

FIG.18 g & h PRESSURE DISTRIBUTION ALONG CENTRE-LINE OF UNDER-SURFACE OF CRAFT WITH STABILITY JETS

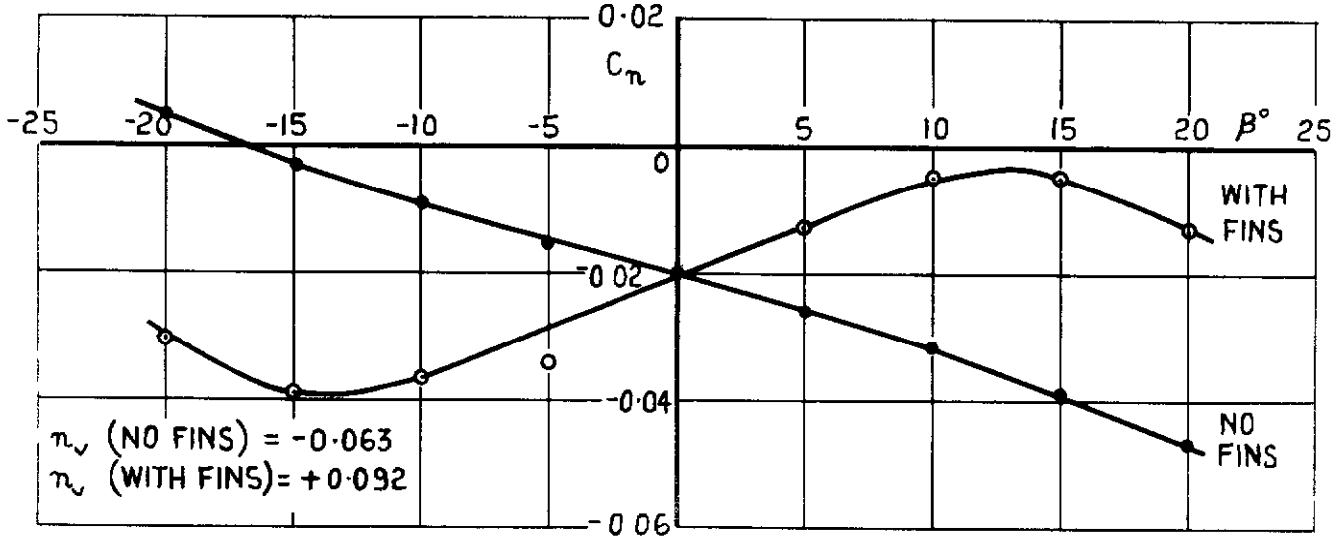

a YAWING MOMENT

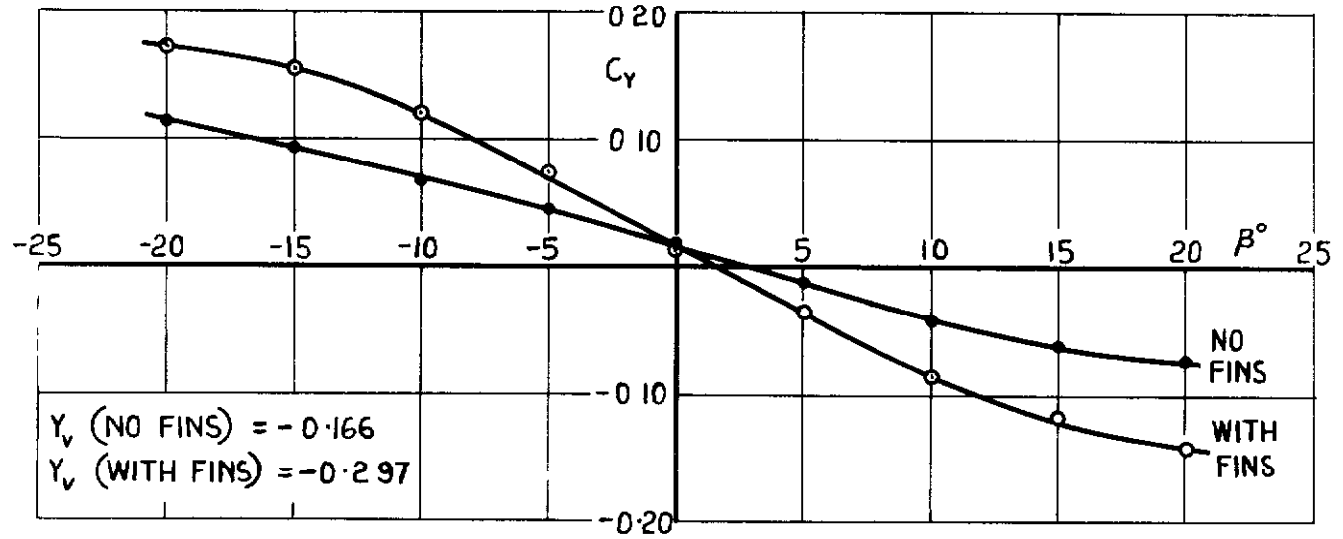

b SIDEFORCE

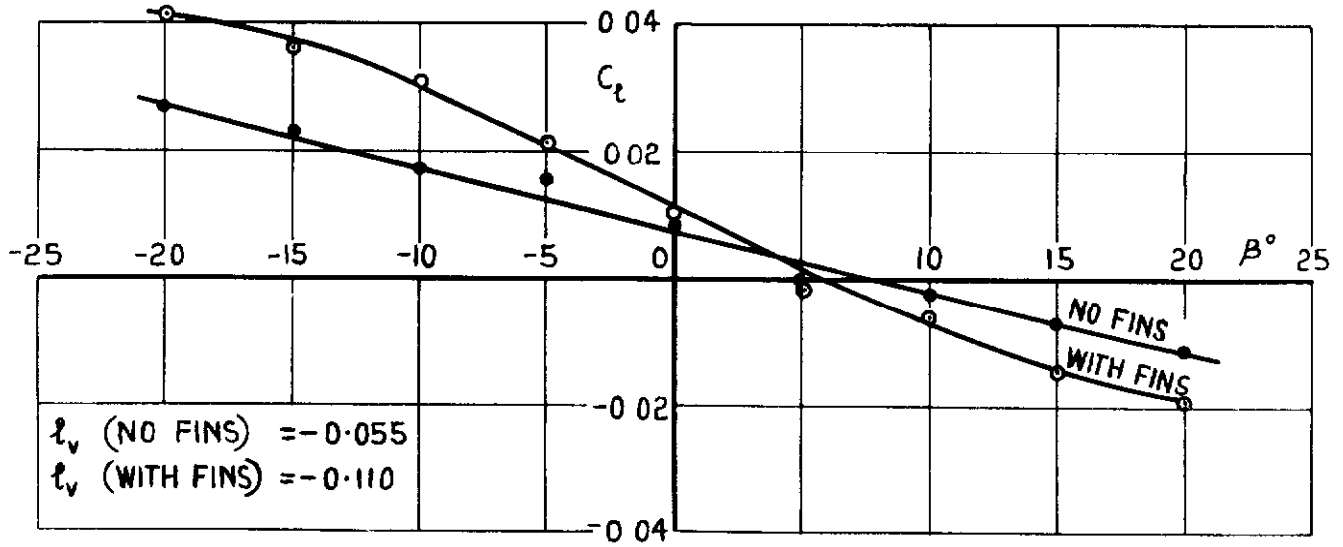

c ROLLING MOMENT

FIG. 19 a-c YAWING MOMENT, SIDEFORCE AND ROLLING MOMENT AT $\sqrt{q_0/p_{c_0}} = 0·87$; $h/t = 3·57$; $\alpha = 0$
ORIGINAL INTAKES ($r_L = 0\,018\,d_1$)

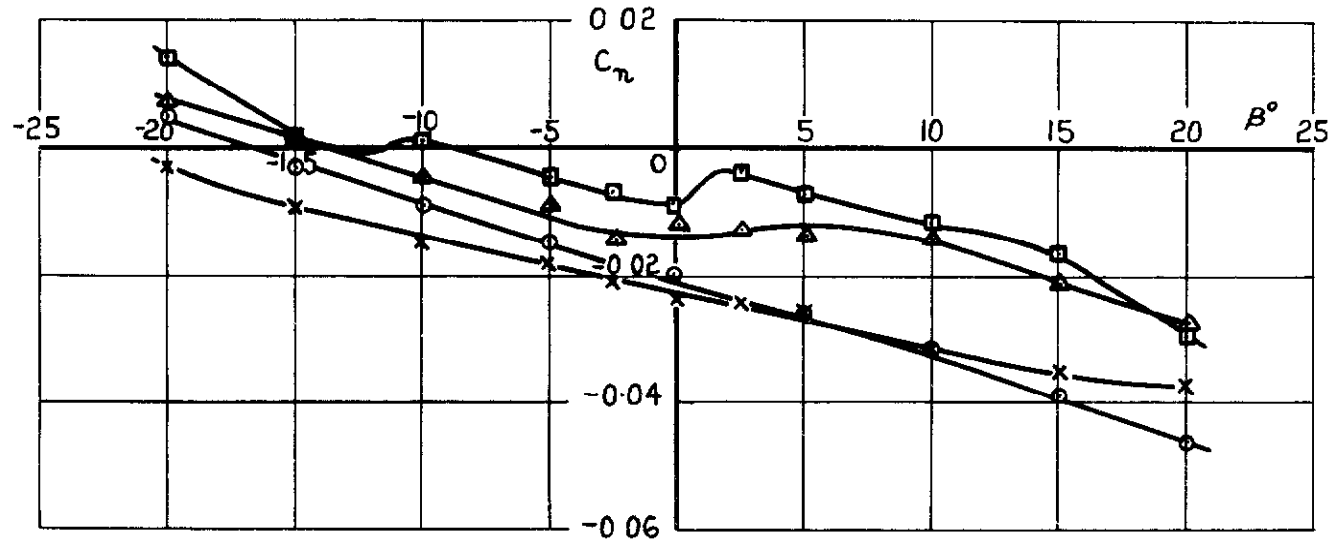

a YAWING MOMENT

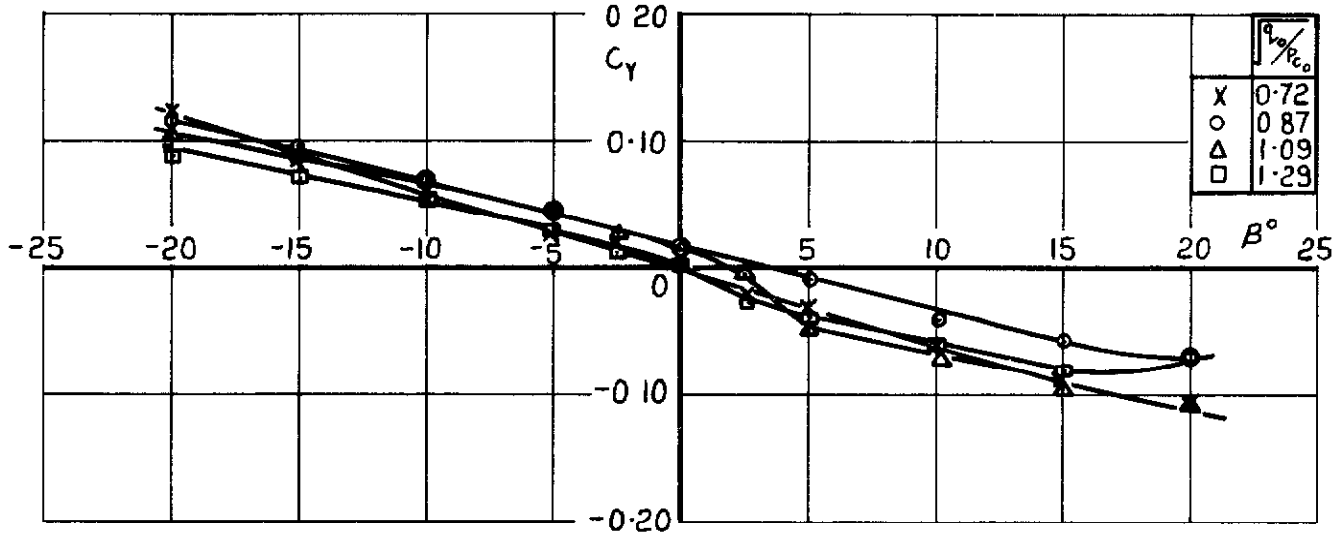

b SIDEFORCE

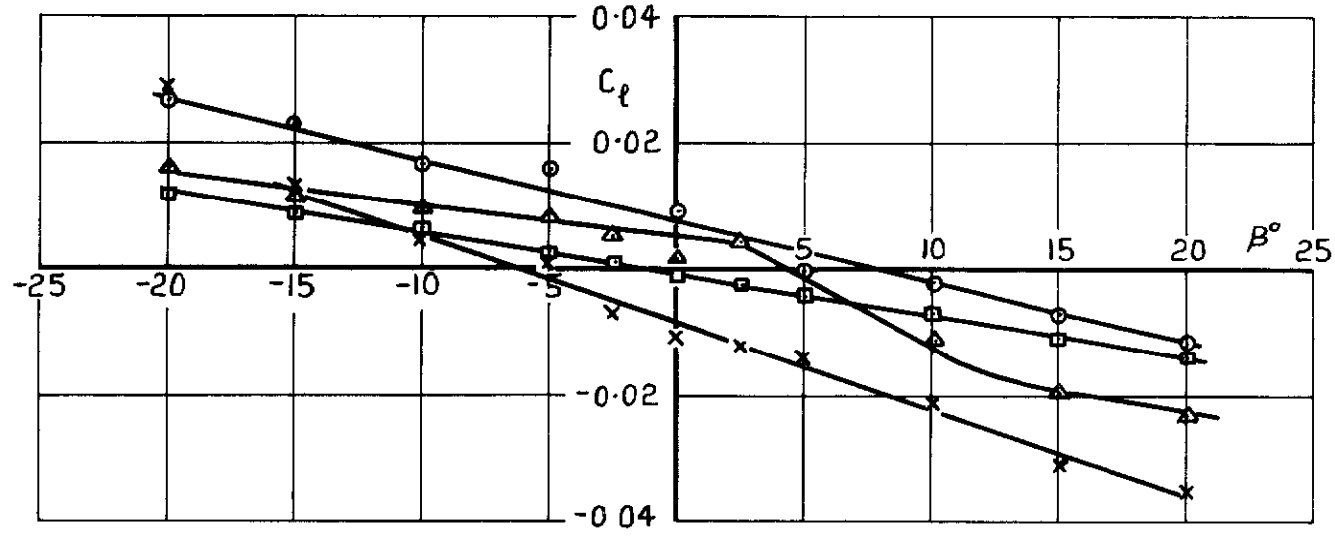

c ROLLING MOMENT

FIG 20 a-c EFFECT OF LIFTING SYSTEM ON LATERAL STABILITY

$h/t = 3{\cdot}57$; $\alpha = 0$; NO FINS

ORIGINAL INTAKES ($r_L = 0{\cdot}018\, d_1$)

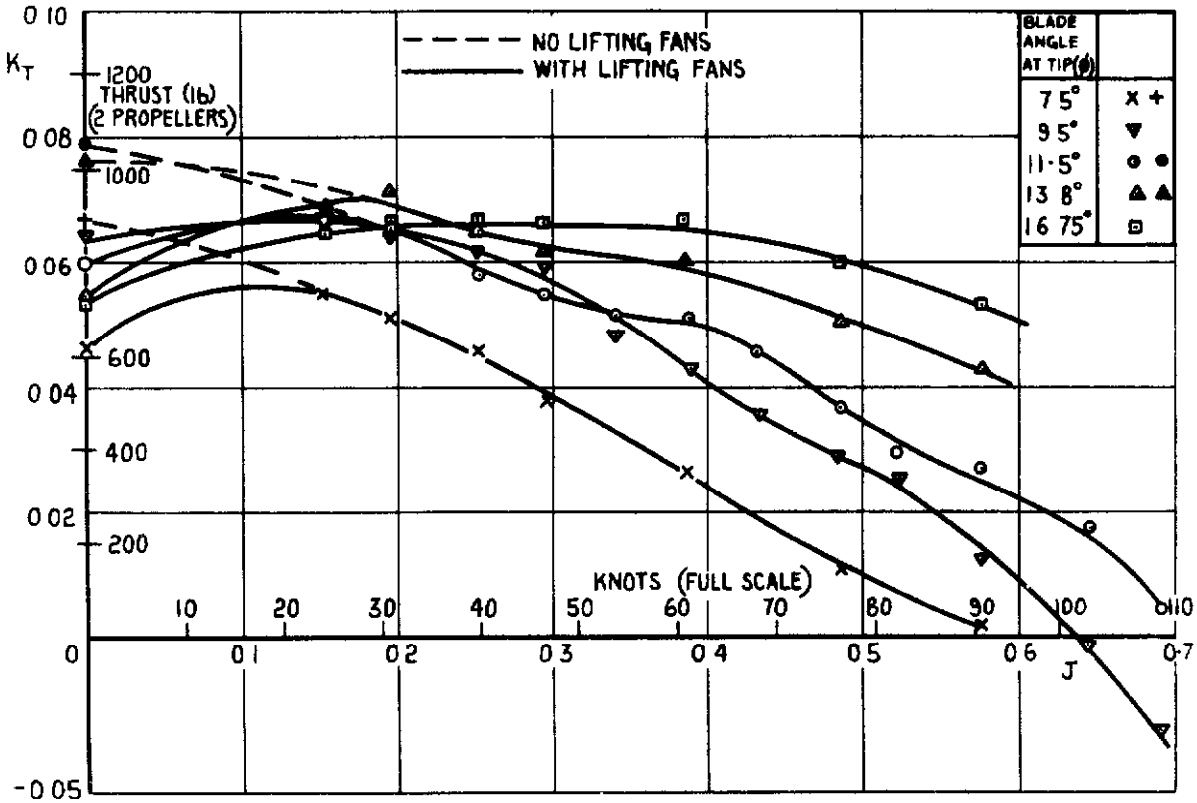

a THRUST INCREMENTS

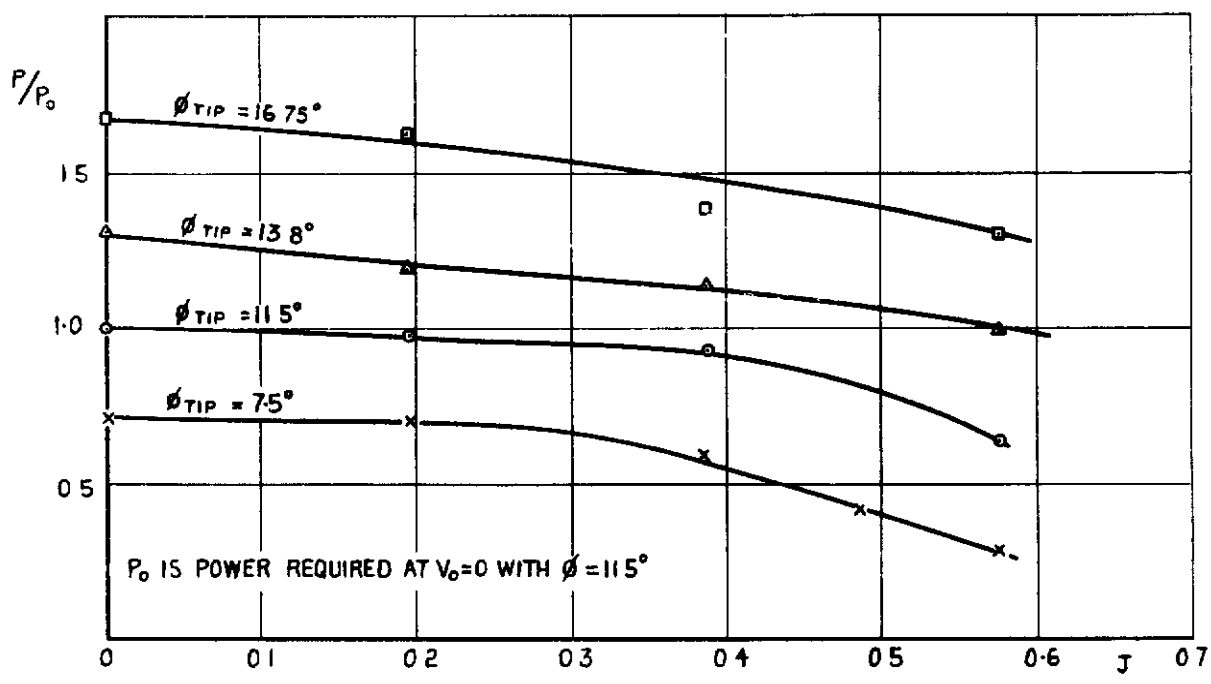

b POWER REQUIREMENTS

FIG. 21 a & b EFFECT OF BLADE ANGLE AND MAINSTREAM SPEED ON THRUST COEFFICIENT AND POWER REQUIRMENTS

$h/t = 3{\cdot}57$; $\alpha = 0$

ORIGINAL INTAKES ($r_L = 0\ 018\ d_i$)

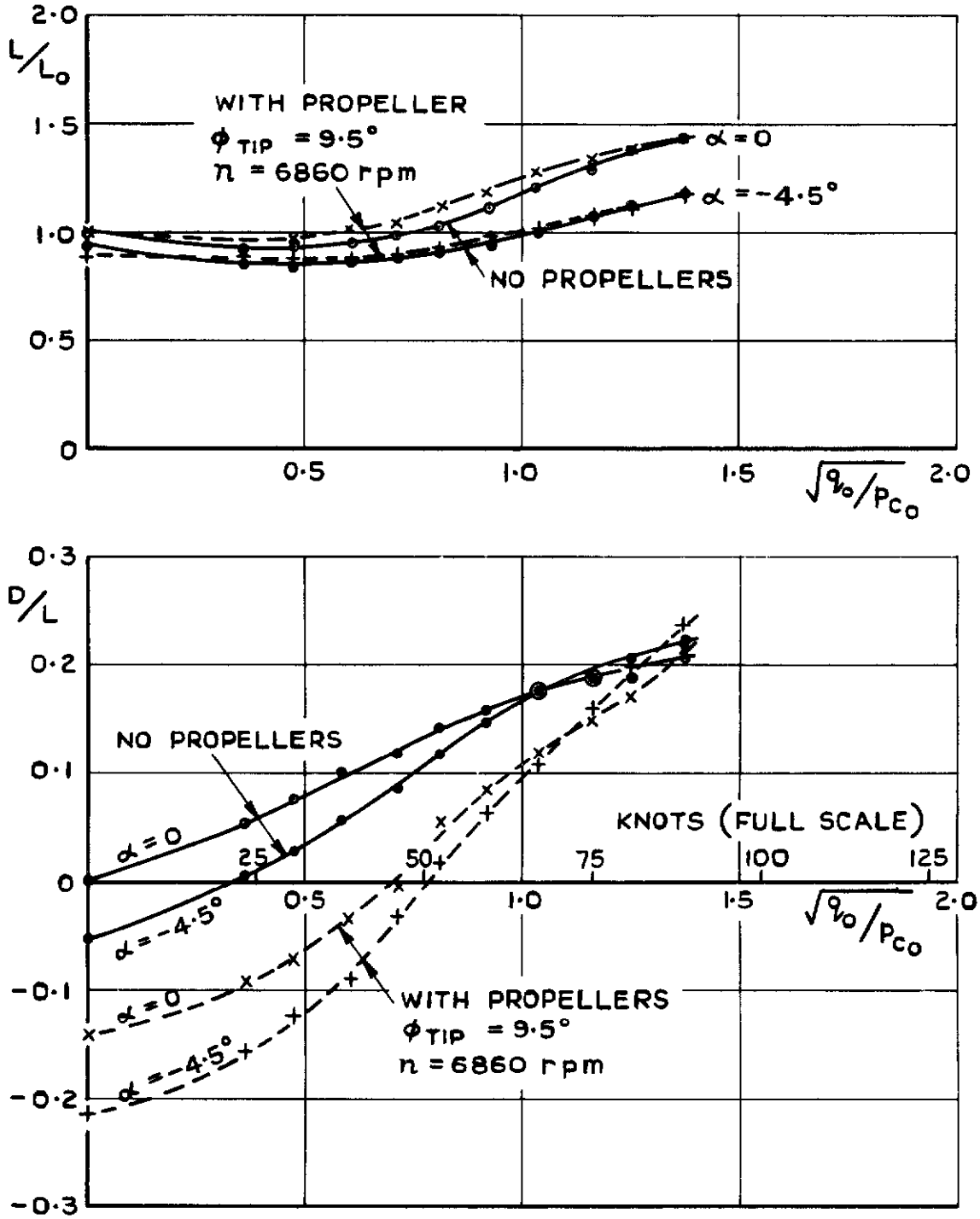

FIG.22 EFFECT OF PROPELLERS ON LIFT AND DRAG

$h/t = 3{\cdot}57$; $P_{C_o} = 2{\cdot}8$ lb/sq ft

ORIGINAL INTAKES ($r_L = 0{\cdot}018\, d_i$)

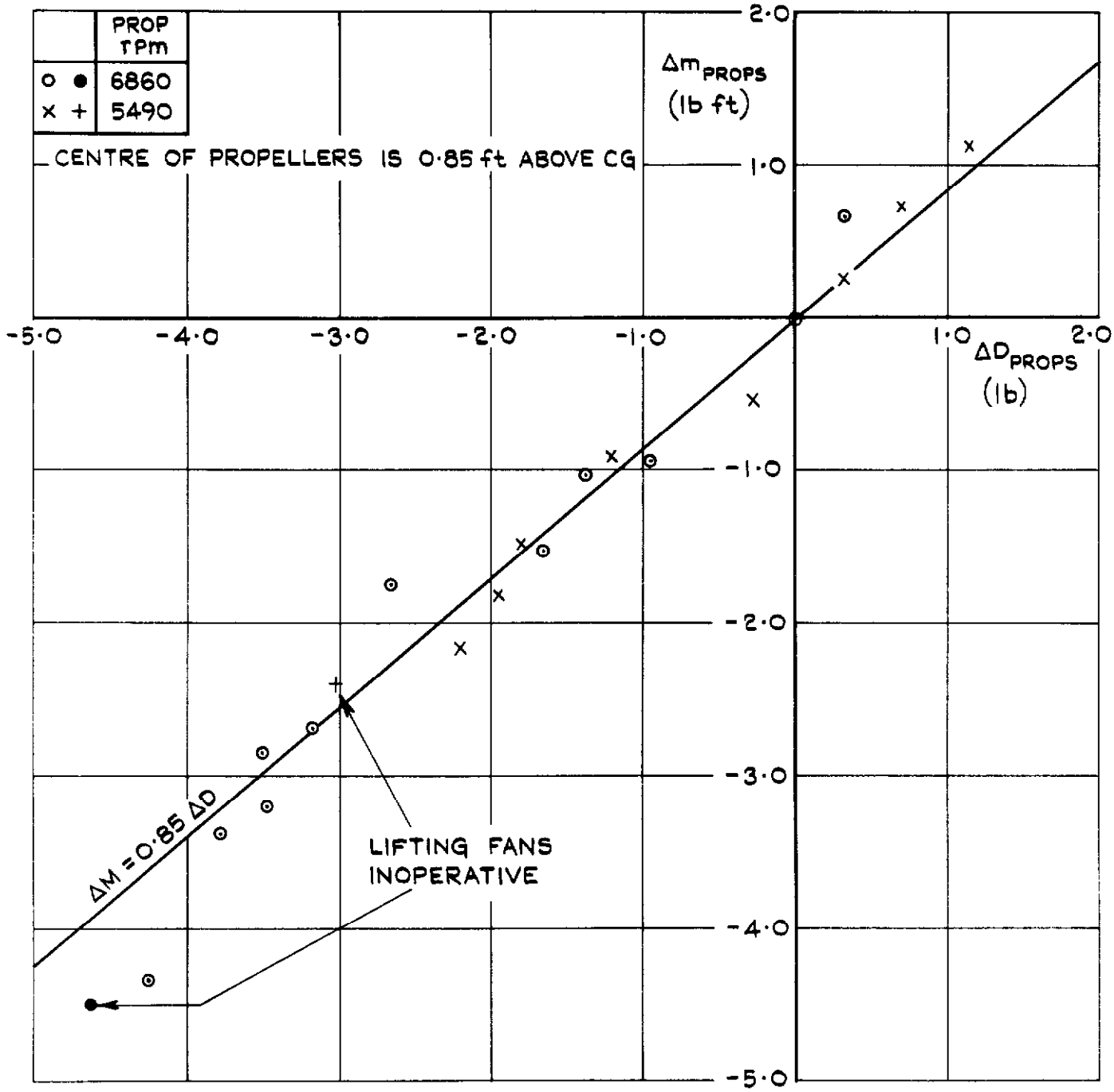

FIG. 23 EFFECT OF PROPELLER THRUST ON PITCHING MOMENT

$\alpha = 0$; $h/t = 3 \cdot 57$

ORIGINAL INTAKES ($r_L = 0 \cdot 018 d_i$)

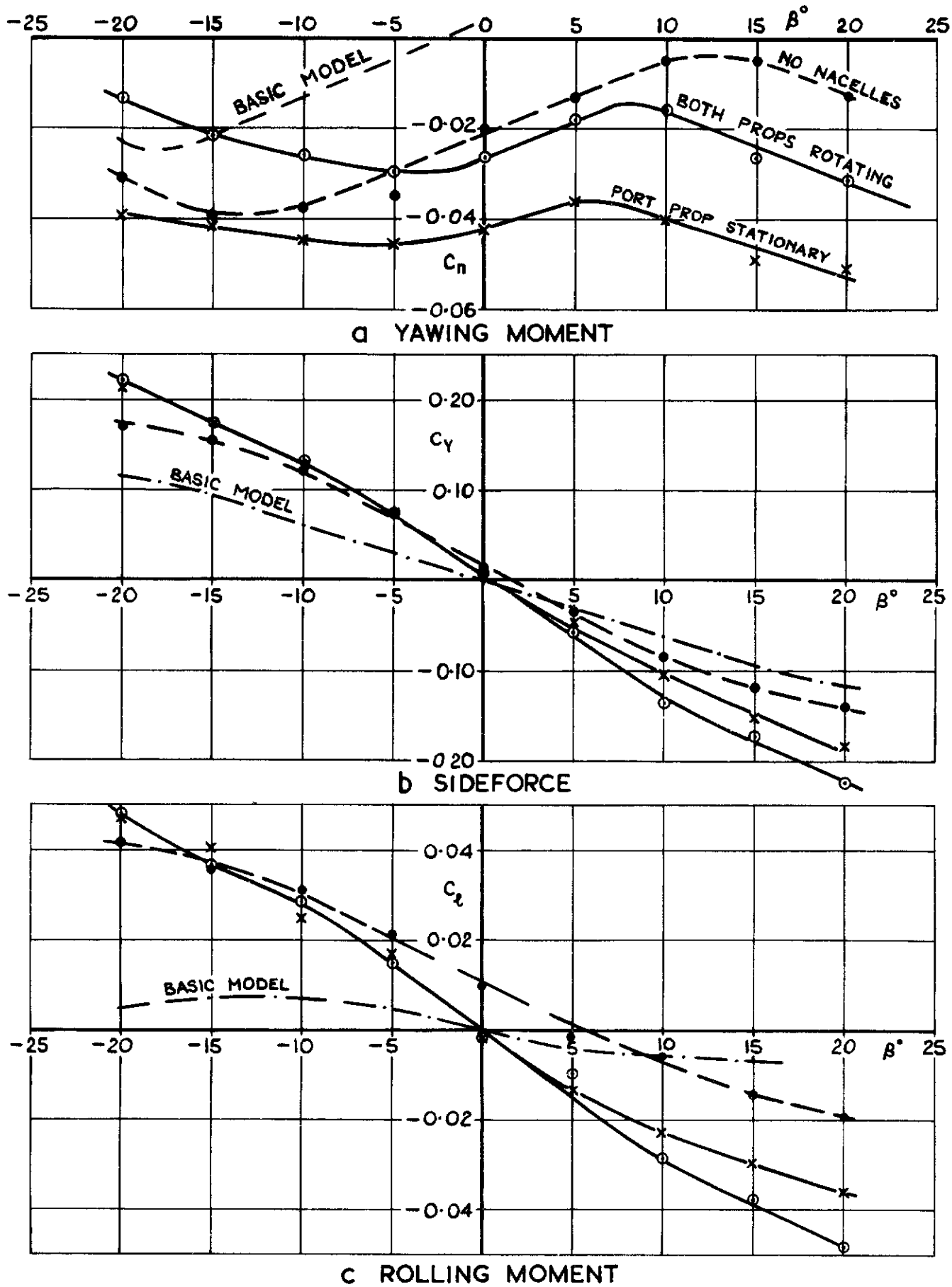

FIG. 24 a-c EFFECT OF STOPPING ONE PROPULSIVE MOTOR ON DIRECTIONAL AND LATERAL STABILITY

$\sqrt{q_o/P_{C_o}} = 0{\cdot}87$, $h/t = 3{\cdot}57$; $\alpha = 0$, UNDEFLECTED RUDDER; $k_T = 0{\cdot}044$

ORIGINAL INTAKES $(r_L = 0{\cdot}018\, d_i)$

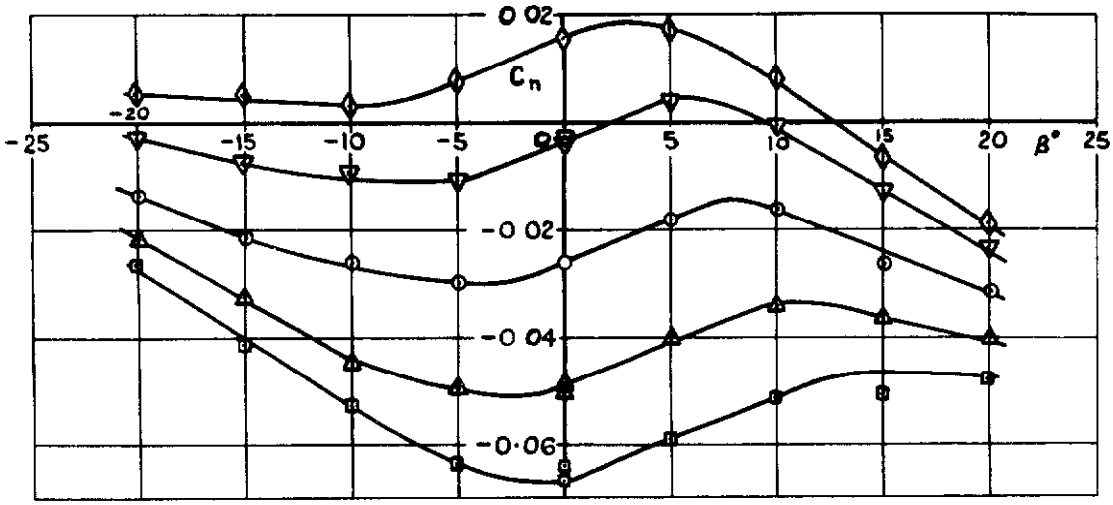

a YAWING MOMENT

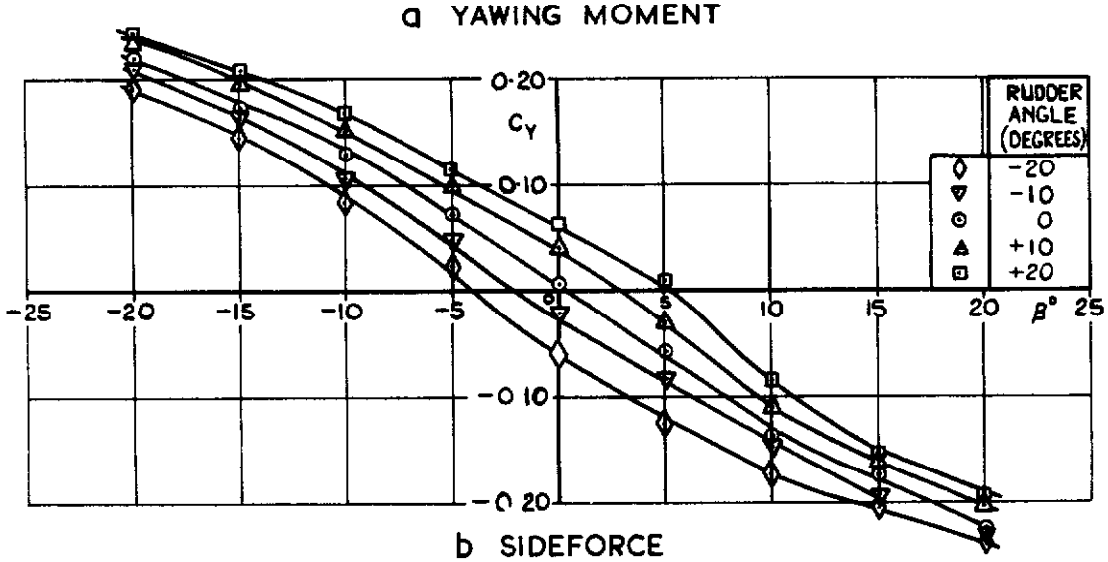

b SIDEFORCE

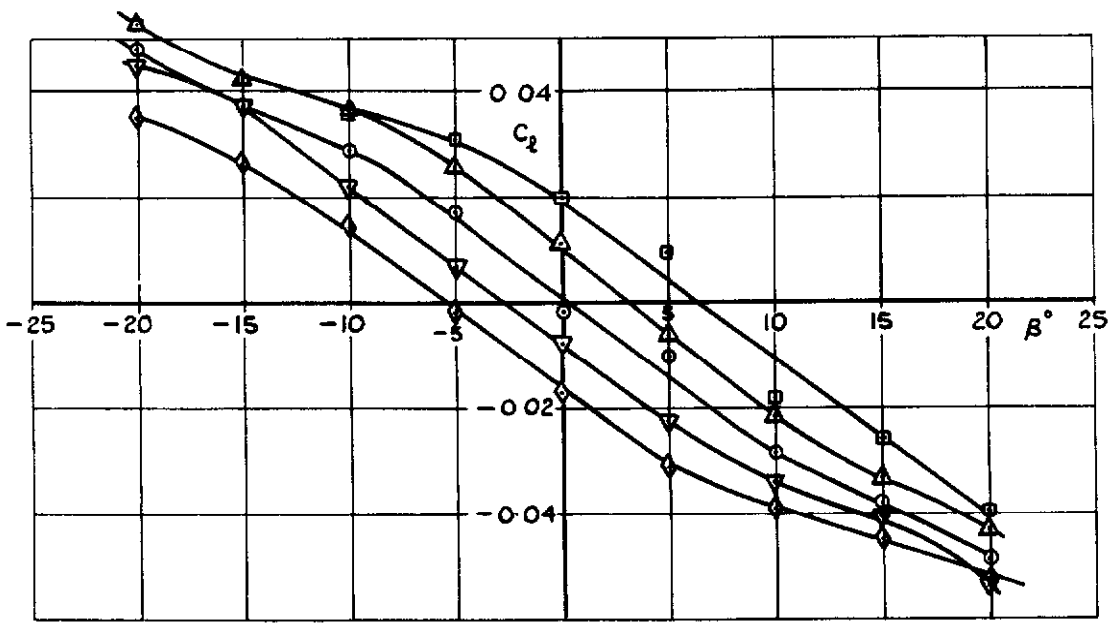

c ROLLING MOMENT

FIG. 25 a-c EFFECT OF RUDDER DEFLECTION IN PRESENCE OF SLIPSTREAM, $k_T = 0{\cdot}044$

$\sqrt{q_0/p_{c_0}} = 0{\cdot}87$, $h/t = 3{\cdot}57$, $\alpha = 0$

ORIGINAL INTAKES ($r_L = 0{\cdot}018\, d_i$)

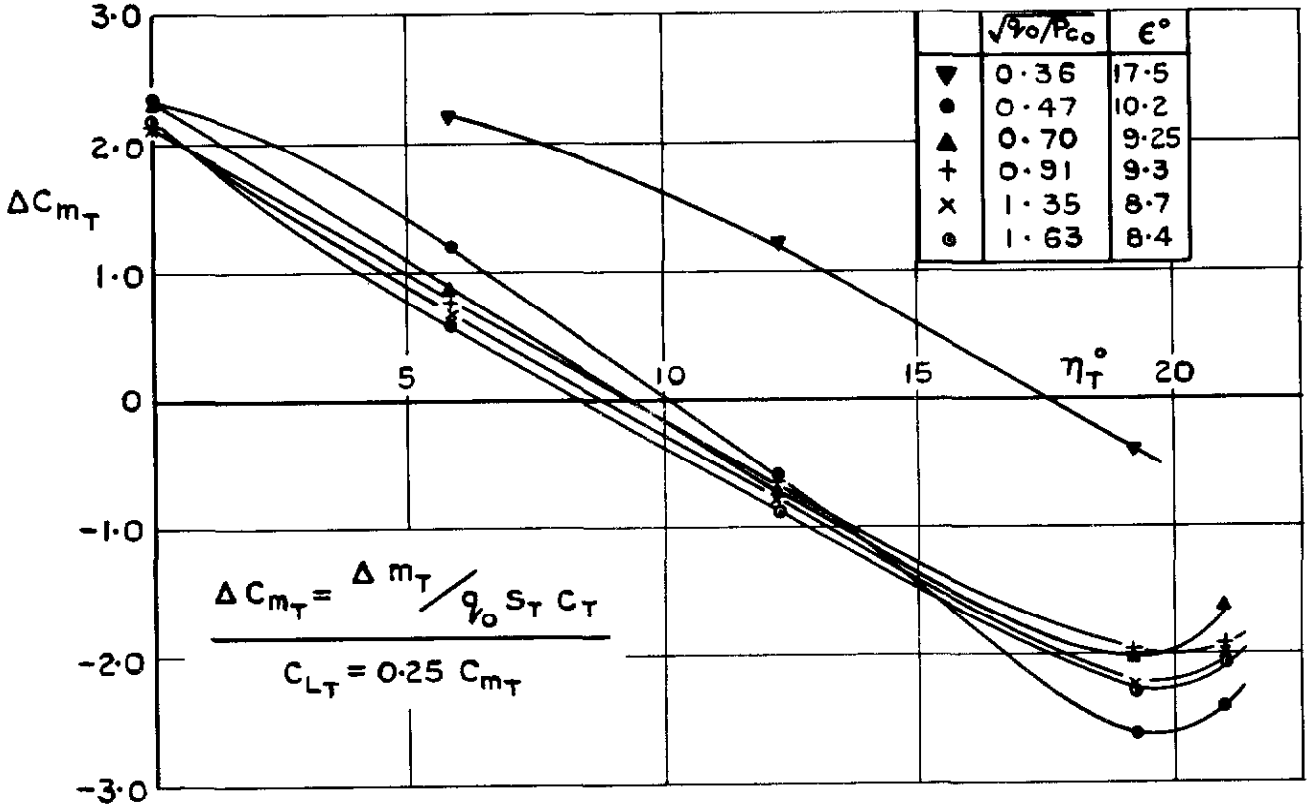

FIG. 26 TAILPLANE CONTRIBUTION TO PITCHING MOMENT

NO NACELLES, HEBA FANS, $h/t = 3{\cdot}57$, $\alpha = 0$, NO STABILITY JETS

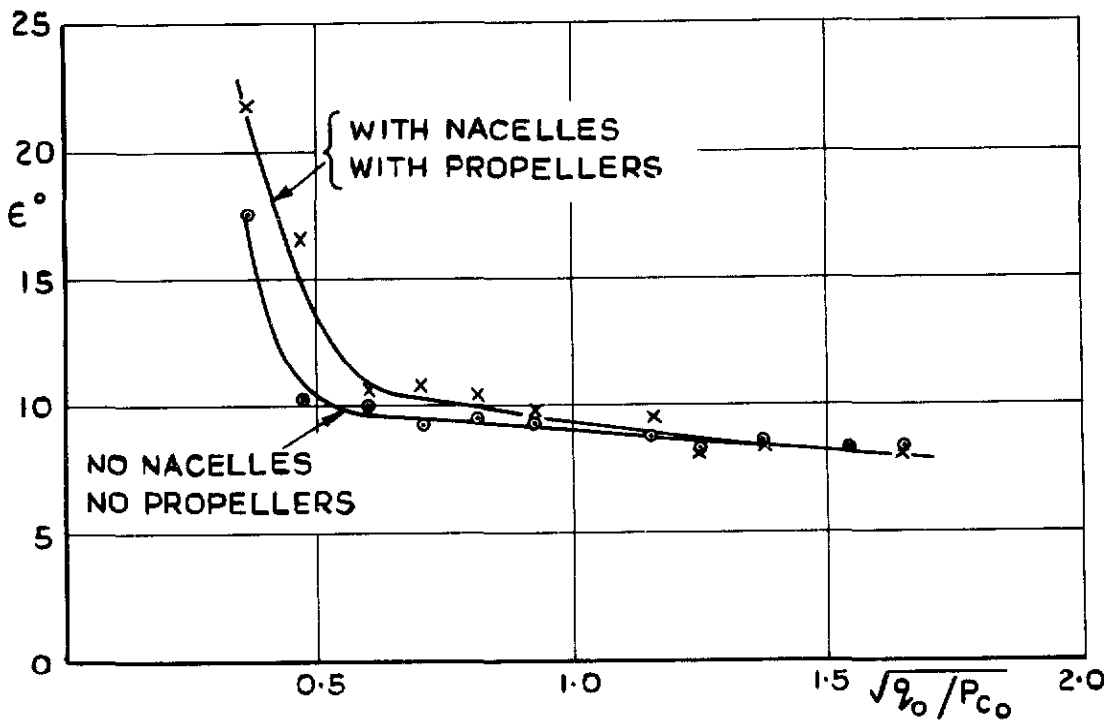

FIG. 27 MEAN DOWNWASH AT TAILPLANE AT ZERO INCIDENCE

$h/t = 3{\cdot}57$, NO STABILITY JETS

ORIGINAL INTAKES ($r_L = 0{\cdot}018\, d_i$)

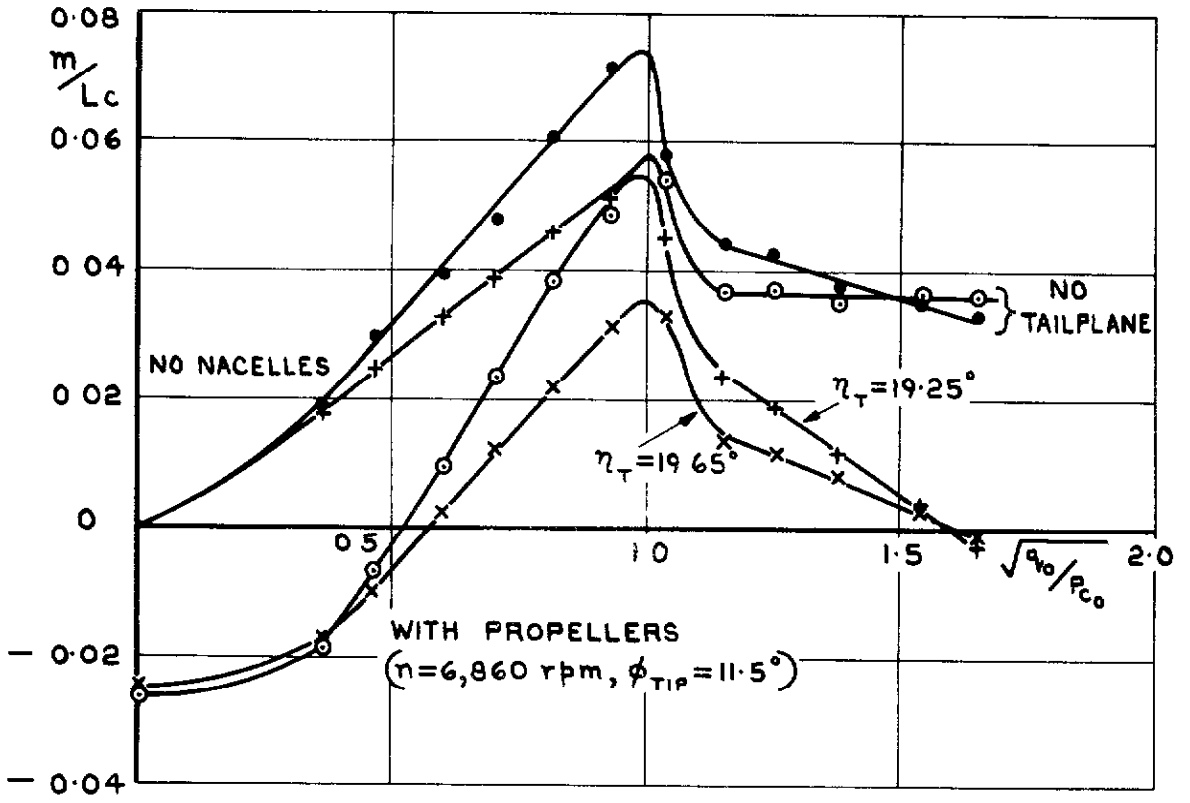

FIG. 28 EFFECT OF TAILPLANE ON CENTRE OF PRESSURE

$^h/_t$ = 3·57; STABILITY JETS CLOSED; α = 0

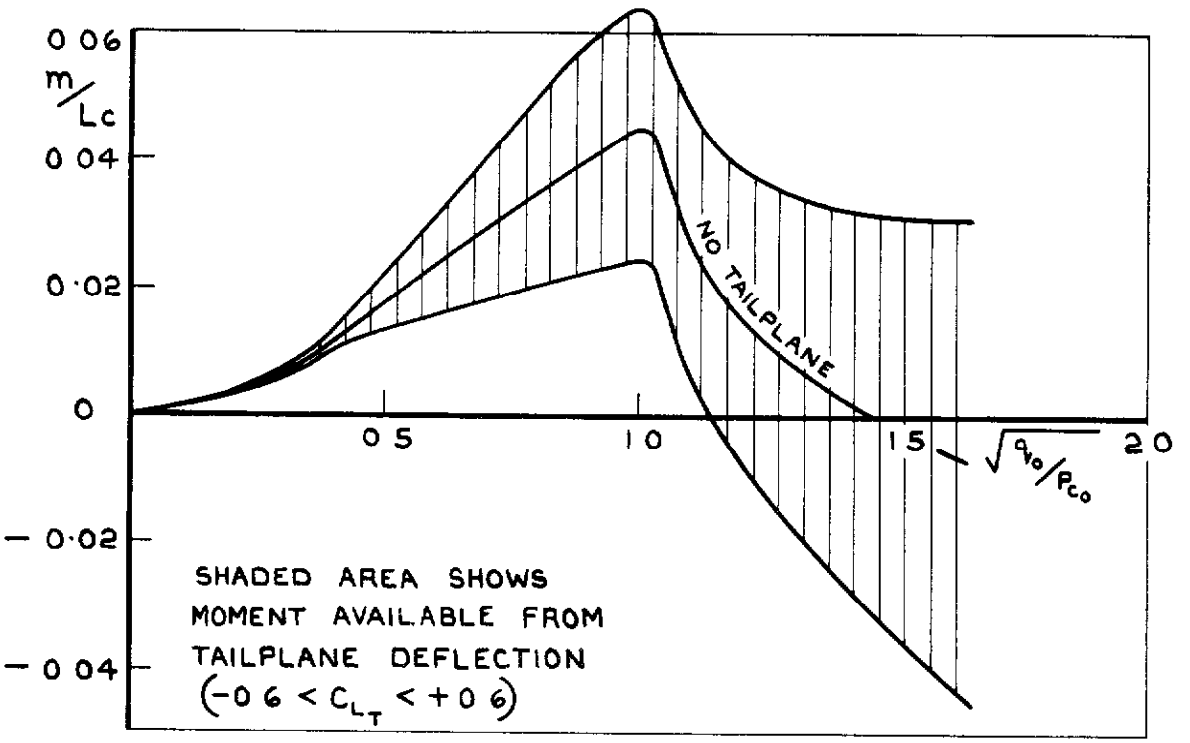

FIG. 29 ESTIMATED PITCHING MOMENT WITH PROPELLER THRUST ADJUSTED TO GIVE ZERO NET DRAG

$^h/_t$ = 3 57, STABILITY JETS CLOSED, α = 0

ORIGINAL INTAKES (r_L = 0·018 d_i)

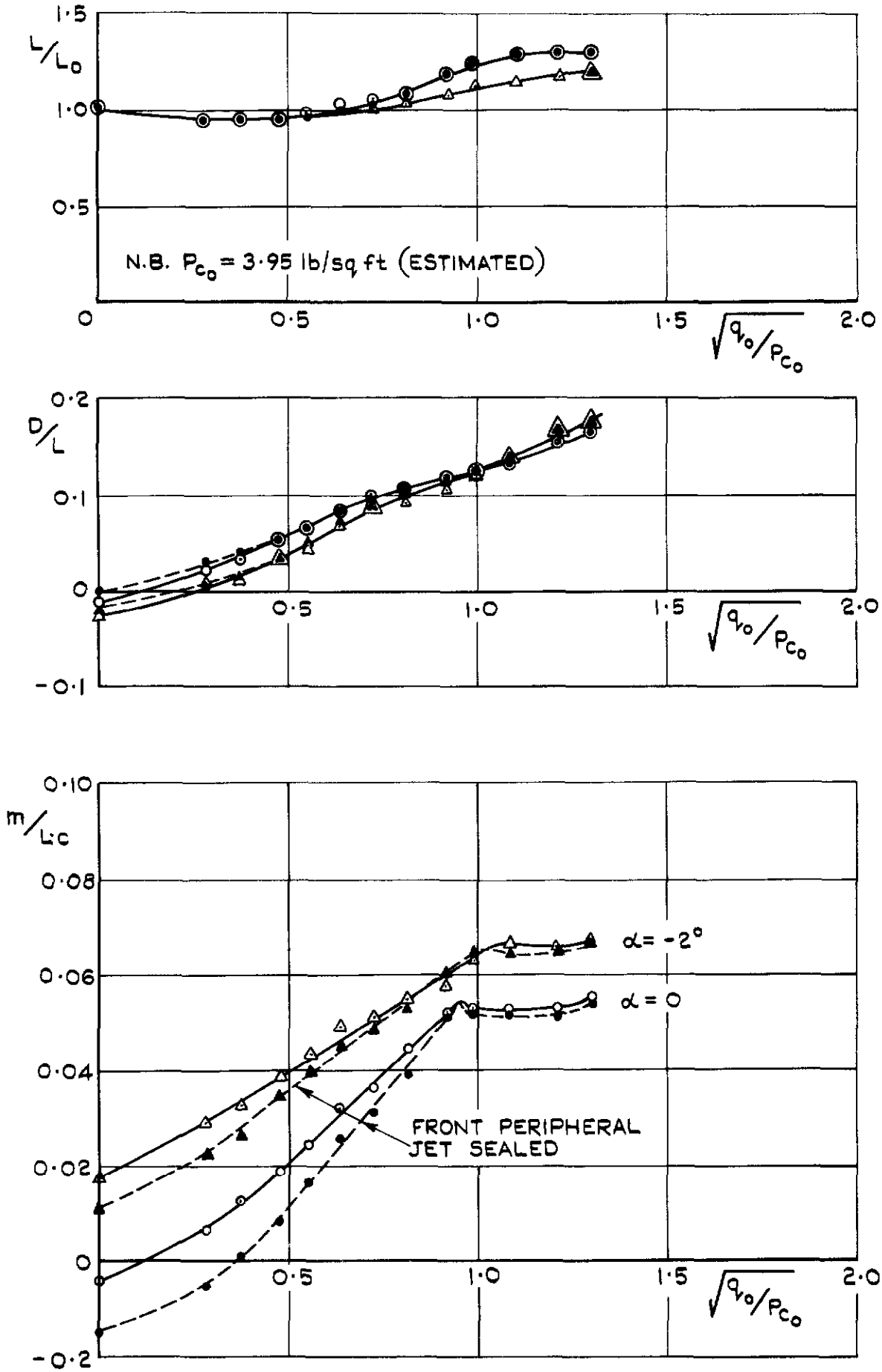

FIG. 30 EFFECT OF SEALING FRONT PERIPHERAL JET

ORIGINAL INTAKES $(r_L = 0 \cdot 018 d_i)$; $h/t = 1 \cdot 73$

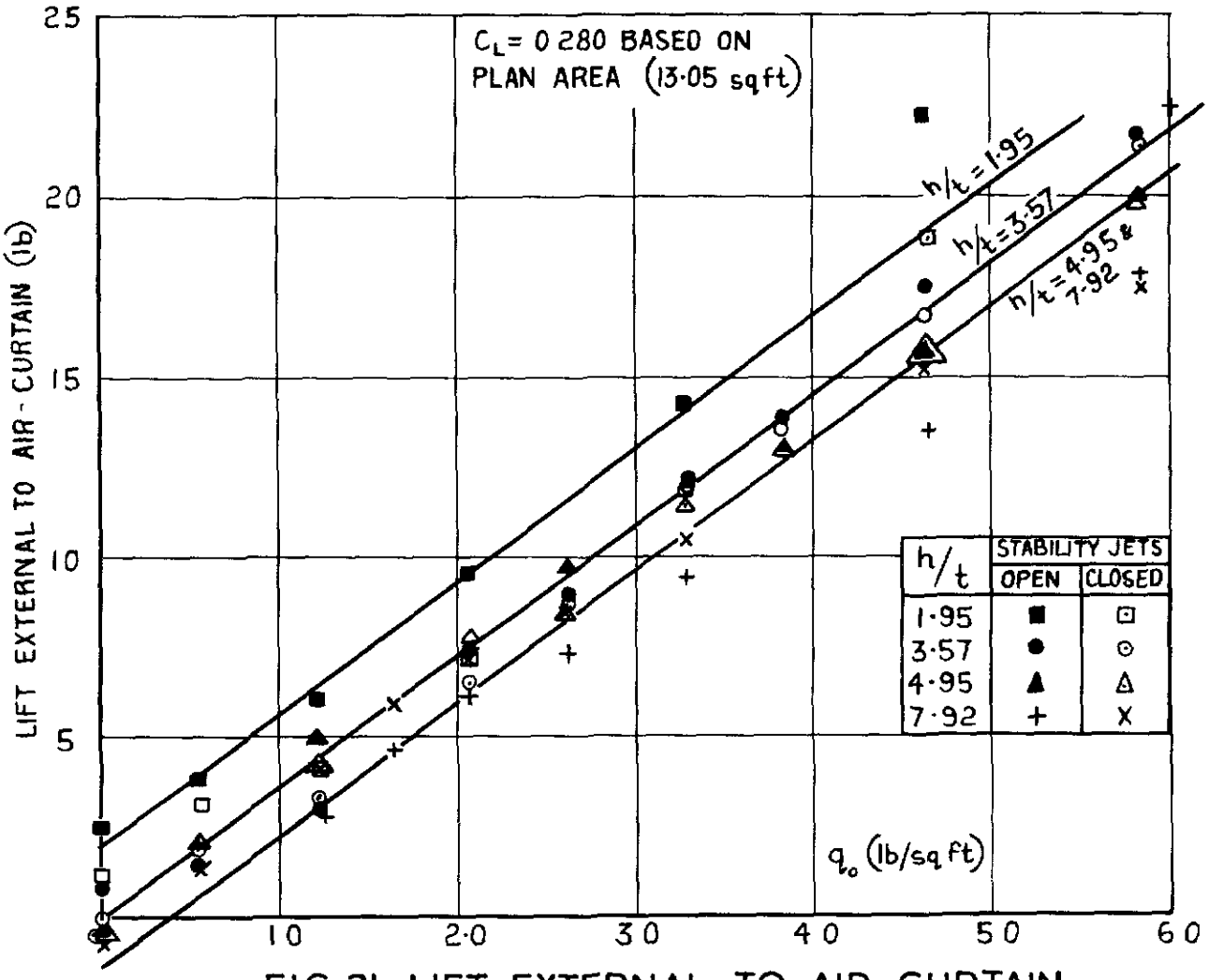

FIG.31 LIFT EXTERNAL TO AIR-CURTAIN

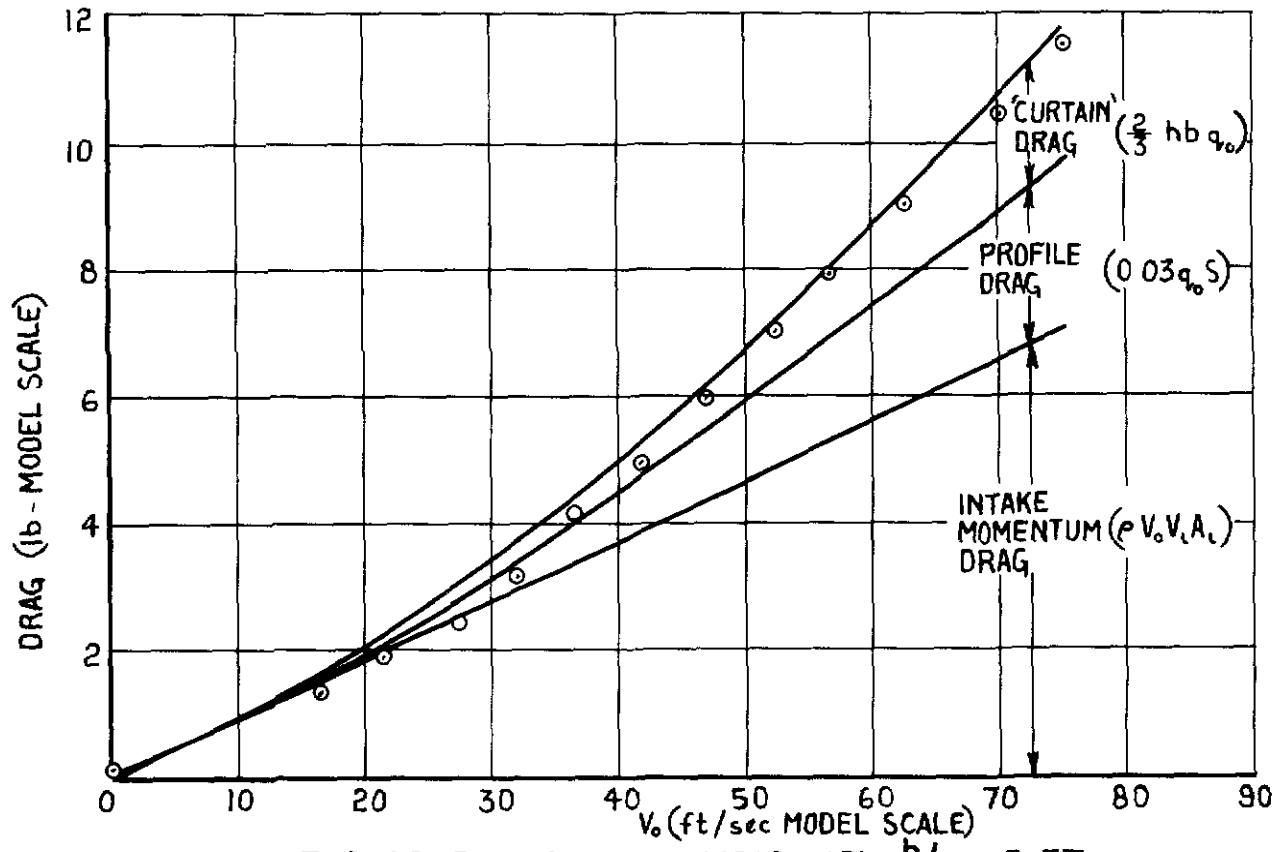

FIG.32 DRAG ANALYSIS AT h/t = 3·57
AND FAN SPEED = 1288 r p m
STABILITY JETS CLOSED ; α = 0

Printed in England for Her Majesty's Stationery Office by the Royal Aircraft Establishment, Farnborough Dd 129528 K.3

A.R.C. C.P. No. 983
December 1966

533.6.013.67 :
533.682

Trebble, W.J.G.

LOW-SPEED WIND-TUNNEL TESTS ON A 1/6TH SCALE MODEL OF AN AIR-CUSHION-VEHICLE (BRITTEN-NORMAN CUSHIONCRAFT C.C.2.)

An investigation has been made into the effects of mainstream speed on the performance and stability of a model of an Air-Cushion-Vehicle. At constant speed of the lifting fan, the lift increases both with reduction in ground clearance and increase in forward speed. The craft has a large drag which is mainly intake momentum drag. Limited speed could be available from tilting the craft bows down, but augmentation from propulsive units would be required for higher speeds.

Large nose-up moments occur at forward speed, reaching a maximum when the mainstream dynamic head is comparable with the cushion pressure. At

(Over)

A.R.C. C.P. No. 983
December 1966

533.6.013.67 :
533.682

Trebble, W.J.G.

LOW-SPEED WIND-TUNNEL TESTS ON A 1/6TH SCALE MODEL OF AN AIR-CUSHION-VEHICLE (BRITTEN-NORMAN CUSHIONCRAFT C.C.2.)

An investigation has been made into the effects of mainstream speed on the performance and stability of a model of an Air-Cushion-Vehicle. At constant speed of the lifting fan, the lift increases both with reduction in ground clearance and increase in forward speed. The craft has a large drag which is mainly intake momentum drag. Limited speed could be available from tilting the craft bows down, but augmentation from propulsive units would be required for higher speeds.

Large nose-up moments occur at forward speed, reaching a maximum when the mainstream dynamic head is comparable with the cushion pressure. At

(Over)

A.R.C. C.P. No. 983
December 1966

533.6.013.67 :
533.682

Trebble, W.J.G.

LOW-SPEED WIND TUNNEL TESTS ON A 1/6TH SCALE MODEL OF AN AIR-CUSHION-VEHICLE (BRITTEN-NORMAN CUSHIONCRAFT C.C.2.)

An investigation has been made into the effects of mainstream speed on the performance and stability of a model of an Air-Cushion-Vehicle. At constant speed of the lifting fan, the lift increases both with reduction in ground clearance and increase in forward speed. The craft has a large drag which is mainly intake momentum drag. Limited speed could be available from tilting the craft bows down, but augmentation from propulsive units would be required for higher speeds.

Large nose-up moments occur at forward speed, reaching a maximum when the mainstream dynamic head is comparable with the cushion pressure. At

(Over)

DETACHABLE ABSTRACT CARDS

higher speeds, the front air curtain breaks down with a resultant rearward movement of the centre of cushion lift thus giving some reduction in the nose-up moment. Pitch stiffness is reduced by an increase in either ground clearance or speed and is reduced to zero when the front curtain breaks down; at higher speeds there is some recovery in stability. Attempts to improve pitch control by means of a tailplane or by throttling the front jet proved inadequate.

higher speeds, the front air curtain breaks down with a resultant rearward movement of the centre of cushion lift thus giving some reduction in the nose-up moment. Pitch stiffness is reduced by an increase in either ground clearance or speed and is reduced to zero when the front curtain breaks down; at higher speeds there is some recovery in stability. Attempts to improve pitch control by means of a tailplane or by throttling the front jet proved inadequate.

higher speeds, the front air curtain breaks down with a resultant rearward movement of the centre of cushion lift thus giving some reduction in the nose-up moment. Pitch stiffness is reduced by an increase in either ground clearance or speed and isreduced to zero when the front curtain breaks down; at higher speeds there is some recovery in stability. Attempts to improve pitch control by means of a tailplane or by throttling the front jet proved inadequate.

Published by
HER MAJESTY'S STATIONERY OFFICE

To be purchased from
49 High Holborn, London W.C 1
423 Oxford Street, London W.1
13A Castle Street, Edinburgh 2
109 St. Mary Street, Cardiff
Brazennose Street, Manchester 2
50 Fairfax Street, Bristol 1
258-259 Broad Street, Birmingham 1
7-11 Linenhall Street, Belfast 2
or through any bookseller

C.P. No. 983

S.O. CODE No. 23-9017-83